

**LEUKOCYTE SPECIFIC PROTEIN-1: A NOVEL REGULATOR OF  
HEPATOCELLULAR MIGRATION AND PROLIFERATION IN LIVER  
REGENERATION AND CANCER**

by

**Kelly Ann Koral**

B.S., Biology, Wheeling Jesuit University, 2008

Submitted to the Graduate Faculty of  
School of Medicine in partial fulfillment  
of the requirements for the degree of  
Cellular and Molecular Pathology

University of Pittsburgh

2016

UNIVERSITY OF PITTSBURGH

SCHOOL OF MEDICINE

This dissertation was presented

by

Kelly Ann Koral

It was defended on

May 19, 2016

and approved by

Wendy M. Mars, Ph.D., Associate Professor

Reza Zarnegar, Ph.D., Professor

Donna Beer Stolz, Ph.D., Associate Professor

Donghun Shin, Ph.D., Assistant Professor

Dissertation Advisor: George K. Michalopoulos, M.D., Ph.D., Professor and Chairman

Copyright © by Kelly Ann Koral

2016

# **LEUKOCYTE SPECIFIC PROTEIN-1: A NOVEL REGULATOR OF HEPATOCELLULAR MIGRATION AND PROLIFERATION IN LIVER REGENERATION AND CANCER**

Kelly Ann Koral, PhD

University of Pittsburgh, 2016

Hepatocellular carcinoma (HCC) is the most commonly diagnosed form of liver cancer with high morbidity and mortality. Copy number variation analysis (CNV) of human HCC revealed that over 50% of the HCC samples examined had CNV in the gene leukocyte specific protein-1 (LSP1). LSP1, a F-actin binding protein, is expressed in hematopoietic cells and interacts with Kinase Suppressor of Ras (KSR), a scaffold for the ERK/MAPK pathway. The expression of LSP1 in liver and its role in normal hepatocellular function and carcinogenesis remains unknown. Therefore, LSP1 mRNA and protein levels were analyzed in normal hepatocytes in culture, rat liver following partial hepatectomy (PHx), and hepatoma cell lines. In culture and after PHx, LSP1 increased after the termination of hepatocyte proliferation and migration. To investigate LSP1 function in HCC, shRNA was utilized to stably knock down LSP1 expression in the JM1 rat hepatoma cell line. Loss of LSP1 in JM1 cells resulted in dramatic upregulation of cyclin D1 and pERK2, as well as increased cell proliferation and migration. Co-immunoprecipitation and immunofluorescence analysis displayed an interaction and co-localization between LSP1, KSR and F-actin in the JM1 cells and liver during regeneration. Conversely, expression of LSP1 in JM2 rat hepatoma cell line led to decreased proliferation. Enhanced expression of LSP1 in mouse hepatocytes during liver regeneration following injection of an LSP1 expression plasmid also led to decreased hepatocyte proliferation, cyclin D1 and pERK expression. LSP1 knockout mice subjected to PHx displayed increased

hepatocellular proliferation on day 4 when compared to control livers as well as increased pERK expression, whereas LSP1 overexpressing transgenic mice (TG) livers displayed a decrease in Ki67 positive hepatocytes on day 4 following PHx and decreased pERK expression. Hepatocytes from KO mice displayed increased proliferation in the absence of growth factors in culture whereas TG hepatocytes proliferated significantly less than WT control hepatocytes. Conclusion: LSP1 is expressed in normal hepatocytes and liver following PHx after the termination of proliferation. In rat hepatoma cell lines and mouse liver in vivo, LSP1 functions as a negative regulator of proliferation and migration. Given the high frequency of LSP1 CNV in human HCC, LSP1 may be a novel target for diagnosis and treatment of HCC.

## TABLE OF CONTENTS

<b>PREFACE.....</b>	<b>XIII</b>
<b>1.0 INTRODUCTION.....</b>	<b>1</b>
<b>1.1 THE LIVER AND REGENERATION.....</b>	<b>1</b>
<b>1.1.1 The liver: its functions and architecture .....</b>	<b>1</b>
<b>1.1.2 Liver regeneration .....</b>	<b>4</b>
<b>1.1.3 Signaling mechanisms involved in the initiation of liver regeneration after partial hepatectomy .....</b>	<b>6</b>
<b>1.1.4 Signaling mechanisms involved in the termination of liver regeneration following PHx .....</b>	<b>8</b>
<b>1.2 LIVER CANCER.....</b>	<b>11</b>
<b>1.2.1 Types of liver cancer and statistics .....</b>	<b>11</b>
<b>1.2.2 Causes of liver cancer.....</b>	<b>12</b>
<b>1.2.3 Liver carcinogenesis mechanisms .....</b>	<b>13</b>
<b>1.2.4 Treatments for liver cancer .....</b>	<b>14</b>
<b>1.3 GENETIC ABNORMALITIES IN LIVER CANCER .....</b>	<b>16</b>
<b>1.3.1 Copy number variation analysis and gene expression profiling in HCC .</b>	<b>16</b>
<b>1.4 LEUKOCYTE SPECIFIC PROTEIN-1.....</b>	<b>19</b>
<b>1.4.1 Structure, expression and basic functions of LSP1 .....</b>	<b>19</b>

1.4.2	Role in leukocyte and endothelial biology .....	21
1.4.3	Role in wound healing and fibrosis .....	24
1.4.4	LSP1 related signaling pathways .....	25
2.0	<b>LEUKOCYTE SPECIFIC PROTEIN-1 EXPRESSION IN HEPATOCYTES, DURING LIVER REGENERATION AND IN HEPATOCELLULAR CARCINOMA CELL LINES.....</b>	<b>29</b>
2.1	<b>INTRODUCTION .....</b>	<b>29</b>
2.2	<b>EXPERIMENTAL METHODS .....</b>	<b>31</b>
2.2.1	Reagents and Antibodies.....	31
2.2.2	Rat hepatocyte isolation and cell culture.....	32
2.2.3	Two-thirds partial hepatectomy of rat liver and isolation of rat hepatocytes after 2/3 partial hepatectomy .....	32
2.2.4	JM1 and JM2 rat hepatoma cell culture .....	33
2.2.5	Immunofluorescence and confocal microscopy .....	33
2.2.6	Cytoskeleton enrichment of JM1 rat hepatoma cells .....	34
2.2.7	Immunohistochemistry .....	34
2.2.8	Immunoprecipitation.....	35
2.2.9	Reverse Transcription and Polymerase Chain Reaction (PCR) .....	35
2.2.10	SDS PAGE and Western blot .....	36
2.2.11	Statistical Analysis.....	36
2.2.12	Approval of Animal Use.....	37
2.3	<b>RESULTS .....</b>	<b>37</b>
2.3.1	LSP1 is expressed in primary hepatocytes in culture .....	37

2.3.2	LSP1 expression in liver regeneration .....	40
2.3.3	LSP1 expression in hepatoma cell lines and interactions with ERK/MAPK scaffold Kinase Suppressor of Ras (KSR).....	44
2.4	DISCUSSION.....	47
3.0	LEUKOCYTE SPECIFIC PROTEIN-1 REGULATES HEPATOCELLULAR MIGRATION AND PROLIFERATION IN VITRO AND IN VIVO .....	50
3.1	INTRODUCTION .....	50
3.2	EXPERIMENTAL METHODS .....	51
3.2.1	Transfection of JM1 cells and creation of stable cell lines.....	51
3.2.2	MTT and Bromodeoxyuridine (BrdU) assays.....	52
3.2.3	Scratch and Transwell migration assays .....	52
3.2.4	Hydrodynamic injection of LSP1 plasmid DNA and 2/3 PHx.....	53
3.2.5	LSP1 knockout mouse model.....	54
3.2.6	Creation of hepatocyte specific LSP1 transgenic mouse model .....	54
3.2.7	Mouse hepatocyte isolation and culturing.....	55
3.3	RESULTS .....	55
3.3.1	Loss of LSP1 expression using shRNA in vitro leads to increased proliferation and migration.....	55
3.3.2	Expression of LSP1 in a LSP1 deficient cell line leads to decreased proliferation .....	62
3.3.3	Expression of LSP1 through hydrodynamic tail vein injection leads to decreased proliferation following partial hepatectomy .....	64

3.3.4	LSP1 KO mice display increased ERK activation and proliferation after partial hepatectomy .....	67
3.3.5	Hepatocytes from LSP1 KO mice exhibit increased proliferation in the absence of growth factors .....	73
3.3.6	LSP1 transgenic mice display decreased proliferation and ERK activation following partial hepatectomy.....	78
3.3.7	Hepatocytes from LSP1 transgenic mice display decreased proliferation and pERK expression .....	83
3.4	DISCUSSION.....	89
4.0	SUMMARY .....	92
5.0	FUTURE DIRECTIONS.....	95
	BIBLIOGRAPHY .....	101

## LIST OF FIGURES

Figure 1. Liver Architecture..	3
Figure 2. Kinetics of DNA synthesis in different cell types of the rat liver after partial hepatectomy..	6
Figure 3. Genomic mapping of LSP1 deletions (blue) and amplifications (red).	18
Figure 4. Schematic of mouse LSP1 protein structure..	20
Figure 5. LSP1 expression in primary rat hepatocytes in culture, rat liver and hepatocytes after PHx..	38
Figure 6. Quantification of BrdU labeling in primary rat hepatocytes in culture.....	39
Figure 7. RT-PCR of rat hepatocytes in culture and rat hepatoma cell lines for LSP1 isoforms..	39
Figure 8. Immunofluoresence of LSP1 and F-actin in rat liver after PHx.....	41
Figure 9. Quantification of LSP1 and f-actin immunofluoresence co-localization in rat liver after partial hepatectomy.....	43
Figure 10. Total and phospho LSP1 expression in rat non-parenchymal cells (NPC) after PHx. .	43
Figure 11. LSP1 expression in rat hepatoma cell lines and analysis of LSP1, KSR and F-actin interactions. ....	45

Figure 12. LSP1 and f-actin immunofluorescence in cytoskeletal extracts of JM1 rat hepatoma cells.....	46
Figure 13. Creation of a LSP1 shRNA expression stable JM1 hepatoma cell line. ....	56
Figure 14. Functional analysis of loss of LSP1 expression in JM1 hepatoma cell line.....	59
Figure 15. Live cell imaging of migration scratch assay of JM1 LSP1 shRNA stable cell line...	60
Figure 16. Transwell Migration Assay of JM1 LSP1 shRNA stable cell line.....	61
Figure 17. JM2 cells were transiently transfected with LSP1 cDNA and pExpress-1 plasmid (control).....	63
Figure 18. In vivo expression of LSP1 in a mouse PHx model.....	66
Figure 19. Western blot analysis of mouse livers after hydrodynamic tail vein injections.. .....	66
Figure 20. LSP1 knockout (KO) mice display increased Ki67 positive hepatocytes on day 4 after PHx and increased hepatocyte numbers on days 4 and 7.. .....	68
Figure 21. Liver to body weight ratios of WT and LSP1 KO mice after PHx.. .....	69
Figure 22. Western blot analysis of LSP1 expression in WT and LSP1 KO mouse livers.. .....	69
Figure 23. Western blot analysis of WT and LSP1 KO mouse livers after PHx.....	71
Figure 24. Immunoprecipitation of KSR in WT and LSP1 KO PHx liver lysates.. .....	72
Figure 25. BrdU incorporation assay in hepatocytes from WT and LSP1 KO mice cultured in the presence of growth factors.. .....	74
Figure 26. BrdU incorporation assay in hepatocytes from WT and LSP1 KO mice cultured in the absence of growth factors. ....	75
Figure 27. Western blot analysis of WT and LSP1 KO hepatocytes cultured in the presence and absence of HGF and EGF.. .....	77

Figure 28. LSP1 transgenic (TG) mice display decreased Ki67 positive hepatocytes and decreased hepatocyte numbers on day 4 after PHx.. .....	79
Figure 29. Liver to body weight ratios of WT and LSP1 TG mice after PHx.....	80
Figure 30. Western blot analysis of LSP1 expression in WT and LSP1 TG mouse livers.....	80
Figure 31. Western blot analysis of WT and LSP1 TG mouse livers after PHx. ....	82
Figure 32. Immunoprecipitation of KSR in WT and LSP1 TG PHx liver lysates.....	83
Figure 33. BrdU incorporation assay in hepatocytes from WT and LSP1 TG mice cultured in the presence of growth factors.. .....	85
Figure 34. BrdU incorporation assay in hepatocytes from WT and LSP1 TG mice cultured in the absence of growth factors.. .....	86
Figure 35. Western blot analysis of WT and LSP1 TG hepatocytes cultured in the presence and absence of HGF and EGF.. .....	88
Figure 36. Schematic of LSP1, KSR, ERK interaction in the cell.....	93
Figure 37. Treatment of LSP1 shRNA JM1 stable cells with sorafenib causes increased cell death in comparison to scrambled control cells.....	98

## **PREFACE**

Graduate school has been one long journey which has taught me not only how to be a good scientist but also helped me to develop confidence in myself. This process has taught me what it means to persevere through hardships and learn from failures (which I will admit I still struggle with). There were many times along this arduous path that I didn't think I could go on but somehow I found the strength to continue on with the support of my mentor, committee, family and friends. Without the unwavering support of all of the people in my life, I know that I would not have accomplished this goal.

There are many people I would like to thank for helping me along the way. First, my mentor Dr. George Michalopoulos has taught me not only how to be a great scientist but also a great human being. George has shown true compassion towards me and has always encouraged me along the way. At times, and there were many, experiments fail or the results obtained are negative but after speaking with George he had a way of turning the failures into a positive and brightening my outlook on my project. He has shown me what it means to have a true passion for science. My committee chairperson: Dr. Wendy Mars has been a great mentor and excellent resource in helping me troubleshoot the problems that I ran into with experiments. She was always willing to sit down and help me figure out what to do differently and challenged me to really think about and understand the experiments. My committee members: Dr. Donna Stolz,

Dr. Reza Zarnegar, and Dr. Donghun Shin have been given me tremendous feedback and helped me to see the bigger picture when at times I was bogged down with some insignificant detail. Through their advice and guidance, I was able to really understand and grasp what experiments were actually measuring and what experiments would help me to address my hypothesis.

To my Mom: You have supported me through it all and always taught me to value an education and reach for my fullest potential. I would not be the person I am today without your unwavering support. My brother Tom: Your humor has helped me get through some of the rough patches in life. You are one of the most intelligent people I know and I am very proud of all that you have accomplished. My husband Kevin: You have been my rock for the past 13 years. You are my soulmate and best friend. You have been by my side through my highest highs and lowest lows. You always believed in me and for that I am forever grateful. I love you and would not have accomplished this without you. To my dearest Hudson: The day you were born was the best day of my life. I love you more than words can describe. I live for your smile and laugh and I hope by achieving this goal you will be proud of me. To my Dad and Grandma: Losing you both were the worst days of my life but out of the grief and tragedy I have tried to find a way to turn it into a positive by dedicating my life to further understand the process of cancer. I hope that I have made you proud. To the rest of my family and friends: I love you all and truly appreciate all that you have done to support me throughout the years.

## **1.0 INTRODUCTION**

### **1.1 THE LIVER AND REGENERATION**

#### **1.1.1 The liver: its functions and architecture**

The liver is a unique organ with a phenomenal ability to regenerate and perform a variety of complex functions. One function of the liver is to detoxify the blood of chemicals found in food delivered from the small and large intestine, the spleen and pancreas.. Liver reprocesses the nutrients from food into secreted proteins such as albumin, coagulation factors and proteins that comprise plasma in the peripheral blood. The liver also produces lipids, which are sent to other tissues as lipoproteins, and carbohydrates stored as glycogen, which function to stabilize glucose levels in the blood. In addition to the previously stated functions, hepatocytes synthesize bile, which is secreted from the apical side of the hepatocyte into the bile canaliculi that lines the area between hepatocytes and coalesces into the bile duct, which are lined with cholangiocytes. Bile is crucial for absorption of fat and other lipophilic nutrients in the small intestine. The liver also acts as the main regulator of ammonia and glucose levels in the blood, which affect normal brain functions. Without a functioning liver, hepatic encephalopathy can occur, which eventually leads to coma and death (1-3).

The liver is a highly specialized tissue consisting of a variety of cell types, which include hepatocytes, cholangiocytes (biliary cells), hepatic stellate cells, Kupffer cells, and sinusoidal endothelial cells. In development, hepatocytes, the main functional cell of the liver, and cholangiocytes, the cells that line the bile ducts, are derived from a common precursor cell, which is known as the hepatoblast. Having a common precursor cell allows hepatocytes and cholangiocytes to transdifferentiate in response to injury when one cell type cannot replicate to replace the lost cells (4, 5) The non-parenchymal cells (NPC) of the liver consist of hepatic stellate cells, sinusoidal endothelial cells, and Kupffer cells. The hepatic stellate cell is a mesenchymal cell that functions in vitamin storage, turnover of extracellular matrix, secretion of growth factors such as HGF, and vascular tone among others and is located in the area between the hepatocytes and sinusoidal endothelial cells, which is known as the space of Disse. Injury to the liver results in the activation of stellate cells to become myofibroblast like cells, which are contractile and secrete extracellular matrix proteins. Hepatic stellate cells share a gene expression profile very similar to the astrocytes of the brain (2, 6, 7). Sinusoidal endothelial cells have fenestrations, which are large cytoplasmic gaps that allow for the movement of macromolecules and lipoproteins into and out of the hepatocytes and blood. Kupffer cells, the resident macrophages of the liver, play a role in immune functions in the liver (Figure 1A) (2, 8).

Hepatocytes form cords along a specialized capillary bed lined with fenestrated sinusoidal endothelial cells. Blood flows into the liver in a unidirectional manner from the portal vein and hepatic artery through the sinusoids to the central vein, which unites with the hepatic vein and finally connects with the inferior vena cava. The liver is organized into hepatic lobules, which are hexagonal units that consist of cords of hepatocytes, the parenchymal cells of the liver, branching out from a central vein. The hepatic artery and portal vein along with the collecting

bile duct form the portal triad, which is found at the corners of the hepatic lobule. Each lobule consists of three broad zones: periportal (zone 1), transitional (zone 2), and pericentral (zone 3). Proceeding from Zone 1 to Zone 3, hepatocytes are exposed to rising levels of processed xenobiotics and toxins and decreasing levels of oxygen (Figure 1B) (2, 9, 10).

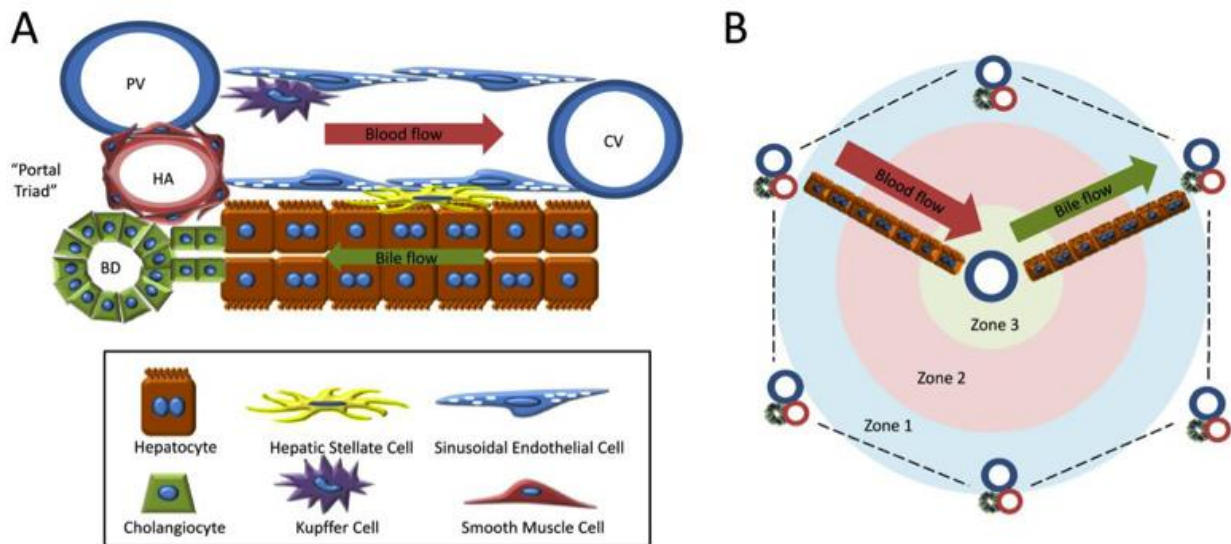


**Figure 1. Liver Architecture.** (A) Schematic depicting the hepatic sinusoid architecture and cell types. Blood flows into the lobule through the portal vein (PV) and hepatic artery (HA) and then into the capillaries, ending at the central veins (CV). Bile moves away from the central vein towards the portal triad and leaves the lobule through the bile ducts (BD). Hepatocytes form “plates” 1-2 hepatocytes thick along the sinusoids. In the “space of Disse” which is the area between the sinusoidal endothelial cells and hepatocytes, the hepatic stellate cells reside. (B) Schematic showing hepatic lobule organization, including the structure of the vasculature and lobule zonation. This structure occurs throughout the liver. Hepatocyte plates are shown for orientation; the entire lobule would contain these plates of hepatocytes and be lined with sinusoids. Adapted from (2).

### 1.1.2 Liver regeneration

The liver has a unique capacity to regenerate after a loss of liver mass. Liver regeneration is a highly complex and organized process, which under normal conditions involves all of the cells of the liver undergoing one to three rounds of replication in order to restore the original number of cells and overall mass of the liver. Hepatotoxic chemicals, such as carbon tetrachloride, can be administered to induce a loss of liver mass. However, this form of injury results in an inflammatory response to remove tissue debris followed by the regenerative process. The most common model to study liver regeneration is the 2/3 partial hepatectomy (PHx) model in which 2/3 of the liver mass is removed surgically (11). Three of the five lobes of the rodent liver are removed without damaging the remaining two lobes, which grow to restore the mass of the original five lobes. The regenerative process is complete within 5-7 days following surgery. Partial hepatectomy is the preferred model for the experimental study of liver regeneration due to its reproducibility in terms of the mass removed and the accuracy of the events that ensue after the procedure. This model is also utilized in a clinical setting in humans to remove primary liver cancer, metastases from other organs or following trauma. However, the main disadvantage of the PHx model is its limited applicability to study liver regeneration in humans, which involves inflammation and necrosis (1, 7, 12-14).

PHx initiates a series of events that progress in a systematic way and can be observed from 5 minutes after the procedure to 5-7 days. The first cells to undergo DNA synthesis are the hepatocytes. DNA synthesis peaks at 24 hours post PHx in the rat and approximately 36 hours post PHx in the mouse (Figure 2). After the first round of replication, a second smaller population of hepatocytes replicates to restore the original number of cells. Hepatocyte proliferation occurs as a wave of mitoses, beginning at the periportal area and moves toward the

pericentral area of the lobule (15). The last hepatocytes to undergo DNA synthesis are the ones around the central vein, which are positive for glutamine synthetase (16). At the end of proliferation, a small number of hepatocytes undergo apoptosis to correct for any extra hepatocytes and restore the mass of the liver to its original size (17). Hepatocytes secrete growth factors and cytokines that stimulate the other cell types of the liver to undergo proliferation. Biliary epithelial cells and stellate cells begin to proliferate about 12 hours after the hepatocytes with a peak of DNA synthesis at about 48 hours in the rat. Endothelial cells begin to proliferate 2-3 days post PHx and finish at 4-5 days. The liver is organized into cell clusters containing 10-14 hepatocytes on day 3 after PHx. On Day 4, the stellate cells send processes into the hepatocyte clusters and start to produce laminin. Next, the sinusoidal endothelial cells penetrate the hepatocyte clusters and restore the normal liver vasculature. Restoration of normal liver mass is complete between 5-7 days post PHx in rodents (in humans, 8-15 days) and is due to the replication of mature adult hepatocytes and other hepatic cells and not by the proliferation of a small population of stem cells. The size of the liver lobules is larger and the hepatocyte plates are almost twice as thick as the original one cell thickness after regeneration. For several weeks following regeneration, lobule reorganization takes place and eventually the histology of the liver is identical to the original liver (1, 7). Since partial hepatectomy is a form of liver injury, it is not unexpected that the same signaling pathways occurring during liver regeneration also play a role in the wound healing process that occurs in other tissues (1).

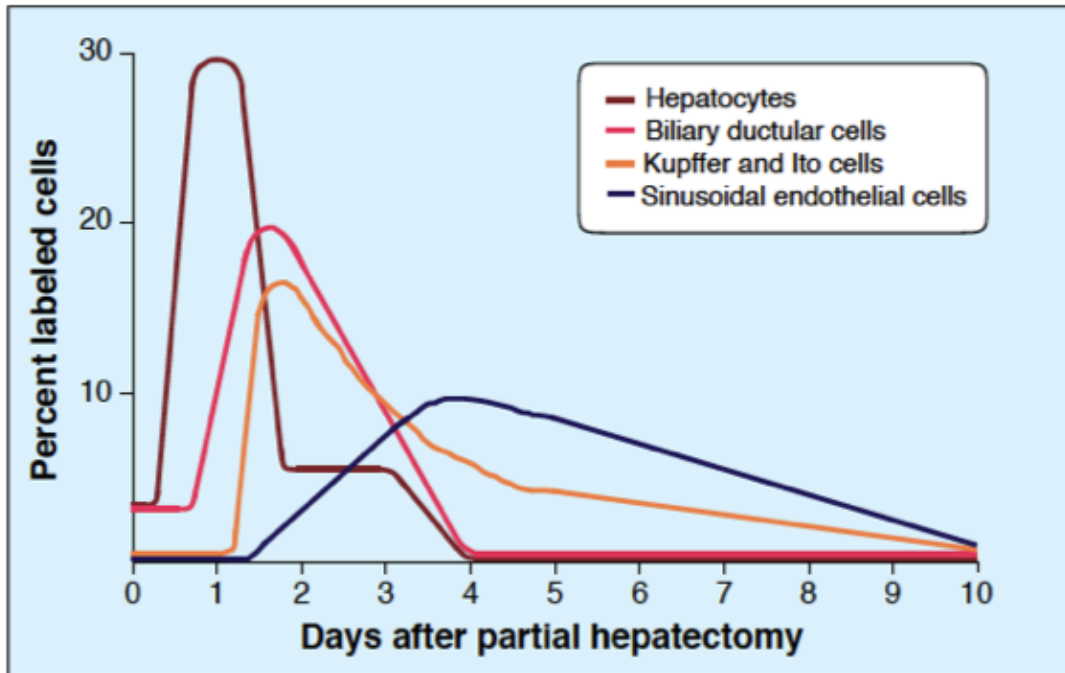


Figure 2. Kinetics of DNA synthesis in different cell types of the rat liver after partial hepatectomy. The four major cell types divide at different times during regeneration. Hepatocytes proliferate first with the peak of DNA synthesis occurring at 24 hours, whereas the other cell types proliferate later. Regenerating hepatocytes secrete growth factors that can stimulate the other cell types to undergo cell division. Adapted from (5).

### 1.1.3 Signaling mechanisms involved in the initiation of liver regeneration after partial hepatectomy

PHx activates the expression of a large number of genes and a sequence of cellular events that are tightly regulated. One of the earliest biochemical events that occur after PHx is an increase in the activity of urokinase plasminogen activator (18), which occurs 5 minutes after PHx (19). uPA

activation is associated with an increase in the activation of plasminogen to plasmin at 10 minutes after PHx and fibrinogen degradation products. Urokinase initiates remodeling of the matrix, which is also seen in wound healing. Studies conducting on wound healing and tumor biology have demonstrated that matrix remodeling initiates integrin signaling along with releasing growth factors and peptides that are bound to the matrix and have signaling capabilities. Extracellular matrix regulation during liver regeneration is a complicated process involving matrix metalloproteinases and tissue inhibitors of metalloproteinases (20). In the extracellular matrix of the liver are many matrix bound growth factors, one of which is hepatocyte growth factor (HGF) (21). uPA activates matrix bound HGF by converting it into its active heterodimeric form. (19) At three hours post PHx, the amount of active and inactive HGF from pre-existing stores is diminished but plasma HGF levels rise by 10 to 20 fold. In the liver, HGF mRNA expression is increased in the stellate and endothelial cells and the lungs, kidney and spleen also produce increased levels of HGF (12). Within 30-60 minutes after PHx, active HGF leads to the activation of the HGF receptor Met. Although epidermal growth factor receptor (EGFR) is constitutively phosphorylated, there is an increase in EGFR phosphorylation at the same time as Met (22). EGF is secreted by the Brunner's glands of the duodenum and is constantly available to the liver through the portal circulation. Studies have shown that cross talk occurs between cMet and EGFR and that Met activation may increase activation of EGFR after PHx. In addition to the increase in HGF expression in the circulation, there is also an increase in the amount of tumor necrosis factor (23), bile acids (24), interleukin-6 (25), serotonin (26), norepinephrine, hyaluronic acid (a main component of the matrix in the liver) and transforming growth factor  $\beta$ I (TGF  $\beta$ I) (1, 7).

Various molecular changes are occurring inside of the hepatocytes following PHx. Between 15-30 minutes following PHx, beta-catenin and Notch-I intracellular domain (NICD) are located in the nuclei of the hepatocytes (27, 28). Within one hour, there is increased Stat3 and NFκB activation. At six hours after PHx, cyclin D1, a protein involved in cell cycle dynamics, is activated in the hepatocytes and amino acids and TOR regulate this activation. On days 2 and 3 after PHx, there is a decrease in the ratio C/EBPα to C/EBPβ, which is believed to play a role in enhancing the synthesis of lipids by hepatocytes. The alterations in gene expression patterns that occur during liver regeneration are reliant on both cytokine and growth factor signaling. (1, 12, 13)

Two of the main signaling molecules that are involved in the initiation of liver regeneration are HGF and the ligands of EGFR. HGF, along with the EGFR ligands (EGF, TGFα, Amphiregulin, HB-EGF, etc.), are the only direct mitogens for hepatocytes, meaning they cause a strong mitogenic response in hepatocytes in culture as well clonal population expansion in the absence of other factors. Injection of HGF, EGF, and TGFα into mice and rats leads to proliferation of hepatocytes and subsequently, enlargement of the liver. Additionally, other substances, such as TNF, norepinephrine, and estrogen, while not direct mitogens, can increase the effect of the direct mitogens and enhance proliferation. (1, 7, 12)

#### **1.1.4 Signaling mechanisms involved in the termination of liver regeneration following PHx**

Termination of liver regeneration is also a highly controlled complex process of which much less is known. Liver mass is highly regulated returning to prehepatectomy mass with great accuracy following regeneration. To correct for inappropriate proliferation, there is a small amount of

hepatocellular apoptosis that occurs at the end of regeneration (17). A recognized inhibitor of hepatocyte proliferation is TGF $\beta$ I and its expression increases within five hours after PHx and remains increased until the end of regeneration (29, 30). However, overexpression of TGF $\beta$ I in a hepatocyte specific transgenic mouse causes elevated levels of TGF $\beta$ I in the blood but does not have an effect on liver regeneration. Activin, a cytokine, is also known to inhibit hepatocyte proliferation and inactivation of its receptor along with inactivation of TGF $\beta$ I receptor leads to prolonged regeneration. Another piece of evidence to demonstrate a role for TGF $\beta$ I in regeneration is that injection of a dominant negative TGF $\beta$ I receptor into unoperated mice led to stimulation of hepatocellular DNA synthesis (31). This suggests that hepatocytes are under a “constant tonic antagonism” between HGF and TGF $\beta$ I in the pericellular area around the hepatocytes. All of this suggests that termination of regeneration is a reverse of initiation in which the formation of extracellular matrix and decorin leads to the binding of HGF and TGF $\beta$ I restoring the pre-hepatectomy balance in the pericellular space.

Extracellular matrix plays an important role in the termination of liver regeneration. ECM not only stores a variety of factors that regulate growth, but also mediates signaling to the surrounding cells through integrins. Previous studies have demonstrated that when integrin linked kinase (32) expression is lost through genetic elimination in the liver, this leads to increased proliferation of hepatocytes and biliary cells in the absence of PHx (33). Following PHx, loss of ILK in the liver results in a termination defect in which the liver grows 59% larger than their pre-hepatectomy weights. These livers lacking ILK expression also expressed increased HGF as well as increased expression of Yap (Yes-associated protein) in the nuclei of hepatocytes, which is a protein involved in the regulation of organ size (34, 35). In vitro, ECM, in the form of matrigel or collagen gels, leads to an inhibition of proliferation with an increase in

hepatocyte differentiation (36). Therefore, ECM signaling through integrins plays an important role in the termination of liver regeneration.

The complex ECM consists of a variety of components including proteins and glycosaminoglycans among others. Another component of the ECM that seems to play a critical role in liver regeneration termination is Glypican 3 (GPC3). GPC3 is highly expressed in the pericellular area surrounding hepatocytes as well as other epithelial cells (37). GPC3 is the most overexpressed protein in human hepatocellular carcinoma (HCC) as well as in other tumors (38) and it is used as a marker of human liver cancer in clinical settings (39). In patients with Simpson-Gholabi-Behmel (SGB) syndrome, a loss of function deletion in GPC3 leads to organomegaly of the liver and other internal organs as well as bone and muscle enlargement (40). Although GPC3 is highly expressed in HCC, the loss of function of GPC3 in SGB leading to increased liver size suggests that GPC3 may act as a growth suppressor and in HCC is produced as a failed growth suppressor, which can no longer suppress tumor growth. Loss of GPC3 function in mice leads to similar symptoms to patients with SGB. (41) During liver regeneration, GPC3 expression increases towards the end of regeneration and loss of GPC3 expression in hepatocytes in culture leads to enhanced proliferation. (42) In a transgenic mouse line expressing GPC3 specifically in hepatocytes, liver regeneration after PHx was suppressed and proliferation of hepatocytes was inhibited indicating that GPC3 functions as a growth suppressor in hepatocytes. (43) These findings demonstrate that the ECM plays a critical role in the termination of liver regeneration following PHx.

## 1.2 LIVER CANCER

### 1.2.1 Types of liver cancer and statistics

Liver cancer is one of the most common and lethal forms of cancer in the world. The term liver cancer consists of a variety of histologically diverse primary hepatic neoplasms, which includes hepatocellular carcinoma (HCC), intrahepatic cholangiocarcinoma (bile duct carcinoma), hepatoblastoma, bile duct cystadenocarcinoma, hemangiosarcoma, and epithelioid hemangioendothelioma. HCC, the most common form of primary liver cancer, accounts for approximately 80% of cases. The second most common form, cholangiocarcinoma, which is cancer of the bile duct cells, represents 10-20% of liver cancer diagnoses (44).

According to the American Cancer Society, in the United States in 2016, there will be 39,320 new cases of liver cancer diagnosed and approximately 27,170 people will die from this disease. Incidence of liver cancer in the United States has tripled from 1980. The relative five-year survival rate for patients with liver cancer in the United States is relatively low at 15%. Liver cancer affects men more than woman with the lifetime risk for an average man being 1 in 81 whereas for an average woman it is 1 in 196. Throughout the world, more than 700,000 people are diagnosed with liver cancer and it remains the leading cause for cancer deaths worldwide, with more than 600,000 deaths each year. Liver cancer is more common in sub-Saharan Africa and Southeast Asia than in the U.S. (45). The high death rates associated with liver cancer are due in part to resistance to current anti-cancer therapies, limitations on the use of chemotherapeutics due to underlying liver conditions as well as a lack of biomarkers to detect liver cancer early (44). Many patients present with cancer symptoms when the cancer is in advanced stages, making it difficult to treat and resulting in death within 3-6 months (46).

### 1.2.2 Causes of liver cancer

The majority of HCC patients have underlying liver cirrhosis. Chronic injury to the liver results in continual rounds of hepatocellular damage and regeneration leading to chronic liver disease. This can then develop into cirrhosis, which occurs when activation of stellate cells into a myofibroblast phenotype leads to deposition of fibrous tissue such as collagen I and loss of hepatocytes due to a decrease in the regenerative capacity of the liver. Over time, the cirrhotic nodules may develop genetic alterations and genomic instability resulting in HCC (47, 48). There are a variety of factors that increase the risk of developing cirrhosis and can ultimately lead to HCC, which includes hepatitis B and C viral infections, alcoholism, consumption of aflatoxin-contaminated foods, nonalcoholic steatohepatitis, diabetes, obesity, and certain hereditary conditions (44, 47, 49). Although cirrhosis infers a greater risk of developing HCC, the relationship between cirrhosis and hepatocarcinogenesis is complex and may involve a patient having a combination of etiologies (47).

Viral induced hepatocarcinogenesis is associated with two main viruses, hepatitis B and C. Hepatitis B virus (HBV) is a partially double stranded DNA virus of the hepadnaviridae family that infects approximately 2 billion people in the world. Around 30-50% of HBV related deaths are due to HCC. Hepatitis C virus is a non-cytopathic RNA virus of the flaviviridae family. Approximately 170 million people are infected with HCV worldwide and 20% of these patients will develop cirrhosis and 2.5% of those will progress to HCC. HCV and HBV differ in three important ways in regards to HCC development. First, HCV is more likely to result in chronic infection than HBV with 60-80% of HCV cases versus 10% of HBV infected patients. Second, HCV infected individuals have a greater propensity to develop cirrhosis which is a

precursor to HCC. Lastly, HCV is an RNA virus without an intermediate DNA form so it is unable to integrate into the genome of the host (44, 50).

Chronic alcohol intake is another risk factor for HCC development. Alcoholism causes activation of monocytes, which leads to increased production of pro-inflammatory cytokines as well as increased endotoxin in the circulation leading to hepatocyte death (51). Hepatocytes develop an increased sensitivity to tumor necrosis factor  $\alpha$  (TNF  $\alpha$ ), resulting in a continuous cycle of hepatocyte death and regeneration, stellate cell activation, cirrhosis and HCC (52). Chronic alcohol consumption can also damage the liver through increased oxidative stress resulting in fibrosis and hepatocarcinogenesis (44).

Another factor that imposes an increased risk for HCC development is ingestion of fungal toxin, aflatoxin B1. Aflatoxin B1 is a mutagen associated with a particular p53 mutation and activation of oncogenes, such as HRAS (53, 54). However, unlike viral and alcohol induced hepatocarcinogenesis, exposure to aflatoxin is not associated with development of cirrhosis suggesting that the toxin induced mutagenesis may be the primary driver of HCC (44).

### **1.2.3 Liver carcinogenesis mechanisms**

Many molecular and genetic pathways are altered and contribute to hepatocarcinogenesis. One common genetic event that occurs in HBV, HCV, and aflatoxin B1 induced HCC is inactivation or mutation of the tumor suppressor protein, p53 (55). Inflammation, constant rounds of necrosis and regeneration, and oxidative stress are hallmarks of viral and alcohol induced HCC, indicating that these processes play a role in the development of HCC. The MAP kinase pathway is also activated in HBV and HCV infected livers suggesting its importance in hepatocarcinogenesis (56, 57). Molecular analysis of human HCC has demonstrated a variety of

genetic and epigenetic alterations that occur in important oncogenes and tumor suppressor genes such as TP53,  $\beta$ -catenin, ErbB receptor family, MET receptor and its ligand hepatocyte growth factor (HGF), p16(INK4a), E-cadherin, and cyclooxygenase 2 (COX2), among others (44).

In addition to genetic alterations in particular oncogenes and tumor suppressor genes, HCC is characterized by genomic instability. A key feature of chronic hyperproliferative liver disease is telomere shortening, which is thought to contribute to the induction of HCC (58). Telomerase is highly activated in ~90% of human HCC suggesting that this process facilitates HCC progression (59, 60). Studies utilizing TERC (essential RNA component of telomerase) null mice have demonstrated that dysfunction of the telomeres resulted in increased initiation of hepatic tumors whereas loss of telomerase activity inhibited progression of HCC (61). Chromosome segregation defects that occur during mitosis cause aneuploidy and an increase in HCC incidence (62).

#### **1.2.4 Treatments for liver cancer**

Treatment options for patients with HCC are limited and the prognosis for patients with advanced HCC remains poor (18). Approximately 30% of patients are eligible for curative treatments such as resection of the tumor, liver transplantation or local ablation, which results in 5-year survival rates around 50% (63). Approximately 20% of patients can receive chemoembolization (64). Tumor resection is usually performed on patients with a non-cirrhotic liver with only one tumor. Liver transplantation mainly helps patients with decompensated cirrhosis and either one tumor less than 5 cm or three small tumors less than 3 cm in diameter (63). The drawback to transplantation is that the shortage of donor livers severely limits its use to treat HCC (63). Percutaneous treatments are utilized in patients with early HCC that is unable to

be resected (63). There are a variety of methods to kill tumor cells in the liver including chemically by using ethanol or acetic acid and by changing the temperature of the cells through radiofrequency, microwave, laser, and cryoablation (65). Arterial embolization is utilized in patients with unresectable HCC in which gelatin is administered along with intra-arterial chemotherapy, most commonly doxorubicin, mitomycin, and cisplatin, along with lipiodol. In approximately 15-55% of patients, this method can achieve partial results and delays progression of the tumor and invasion of the vasculature (66, 67).

The only molecular targeted therapy that is FDA approved to treat advanced HCC is sorafenib. Sorafenib is an oral inhibitor of multiple tyrosine kinases as well as an angiogenesis inhibitor that is active against vascular endothelial growth factor (VEGF), platelet derived growth factor receptor (PDGFR), c-KIT receptor, BRAF and p38 signaling pathways (18). Patients with advanced HCC taking sorafenib have a median time to disease progression of 5.5 months and median overall survival of 10.7 months (68). Sorafenib significantly improved overall survival in comparison to placebo in two large phase III trials (68, 69). There are currently no additional therapies for patients whose cancer progresses while taking sorafenib or are unable to tolerate this treatment (18). Since the efficacy of the currently available treatments is low, there remains a great need to develop novel therapeutics to treat HCC.

## **1.3 GENETIC ABNORMALITIES IN LIVER CANCER**

### **1.3.1 Copy number variation analysis and gene expression profiling in HCC**

Global gene expression profiling of HCC is utilized to identify novel therapeutic targets as well as to improve the prognosis and diagnosis of HCC by identifying genetic alterations in the tumors. Data from these studies provides vital information to characterize HCC into different molecular subgroups, which improves the selection of specific treatments and overall outcome for patients with HCC. DNA microarrays are utilized to analyze the expression of thousands of genes and can successfully predict prognosis as well as organize different types of cancer into specific molecular subgroups (70). Understanding the heterogeneity of HCC by utilizing genomic expression profiling will improve patient response to treatment because certain therapeutics will only be successful in particular subtypes of the disease (70, 71).

Several recent studies have identified large deletions and point mutations as well as copy number variations, meaning genome amplifications and deletions of a large size in HCC. One study identified alterations in four genes not previously described in HCC. One of these genes IRF2 has potential tumor suppressor properties and when inactivated leads to impairment of TP53 function in HBV related tumors (72). Exome sequencing of HCC lead to the identification of 161 potential driver mutations, which are associated with 11 pathways that are altered in HCC (73).

A recent publication from our laboratory focused on identifying CNVs of a small size unlike other recent studies, which focused on large CNVs (74). The rationale is that important small CNVs would be missed in a study that only detects large CNVs, which would be likely to have many genes in each CNV. This would make it difficult to determine which genes in the

CNV are promoting hepatocarcinogenesis. In our study, LSP1 was the most frequent CNV detected in HCC (51 out of 98 human HCCs sampled). All of the CNVs (5 amplifications and 46 deletions) affected the C-terminal region of the gene, which contains the F-actin binding domain of LSP1 (Figure 3). Deletions of LSP1 along with *KIAA1217* were associated with larger tumor size in comparison to tumors lacking these deletions. LSP1 has not been studied in liver biology and therefore no known role for LSP1 in liver exists. Since greater than 50% of tumors have CNV in the LSP1 gene it is important to determine if LSP1 plays a role in normal hepatocellular function as well as in carcinogenesis (74).

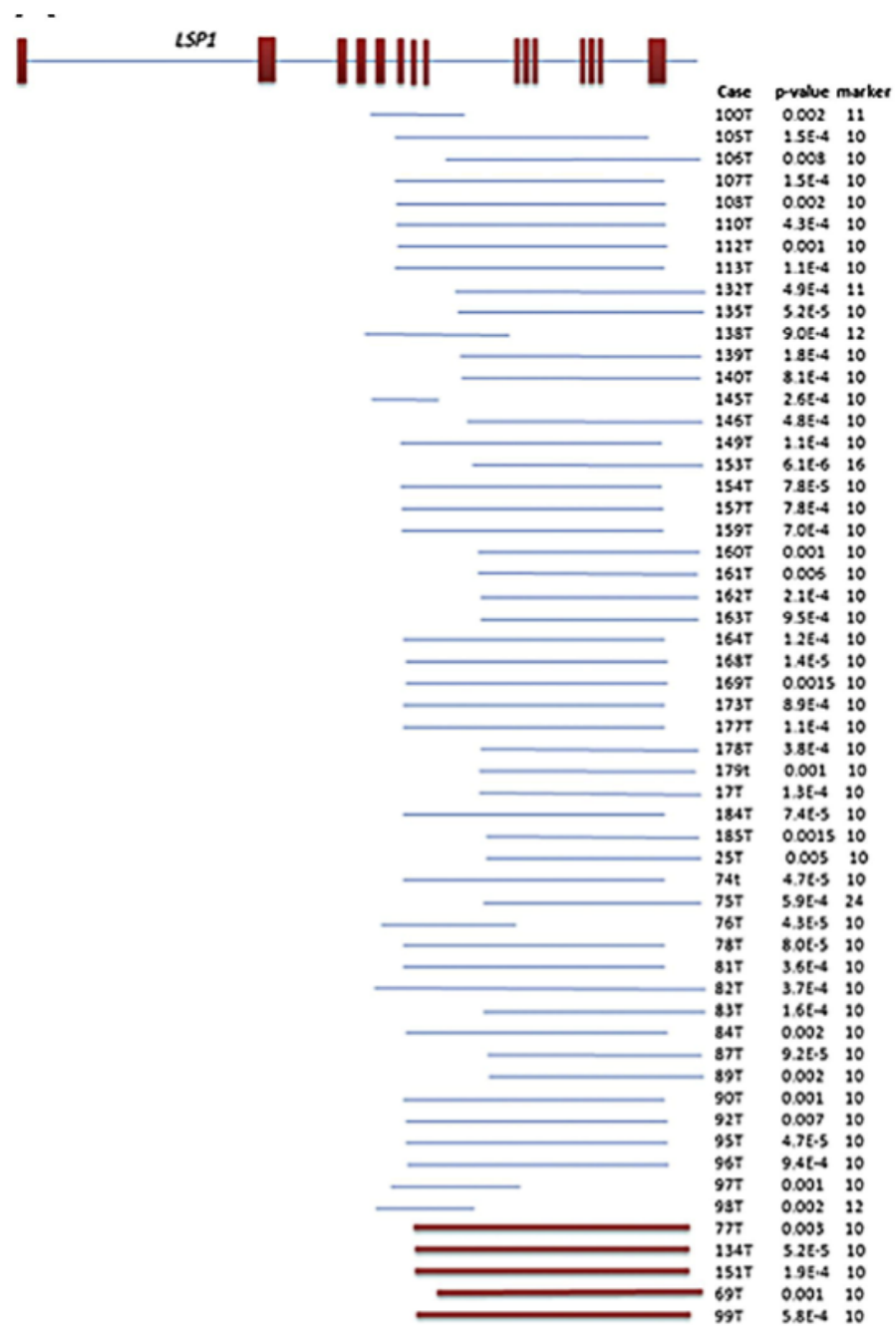


Figure 3. Genomic mapping of LSP1 deletions (blue) and amplifications (red). Vertical Bars represent exons and horizontal bars represent introns. The minimal number of markers utilized for detection is indicated as well as p values. All LSP1 CNVs affect the C-terminal region of the gene. Adapted from (71)

## 1.4 LEUKOCYTE SPECIFIC PROTEIN-1

### 1.4.1 Structure, expression and basic functions of LSP1

Leukocyte specific protein-1 (LSP1), an F-actin binding protein, is expressed in lymphocytes as well as macrophages, neutrophils and endothelial cells (75). LSP1, a 339 and 330 amino acid protein in humans and mice, respectively, is composed of two distinct domains, the acidic N-terminal region, which contains two putative calcium EF hand motifs, and the basic C-terminal region, which contains the F-actin binding region of the protein as well as serine and threonine phosphorylation sites. These sites are phosphorylated by MAPKAP2 (MK2) at serines 195 and 243 and protein kinase C (PKC) at serines 202 and 283 of the mouse LSP1 (Figure 4) (75, 76). The LSP1 c-terminal region also binds to PKC $\beta$ I, targeting it and the ERK/MAPK pathway to the cytoskeleton. LSP1 binds to F-actin between amino acid residues 300-330 with a high affinity ( $K_d= 0.2\mu\text{M}$ ) (77). LSP1 does not play a role in actin polymerization kinetics nor does it directly bind to G-actin but it does facilitate bundle formation from polymerized F-actin filaments (76).

LSP1 protein is highly conserved in humans and mice with 67% of the amino acid sequence identical. However, the majority of the identical sequences occur in the C-terminal region of the protein with 85% sequence homology whereas there is only a 53% homology between human and mouse LSP1 in the N-terminal region (2, (78).



LSP1 is found predominantly on the cytoplasmic side of the plasma membrane in lymphocytes but can also be found in the soluble cytoplasm and attached to the F-actin cytoskeleton during chemotaxis (80). During chemotaxis, LSP1 localizes with F-actin in filopodia, lamellipodia and membrane ruffles of the neutrophils. In endothelial cells, LSP1 is located mainly in the nucleus with low levels of the protein interacting with the F-actin cytoskeleton. LSP1 co-localizes to F-actin aggregates with anti-IgM induced B cell receptor caps in B cells (75).

#### **1.4.2 Role in leukocyte and endothelial biology**

The main function of LSP1 is regulating cellular migration and chemotaxis. LSP1 negatively regulates the migration of leukocytes and this regulation is dependent on the level of LSP1 interacting with F-actin. High levels of LSP1 bound to F-actin microfilaments leads to decreased leukocyte movement. Utilizing a LSP1 knockout mouse model, two different models of inflammation were induced; the first involved injection of thioglycollate into the peritoneum and the second involved injection of zymosan into the knee joint. Loss of LSP1 lead to increased numbers of leukocytes migrating to the site of inflammation in the LSP1 deficient mice in comparison to wild type controls (81). Neutrophils from a patient with neutrophil actin dysfunction syndrome (NAD47/89), which express high levels of LSP1 in their neutrophils, displayed decreased motility in vitro (82, 83). Patients with NAD47/89 experience frequent severe infections due to neutrophils exhibiting impaired actin polymerization, chemotaxis induced by fMLP and capacity to kill bacteria (84). Expression of LSP1 in an LSP1 deficient melanoma and U937 monocyte cell lines also led to decreased motility and the formation of F-actin bundle enriched hair like structures. The negative effect of LSP1 on U937 cell motility was

only observed in cells expressing LSP1 levels similar to that of neutrophils. Expression of lower levels of LSP1 actually led to increased migration in U937 cells in comparison to control cells (82, 85). LSP1 is a negative regulator of leukocyte migration and its role in cellular motility is dependent on the level of LSP1 interacting with F-actin.

The data on the role of LSP1 in leukocyte chemotaxis is conflicting. One group found that LSP1 deficient neutrophils displayed impaired chemotaxis in comparison to controls, which contradicts the previous findings that LSP1 negatively regulates leukocyte migration and chemotaxis (86). However, the role of LSP1 in migration is highly dependent on the type of integrin involved. Chemotaxis assays were performed with LSP1  $-/-$  neutrophils on two different substrates, fibrinogen or fibronectin, in which loss of LSP1 only accelerated migration on fibrinogen. These results demonstrate that the role LSP1 plays in negatively regulating migration and chemotaxis is likely through adhesion to specific integrins such as Mac-1 (87). Studies have shown the integrin Mac-1 is negatively regulated by LSP1 and that through inhibition of Mac-1, LSP1 also inhibits superoxide production in neutrophils induced with thioglycollate (86, 88). LSP1 both negatively and positively affects the chemotaxis of neutrophils depending on the integrins involved and the substrate on which the cells are migrating.

In addition to its role in migration and chemotaxis, LSP1 functions as a positive regulator of B cell antigen receptor (BCR) induced apoptosis. Upon stimulation with IgM, LSP1 co-localizes with membrane IgM in B cells. Treatment of B cells with anti-immunoglobulin antibodies imitates the high affinity binding of cross-linking antigens to the BCR, which leads to arrest of growth in late G<sub>1</sub> phase of the cell cycle and apoptosis. To demonstrate a role for LSP1 in BCR mediated apoptosis, normal immature B cells were isolated from LSP1 knockout mice as well as WT mice and treated with lipopolysacchride, which results in cells enriched for an

IgM<sup>high</sup> IgD<sup>low</sup> phenotype. These cells were treated with anti-immunoglobulin antibody to induce apoptosis. Loss of LSP1 expression lead to decreased anti-IgM induced apoptosis in comparison to wild type cells demonstrating that LSP1 is a pro-apoptotic protein in B cells (89). Additionally, expression of the C-terminal region of LSP1 (B-LSP1) in the LSP1 positive W10 B cell line leads to increased anti-IgM induced apoptosis because B-LSP1 inhibits translocation of PKC $\beta$ I to the plasma membrane. This causes inhibition of ERK2 (extracellular signal regulating kinase) activation, which contributes to increased anti-IgM induced apoptosis (90). Therefore, in addition to its role as a negative regulator of cellular motility, LSP1 also functions as a positive regulator of apoptosis in B cells.

In resting endothelial cells, LSP1 is predominantly expressed in the nucleus with lower levels of LSP1 co-localizing with the F-actin microfilaments. However, upon activation of the endothelium, LSP1 interacts with the F-actin cytoskeleton (91). In a LSP1 knockout mouse model, loss of LSP1 resulted in decreased permeability in the microvasculature in response to histamine (92). Utilizing a chimeric LSP1  $-/-$  model in which the endothelial cells lacked LSP1 expression and the leukocytes were wild type, neutrophil extravasation was inhibited in response to tumor necrosis factor  $\alpha$  (TNF $\alpha$ ) injection into the cremaster muscle (92). Endothelial LSP1 plays a role in the formation of endothelial domes, which are crucial for neutrophil transendothelial extravasation, in response to the neutrophil chemokine keratinocyte-derived chemokine (KC) (91). The ability of leukocytes to adhere to endothelial cells is also facilitated by endothelial LSP1. The adhesion of leukocytes to ICAM-1 expressed on the endothelium leads to phosphorylation and activation of LSP1 through the activation of p38 MAPK (93). LSP1 expressed in both endothelial cells and leukocytes facilitates the migration and extravasation of leukocytes to sites of inflammation.

### 1.4.3 Role in wound healing and fibrosis

Wound healing is a highly intricate process facilitated by a variety of cell types, growth factors, chemokines, and the extracellular matrix. Skin wound healing involves several stages, which include inflammation, cellular proliferation and migration, angiogenesis and formation of extracellular matrix (94). In the inflammation phase, neutrophils and macrophages are recruited to the site of injury. During the proliferation stage, tissue granulation and re-epithelialization occurs due to the migration and proliferation of keratinocytes, endothelial cells and fibroblasts. Finally in the remodeling stage of wound healing, proteolytic enzymes degrade excess collagen in the wound, which completes repair of the skin (94, 95).

Since LSP1 is expressed in leukocytes, which play an important role in inflammation and wound healing, the role of LSP1 in skin wound healing was assessed. Using a global LSP1 knockout mouse model, loss of LSP1 expression led to accelerated full thickness skin wound healing in comparison to wild type controls. There was a significant increase in the number of neutrophils, macrophages and fibrocytes recruited during the inflammatory stage to the wound in the LSP1 null mice. Re-epithelialization, synthesis of collagen, and angiogenesis were also enhanced in the LSP1 knockout mice, which correlates with the increase in inflammatory cells in the wound. Additionally, expression of macrophage derived chemokines, macrophage inflammatory proteins MIP-1 $\alpha$  and MIP-2 as well as monocyte chemoattractant protein-1 (MCP-1) and growth factors, vascular endothelial growth factor (VEGF) and transforming growth factor- $\beta$ I (TGF  $\beta$ I) were increased in the LSP1 null mice in comparison to wild type mice. Therefore, loss of LSP1 expression leads to increased skin wound healing due to the increased recruitment of leukocytes to the site of injury, which leads to elevated expression of chemokines and growth factors that promote healing (95).

The function of LSP1 in skin fibrosis was studied since inflammation plays a key role in both wound healing and fibrosis. During tissue repair, an inflammatory response occurs in which cytokines are produced and released from leukocytes at the site of injury. This stimulates fibroblast to become activated and proliferate. When this process becomes unregulated, the result is fibrosis, in which myofibroblasts secrete extracellular matrix (ECM) proteins and pro-inflammatory cytokines at the site of injury. The myofibroblasts are derived from resident fibroblasts, which are stimulated by pro-fibrotic growth factors, such as TGF- $\beta$ . To determine the role of LSP1 in skin fibrosis, LSP1 null mice were injected subcutaneously with bleomycin, which produces a dermal lesion similar to scleroderma. Lack of LSP1 expression led to a significant increase in skin fibrosis with increased recruitment of neutrophils, macrophages and fibrocytes as well as enhanced collagen synthesis and upregulation of growth factor and chemokine expression (96). Therefore, the function of LSP1 in the process of skin fibrosis is to regulate leukocyte recruitment to the site of injury leading to increased growth factor and chemokine production.

#### **1.4.4 LSP1 related signaling pathways**

In human neutrophils, MAPKAPkinase 2 (MK2), a target of p38 MAPK, phosphorylates LSP1 after treatment with fMLP, a chemotactic protein (97, 98). Inhibition of p38 MAPK activation in neutrophils leads to inhibition of both LSP1 and MK2 phosphorylation demonstrating that p38 MAPK is upstream of LSP1 and MK2 activation (99). Additionally, use of the PI3kinase (PI3K) inhibitor wortmannin leads to inhibition of p38 MAPK, MK2 and LSP1 activation revealing that PI3K is upstream of p38 MAPK in this pathway (98). In neutrophils, PI3K regulates the activation of p38MAPK, which phosphorylates MK2 followed by MK2 phosphorylating LSP1.

Additional evidence to demonstrate the role MK2 plays in LSP1 phosphorylation is that MK2  $-/-$  mice display a similar phenotype to LSP1  $-/-$  mice. In vitro, MK2  $-/-$  neutrophils induced by fMLP exhibited increased migration on fibrinogen, which recognizes the integrin Mac-1. In response to fMLP in vivo, loss of MK2 lead to increased migration of neutrophils into the peritoneum in comparison to wild type (100, 101). Therefore, LSP1 negatively regulates neutrophil migration and chemotaxis through its phosphorylation by MK2.

LSP1 is a target of protein kinase C (PKC) because treatment of cells with the phorbol ester, PMA, as well as diacylglycerol, which activates PKC, leads to increased phosphorylation of LSP1. However, in neutrophils treated with fMLP, Bim1, a PKC inhibitor, was not able to block phosphorylation of LSP1 indicating that PKC likely functions in regulating the p38MAPK/MK2 pathway induced by fMLP in these cells (98). Previous studies have demonstrated that LSP1 interacts with PKC $\beta$ I, which is required for activation of ERK2, but not PKC $\alpha$  or  $\beta$ II. PKC $\beta$ I activation of ERK2 acts to prevent anti-IgM induced apoptosis in B lymphoma cells (90). LSP1 and PKC $\beta$ I interact in a larger signaling complex, which contains kinase suppressor of Ras (KSR), an ERK scaffold protein, ERK2 and MEK1, which activates ERK. The role of LSP1 is to target this KSR/ERK complex to the actin cytoskeleton. Expression of a truncated LSP1, which contains the c-terminal region of the protein, blocks translocation of PKC $\beta$ I to the plasma membrane and activation of ERK2 in response to anti-IgM leading to increased apoptosis. Treatment of a B-lymphoma cell line with anti-IgM leads to activation of LSP1 associated MEK1 but this MEK1 activation is inhibited when the truncated LSP1 is expressed. This suggests that activation of MEK1 associated with LSP1 is dependent on PKC $\beta$ I activation (102). Therefore, in response to anti-IgM, LSP1 functions to target PKC $\beta$ I, KSR, MEK1 and ERK2 to the actin cytoskeleton facilitating PKC $\beta$ I activation of the ERK pathway.

The ERK/MAPkinase signaling pathway functions to transmit signals from extracellular stimuli at the plasma membrane to numerous downstream targets in both the nucleus and cytoplasm to induce a variety of cellular processes such as proliferation, migration and differentiation among others. ERK signaling is able to elicit cellular responses to different external stimuli through its targeting to the correct intracellular location. Activated ERK can translocate to the nucleus to phosphorylate transcription factors while a different group of ERK can phosphorylate cytoplasmic substrates (103). The MAP kinases ERK1 and ERK2 are activated and phosphorylated by the ERK/MAP kinase kinases (MAPK), MEK1 and MEK2, which are activated through phosphorylation by the MAP kinase kinase kinases (MAPKKKs) such as Raf. The ERK/MAPK pathway is activated by Ras and PKC through Raf-1 (104).

A scaffold protein that ensures ERK is targeted to the proper intracellular location is kinase suppressor of Ras (KSR), which binds directly to ERK and its upstream activator, MEK as well as LSP1 (105-108). KSR was identified in genetic screens of *Drosophila* and *C. elegans* for Ras related genes. KSR shares the most similarity with Raf kinases, however KSR and Ras differ in three major ways: first, KSR does not contain Ras binding domains; second, the N terminus contains a unique conserved region of ~40 amino acids, called Conserved Area 1 (CA1); and lastly instead of containing a lysine residue in the kinase subdomain II, which is critical for the phosphotransfer reaction, KSR has an arginine residue suggesting that KSR lacks kinase activity (105). KSR is localized to the cytoplasm in unstimulated cells but upon stimulation with growth factors, KSR translocates to the plasma membrane along with MEK and ERK (107, 109-111).

There is some controversy as to the function of KSR. Some previous studies have demonstrated that KSR blocks MEK1 activation, which reduces Ras induced NIH3T3 mouse

fibroblast transformation. Overexpression of KSR in chicken embryonic neuroretina (NR) cells inhibited Ras and B-raf induced proliferation but was unable to inhibit proliferation induced by constitutively active MEK1 indicating that KSR inhibits these cellular processes by blocking MEK1 activation (106). However, others have found that KSR, in a Ras dependent manner, acts to coordinate a RAF/MEK complex, which promotes phosphorylation of MEK and propagates the signal through the ERK/MAPK pathway (105, 112). This discrepancy in the function of KSR is thought to be due to the expression level of KSR. If there is excess KSR present in the cell due to transfection, this may lead to sequestration of components of the MEK/ERK pathway from each other preventing their activation (113). In dendritic cells, LSP1, along with KSR and CNK, modulate Raf-1 activation when mannose-expressing pathogens bind to the pattern recognition receptor, DC-SIGN (114). The function of KSR in modulating the ERK/MAPK pathway is controversial and appears to depend mainly on the level of KSR expression and the cell type involved.

## **2.0 LEUKOCYTE SPECIFIC PROTEIN-1 EXPRESSION IN HEPATOCYTES, DURING LIVER REGENERATION AND IN HEPATOCELLULAR CARCINOMA CELL LINES**

Portions of Chapter 2 are adapted from: **Kelly Koral, Shirish Paranjpe, William C. Bowen, Wendy Mars, Jianhua Luo, and George K. Michalopoulos. Leukocyte specific protein-1: a novel regulator of hepatocellular proliferation and migration deleted in human hepatocellular carcinoma. Hepatology. 2015 Feb 6;61(2):537-47.**

### **2.1 INTRODUCTION**

Hepatocellular carcinoma (HCC), the most common form of liver cancer, is characterized by high rates of mortality. The 5-year survival rate of individuals with HCC is relatively low at approximately 15%, which stems in part from the lack of effective treatment modalities. HCC is often resistant to current anticancer therapies and underlying diseases of the liver, such as cirrhosis, can limit the use of chemotherapeutic agents leading to increased lethality of HCC. An effective therapeutic alternative is surgical tumor resection; however this can only be implemented in patients with localized disease and liver transplant can only be performed in patients that meet strict criteria (44). Since there is only a basic understanding of the molecular,

cellular and environmental processes that lead to this disease and limited treatment options, additional studies must be conducted to gain a better understanding of the development and progression of HCC in order to develop novel therapeutic modalities to combat this lethal disease.

In a previous publication from our laboratory, copy number variation (CNV) analysis was performed on 98 human HCC samples. The results revealed a portion of the gene for leukocyte-specific protein (LSP1), an intracellular F-actin binding protein expressed in neutrophils, macrophages and endothelial cells, is deleted or amplified (in its carboxy-terminal F-actin binding site) in a majority of HCCs evaluated (51 of 98 cases) (74, 75). All of the deletions and amplifications of LSP1 affected the C-terminal F-actin binding region, indicating alteration of this portion of the LSP1 gene may play an important role in the development or progression of HCC (74). There are no previous reports defining a role for LSP1 in the liver or establishing the expression of LSP1 in normal liver cells. Therefore, given the very high frequency of LSP1 CNV in human HCC, the expression and function of LSP1 in normal hepatocytes should be fully elucidated.

Previous studies have demonstrated that mice deficient in LSP1 display accelerated skin wound healing and that LSP1 functions to negatively regulate migration of neutrophils (95). LSP1 acts as a scaffold through KSR for the extracellular signal-regulated kinase/mitogen activated protein kinase pathway (ERK/MAPK) and targets proteins of this pathway to the actin cytoskeleton (102). Signaling through the ERK/MAPK pathways leads to a variety of cellular processes including migration, proliferation, differentiation, and survival and is a key signaling pathway in the progression of proliferating hepatocytes through G1 phase of the cell cycle during

liver regeneration (115). LSP1 specifically binds to Kinase Suppressor of Ras (KSR), a key regulator of cellular growth due to its function as a scaffold for MAPK and Raf kinase (116, 117). Therefore, loss of LSP1 function may remove suppressing effects on KSR and ERK/MAPK signaling, leading to aberrant hepatocyte proliferation and facilitation of HCC development. In the present study, we demonstrate that LSP1 is expressed in cultured hepatocytes and after the termination of proliferation. Further, the rat hepatoma cell line JM1 expresses LSP1 protein, which, through co-immunoprecipitation analysis, interacts with KSR and F-actin in these cells. Loss of LSP1 expression in the hepatoma cell line leads to increased migration and proliferation, suggesting that LSP1 acts as a negative regulator for these processes. Expression of LSP1 by suitable expression vectors both in vitro (JM2 rat hepatoma cell line) leads to decreased proliferation. Therefore, loss of LSP1 expression and function could promote HCC development and metastasis (118).

## **2.2 EXPERIMENTAL METHODS**

### **2.2.1 Reagents and Antibodies**

Rabbit anti-LSP1 primary antibody was a generous gift from Dr. Jan Jongstra (University Health Network, Toronto, CA). Additional antibodies that were utilized for western blotting, immunofluorescence, immunohistochemistry and immunoprecipitation include cyclin D1 (Neomarkers), phospho-LSP1 (S252) (Abcam), F-actin (Abcam) KSR (Santa-Cruz), phosphoERK1/2 (tyr202/204) (Cell Signaling Technologies), and total ERK1/2 (Cell Signaling Technologies), HNF4 $\alpha$  (Santa Cruz), Proliferating cell nuclear antigen (PCNA) (Santa Cruz),

Ki67 (ThermoFisher), FITC-phalloidin (ThermoFisher) and  $\beta$ -actin (Sigma). GFP tagged rat LSP1 shRNA plasmid and control scrambled shRNA GFP plasmid were purchased from Origene (#TG702934). Rat LSP1 cDNA plasmid was purchased from Open Biosystems Dharmacon (#MRN1768-202784006) GenJet In Vitro DNA Transfection Reagent (Ver. II) was purchased from SignaGen Laboratories for transfection studies.

### **2.2.2 Rat hepatocyte isolation and cell culture**

Rat hepatocytes were isolated from normal male Fisher 344 rats using an adaptation of Seglen's calcium two-step collagenase perfusion technique described previously (119, 120). Isolated rat hepatocytes (300,000 cells/ml) were cultured on collagen-coated six well plates in hepatocyte growth medium supplemented with HGF (40ng/ml) and EGF (20ng/ml) (36, 121). Hepatocyte and NPC pellet were harvested along with hepatocytes cultured for 1, 3, 6, 8 and 10 days for protein and RNA analysis. Protein samples were collected in RIPA buffer and RNA samples were prepared using Trizol reagent (ThermoFisher).

### **2.2.3 Two-thirds partial hepatectomy of rat liver and isolation of rat hepatocytes after 2/3 partial hepatectomy**

Male Fisher 344 rats were subjected to 2/3 partial hepatectomy as previously described (11, 121). Briefly, rats were anesthetized using Nembutal (50mg/kg). Rats (n=3 for each time point) were sacrificed on days 1, 2, 3, 5, 7 and 10. Regenerating liver tissue was harvested at the various time points and either snap frozen for protein and RNA analysis, fixed in 10% formalin for paraffin embedding, and embedded into OCT media and frozen at -80°C for cryosectioning.

At various time points after PHx, livers were perfused using an adaptation of Seglen's calcium two-step collagenase perfusion techniques as previously described (119, 120). Hepatocyte and NPC pellets were collected for protein and RNA analysis on days 1, 2, 3, 5, and 7 after partial hepatectomy.

#### **2.2.4 JM1 and JM2 rat hepatoma cell culture**

JM1 and JM2 rat hepatoma cell lines (122) were cultured in Dulbecco's Modified Eagle's Medium (DMEM) supplemented with 10% fetal bovine serum (FBS) (Atlas) and gentamicin (1:1000) and maintained in an incubator at 37°C with 5% CO<sub>2</sub>.

#### **2.2.5 Immunofluorescence and confocal microscopy**

Frozen rat and mouse liver tissue after PHx were cut into 5-micron thick sections and fixed to glass slides. Tissue was fixed in 5% paraformaldehyde for 5 minutes and washed with PBS. Sections were blocked in 2% bovine serum albumin (BSA) for 45 minutes, washed in 0.5% BSA and incubated in primary antibody ( $\alpha$ LSP1 1:50) in 0.5% BSA for 1 hour. Following primary antibody incubation, the tissue was washed in BSA and Cy3 conjugated secondary antibody (1:1000) along with FITC-phalloidin (1:500) was added to the sections for 1 hour. Hoechst dye was used to stain the nuclei and gelvatol was used to fix the glass coverslips to the tissue. Slides were stored at 4°C and images were taken at the Center for Biologic Imaging at the University of Pittsburgh using an Olympus Fluoview II inverted confocal microscope at both high and low power oil immersion objectives for the rat liver tissue. The mouse liver tissue was co-stained

with LSP1 (1:50) and HNF4 $\alpha$  (1:50 (Santa Cruz)) and imaged using Olympus Provis inverted epi-fluorescence microscope in the Center for Biologic Imaging at the University of Pittsburgh.

### **2.2.6 Cytoskeleton enrichment of JM1 rat hepatoma cells**

JM1 cells were grown on collagen coated glass coverslips under normal growth medium conditions (DMEM +10% FBS+ gentamicin). After 48 hours in culture, the cells were washed in a stock solution of 100mM PIPES, pH6.9, 0.1mM EDTA, 0.5mM MgCl<sub>2</sub>, and 4M glycerol. Following the wash, the cytoskeleton was enriched using an extraction buffer which contained the stock solution with 0.75% Triton X-100 for 5 minutes at 37°C. After the extraction, the cells were washed and then fixed with fixation buffer (stock solution with 2% paraformaldehyde and 0.01% glutaraldehyde) for 1 hour. The coverslips were stored in PBS at 4°C until they were utilized for immunofluorescence. All solutions (wash, extraction, and fixation buffers) were kept at 37°C.

### **2.2.7 Immunohistochemistry**

Paraffin embedded liver tissue was sectioned into 5 $\mu$ m sections and stained with Ki67 proliferation marker (ThermoFisher) using the avidin-biotin-peroxidase complex technique (Vectastain ABC kit and DAB peroxidase substrate kit, Vector Laboratories). The sections were counterstained with hematoxylin. The stained tissue sections were imaged using Olympus Provis inverted microscope at 200x magnification. The percentage of Ki67 positive hepatocytes was quantified using ImageJ software in at least 10 random fields per tissue section.

### **2.2.8 Immunoprecipitation**

Five hundred micrograms of whole cell lysates from JM1 cells were prepared in RIPA buffer and diluted to a final volume of 500 $\mu$ l. Protein complexes were immunoprecipitated with 10 $\mu$ g of LSP1 (Santa Cruz), F-actin (Abcam), and KSR (Santa Cruz) antibodies overnight at 4°C with end-over-end mixing followed by incubation with protein A/G beads (Santa Cruz) overnight at 4°C. Complexes were centrifuged at 1,000xg for 5 minutes and washed three times in RIPA buffer before resuspension in 2x loading buffer and boiled at 95°C for 15 minutes. Immunoprecipitated protein complexes were separated by SDS-PAGE electrophoresis and transferred to Immobilon-P PVDF membranes (Millipore). Blots were probed with antibodies for total LSP1 using rabbit polyclonal serum (generous gift from Dr. Jan Jongstra), kinase suppressor of Ras (KSR) (Santa Cruz Biotechnology) and F-actin (Abcam). The membranes were processed with SuperSignal West Pico chemiluminescence substrate (Pierce, Rockford, IL) and exposed to X-ray film (Lab Product Sales, Rochester, NY).

### **2.2.9 Reverse Transcription and Polymerase Chain Reaction (PCR)**

RNA was obtained by homogenizing rat livers, hepatocytes and cell lines in Trizol<sup>®</sup> reagent (Invitrogen). RNA was DNase treated using the DNase free Kit from Ambion in order to remove any contaminating genomic DNA. Two micrograms of total DNase treated RNA from each sample was reverse transcribed into cDNA using Superscript reverse transcriptase (Invitrogen). PCR using primers specific for LSP1 (primers) and GAPDH (primers) was performed using Taq polymerase (Invitrogen) on a Thermo Hybaid PCR sprint thermal cycler (Thermo Scientific).

### **2.2.10 SDS PAGE and Western blot**

Whole cell protein lysates of liver tissue and cells were prepared using 1% sodium dodecyl sulfate (SDS) in RIPA buffer (10mM Na<sub>2</sub>HPO<sub>4</sub>, 10 mM NaH<sub>2</sub>PO<sub>4</sub>, 150 mM NaCl, 1% NP-40, protease inhibitor cocktail (P8340, Sigma), phosphatase inhibitor cocktail I and II (P2850 and P5726, Sigma), 0.26 mg/ml amiloride and 0.05 mg/ml AEBSF) and homogenized. Protein concentrations were determined using Bicinchoninic acid (BCA) assay (Pierce Chemical Co., Rockford, IL) and 30µg protein was loaded and separated on 10% SDS polyacrylamide gels and transferred to Immobilon-P membranes (Millipore, Bedford, MA). Following transfer, membranes were stained with Ponceau S to evaluate efficient loading and transfer of proteins. Blots were probed for 1 hour with primary and horseradish peroxidase (HRP) conjugated secondary antibodies separately in Tris-buffered saline (TBS) with Tween 20 containing 5% fish gelatin (Sigma, St. Louis, MO). The membranes were processed with SuperSignal West Pico chemiluminescence substrate (Pierce, Rockford, IL) and exposed to X-ray film (Lab Product Sales, Rochester, NY).

### **2.2.11 Statistical Analysis**

All statistical analyses and graphs were prepared on Excel software (Microsoft) utilizing the student t-test. Statistical significance was fixed to p values less than 0.05. Error bars on graphs represent +/- standard error of the mean (SEM). Densitometry of western blot images was analyzed using the National Institute's of Health ImageJ 4 software and protein loading was normalized to either the corresponding Ponceau S staining or β-actin western blots.

### **2.2.12 Approval of Animal Use**

All procedures performed on mice and rats were approved under University of Pittsburgh Institutional Animal Care and Use Committee (IACUC) protocols and conducted in accordance with the National Institute of Health animal care and use guidelines.

## **2.3 RESULTS**

### **2.3.1 LSP1 is expressed in primary hepatocytes in culture**

We demonstrate that LSP1 is expressed in primary rat hepatocytes in culture (Figure 5A and B). Expression of LSP1 protein is not seen in the hepatocyte pellet after isolation by collagenase perfusion or on day 1 in culture but begins to be expressed starting on day 3 in culture and expression steadily increases to day 10 in culture (Figure 5A and B). The peak of hepatocyte proliferation occurs between days 2 and 4 in culture with growth factors HGF and EGF and after day 4 in culture proliferation starts to decrease (Figure 6) (36). The correlation between LSP1 expression and decreased proliferation rates suggests that LSP1 is functioning at the termination stage of hepatocyte proliferation in culture. Utilizing RT-PCR we analyzed expression of the two LSP1 isoforms in primary rat hepatocytes in culture revealing that in the primary rat hepatocytes only isoform 1 is expressed while in the rat hepatoma cell lines both isoforms are expressed (Figure 7).

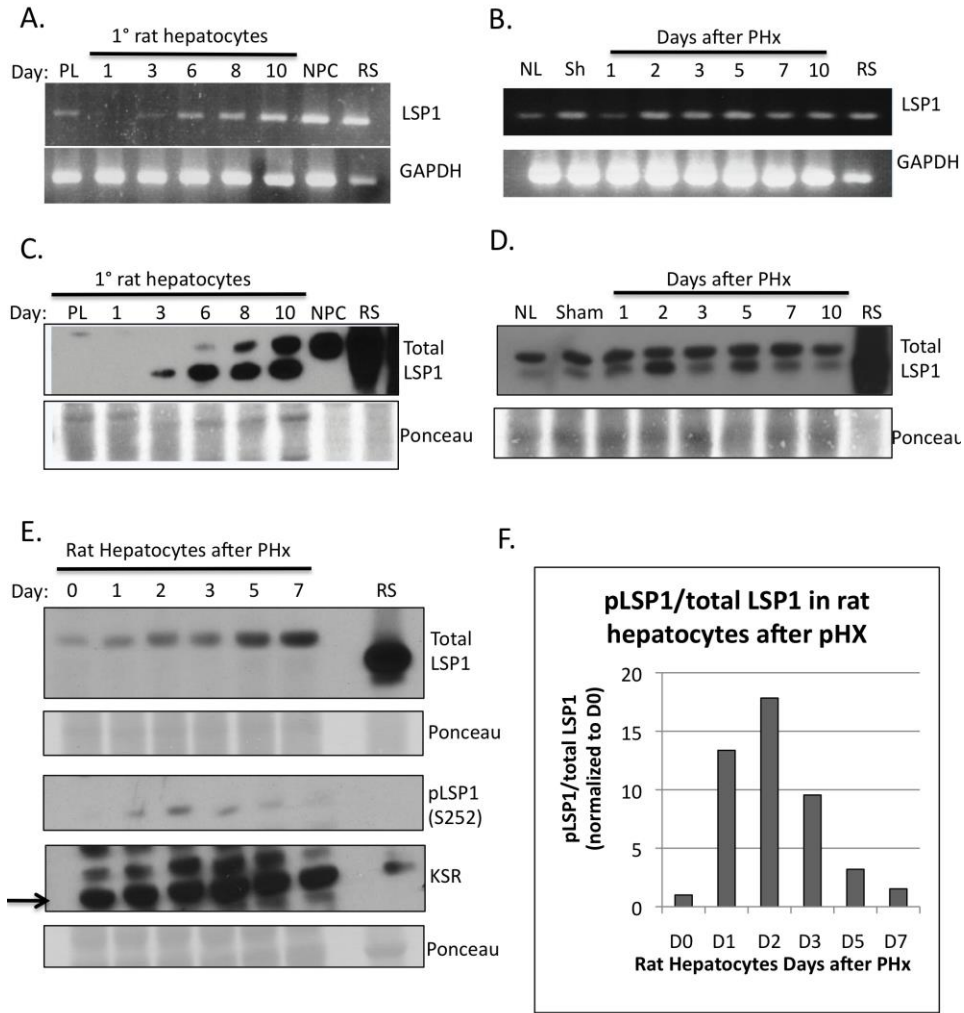


**Figure 5. LSP1 expression in primary rat hepatocytes in culture, rat liver and hepatocytes after PHx.** Primary rat hepatocytes were cultured in the presence of HGF and EGF and harvested for **A.** mRNA expression using semi-quantitative RT-PCR (upper panel, LSP1 and bottom panel GAPDH as loading control), and **B.** protein expression by western blot (upper panel, total LSP1, bottom panel, Ponceau S stain, loading control). PL: Hepatocyte Pellet; NPC: Non-parenchymal cell fraction; RS: Rat spleen, used as positive control. Whole rat liver was harvested after PHx and LSP1 expression was analyzed using **C.** RT-PCR (upper panel, LSP1, bottom panel GAPDH) and **D.** western blot of LSP1 (upper panel) and Ponceau S (bottom panel, loading control). NL: Normal whole liver lysate; RS: Rat spleen. Rat hepatocytes were isolated from liver after PHx by collagenase perfusion and analyzed by **E.** western blot for total LSP1 (upper panel), phosphoLSP1 (S252) (3rd panel down) and KSR (4th panel down). **F.** Quantification of phosphoLSP1 to total LSP1 in the rat hepatocytes after PHx.

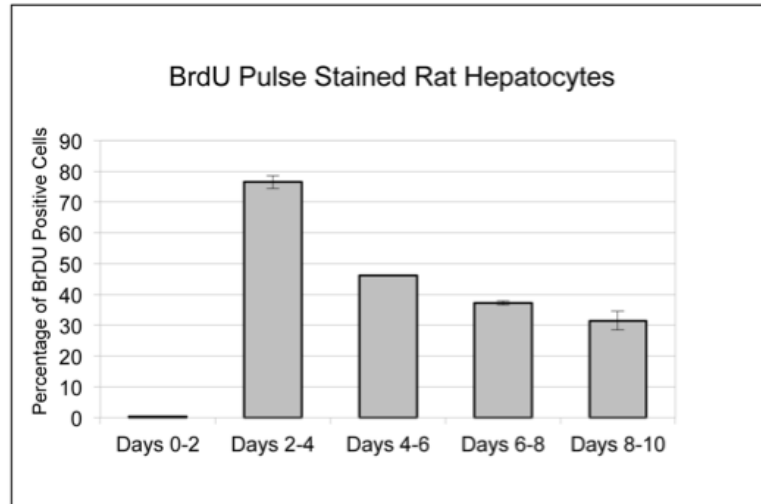


**Figure 6. Quantification of BrdU labeling in primary rat hepatocytes in culture.** Primary rat hepatocytes were pulsed with 2 $\mu$ l of concentrated BrdU solution in 1ml of complete growth media supplemented with HGF and EGF. Every two days, cells were fixed in 10% formalin and stained with BrdU antibody. Percentage of BrdU positive hepatocytes were quantified by counting cells in at least three random fields per well.

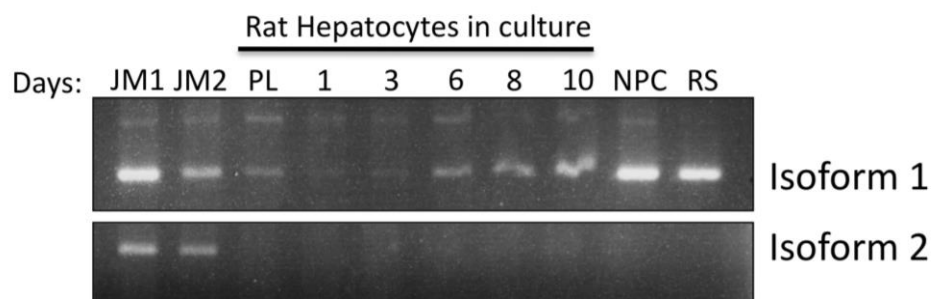


**Figure 7. RT-PCR of rat hepatocytes in culture and rat hepatoma cell lines for LSP1 isoforms.** Primers were designed for the two most common isoforms of LSP1. Top panel: Isoform 1. Bottom panel: Isoform 2.

### 2.3.2 LSP1 expression in liver regeneration

Next, we analyzed the expression of LSP1 during liver regeneration using the commonly utilized 2/3 partial hepatectomy (PHx) model (7, 12). LSP1 mRNA and protein expression was observed at low levels in whole lysates from normal resting liver and 1 day after PHx (Figure 5C and D), which corresponds to the peak of hepatocyte proliferation after PHx in the rat (7, 12). Increased LSP1 expression is observed by western blot and immunofluorescence on days 2 and 5 after PHx (Figure 5D and 8). Day 2 after PHx, hepatocyte proliferation in the rat is decreased (7, 12) and this corresponds with the increased LSP1 expression, which suggests that LSP1 may play a role in the termination of proliferation *in vivo* during regeneration. Since LSP1 expression was measured in whole liver after PHx, we are unable to determine which specific cell types of the liver are contributing to the signal. This is because LSP1 is heavily expressed in the non-parenchymal hepatic cell populations (see NPC in Fig. 5B). Therefore, we isolated rat hepatocytes from PHx livers by collagenase perfusion at various time points after PHx and measured LSP1 expression. Western blot analysis for total LSP1 revealed that LSP1 is expressed at low levels at time 0 but steadily increases until day 7 (Figure 5E). The percentage of hepatocytes in comparison to NPCs after perfusion was not determined therefore it is possible that some of the LSP1 expression detected is due to the presence of NPCs. Analysis of phospho-LSP1 levels indicates a peak of expression at day 2 after PHx in the hepatocytes (Figure 5E and F). Upon phosphorylation of LSP1 at serine 252, LSP1 localizes to the F-actin filaments (75) which corresponds to the co-localization of F-actin and LSP1 observed in rat liver after PHx (Figure 8 and 9). Western blot analysis of total LSP1 in isolated NPCs after PHx showed a marked increase in expression on day 3 after PHx (Figure 10).

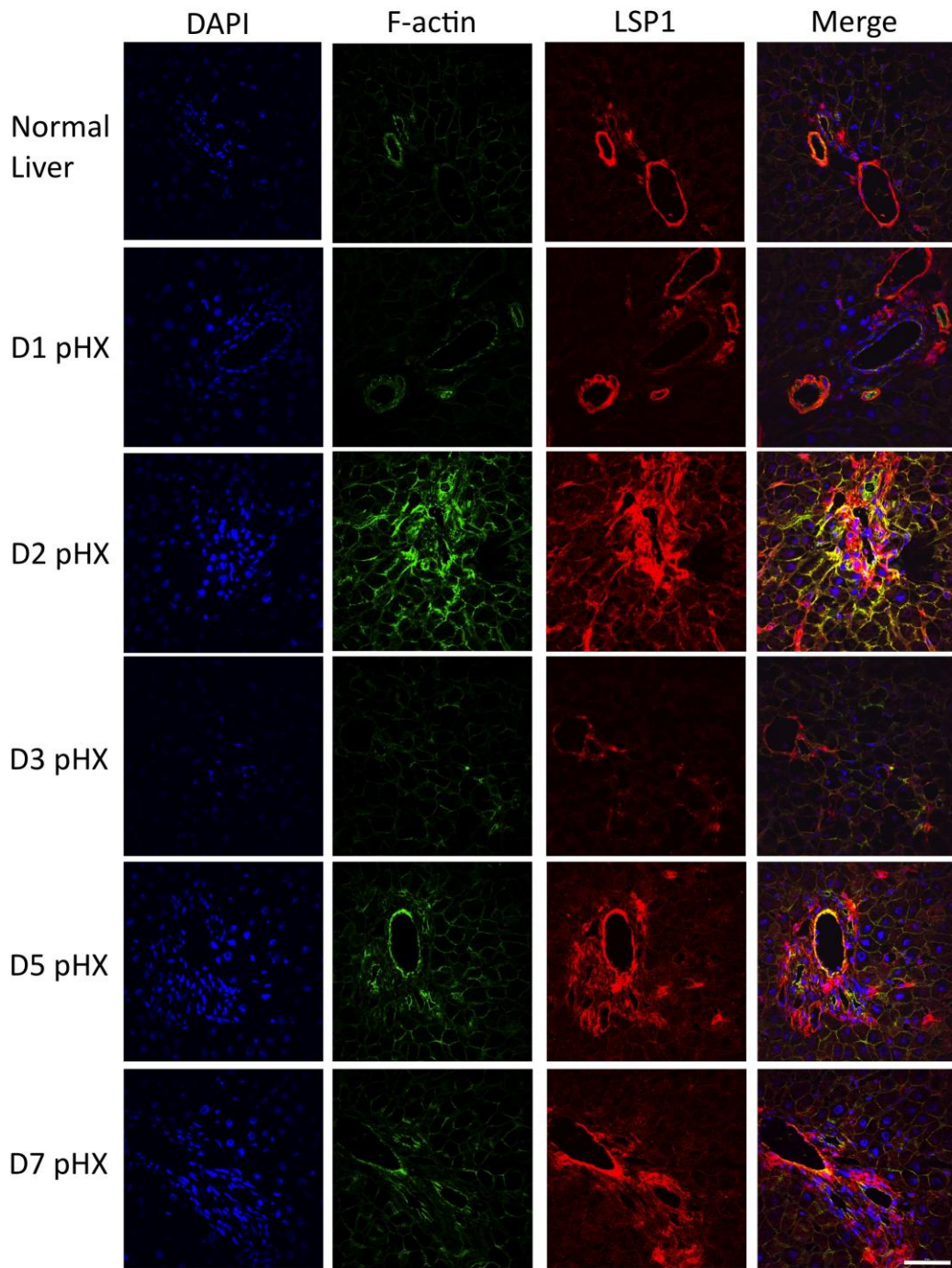


Figure 8. Immunofluorescence of LSP1 and F-actin in rat liver after PHx. Rat liver was harvested at various time points after PHx and was probed for LSP1 and F-actin. First panel is DAPI to stain the nuclei, second panel shows the F-actin signal, third panel shows the signal for total LSP1 and the last panel displays a merge of the DAPI, F-actin, and total LSP1 signals. 600x magnification. Scale bar =50µm

Since LSP1 is an F-actin binding protein in hematopoietic cells, we utilized immunofluorescence to determine if LSP1 and F-actin co-localize in hepatocytes during liver regeneration. LSP1 and F-actin do co-localize at day 2 after PHx as indicated by the yellow signal observed in the merged images and this co-localization appears to be hepatocellular, since the size, shape and morphological characteristics of the LSP1 positive cells is consistent with hepatocytes (Figure 8 and 9). It is possible that the LSP1 expression observed is due to cells surrounding the hepatocytes such as stellate cells. This possibility could be tested by performing IF with stellate cell markers such as GFAP or desmin along with LSP1 staining and measuring co-localization. Strong expression of LSP1 in the vascular endothelium and portal mesenchyme (Figure 8) is expected since previous literature has demonstrated LSP1 expression in endothelial and mesenchymal cells (79, 92).

LSP1 has been shown to interact with Kinase Suppressor of Ras (KSR), an ERK/MAPK pathway scaffold, and target these proteins to the actin cytoskeleton (102). Therefore, we also measured the expression of KSR in the isolated rat hepatocytes after PHx. KSR expression is observed in normal resting hepatocytes and it slightly increases towards the end of regeneration (Figure 5E).

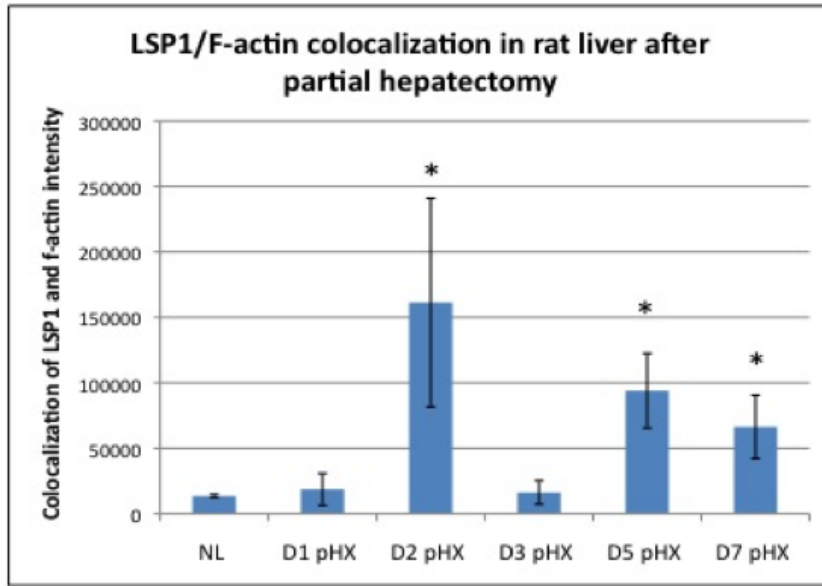


Figure 9. Quantification of LSP1 and f-actin immunofluorescence co-localization in rat liver after partial hepatectomy. Co-localization intensity was quantified from at least three independent fields using Metamorph software. Representative IF images are shown in figure 8.

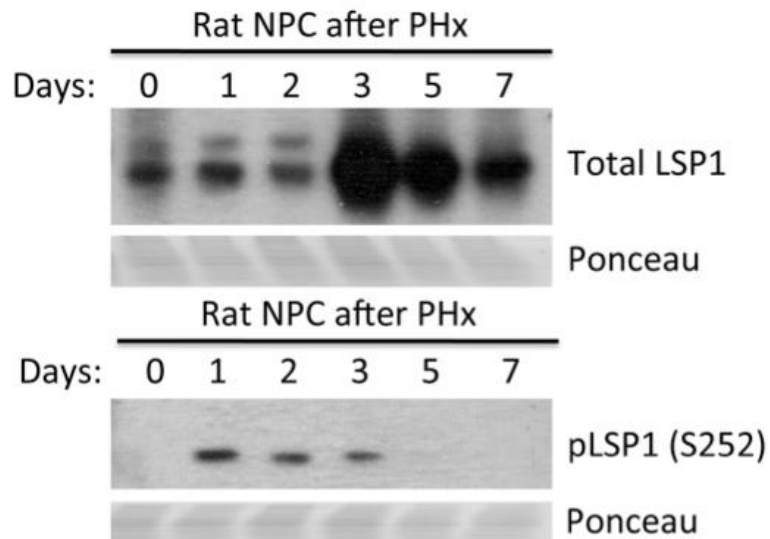
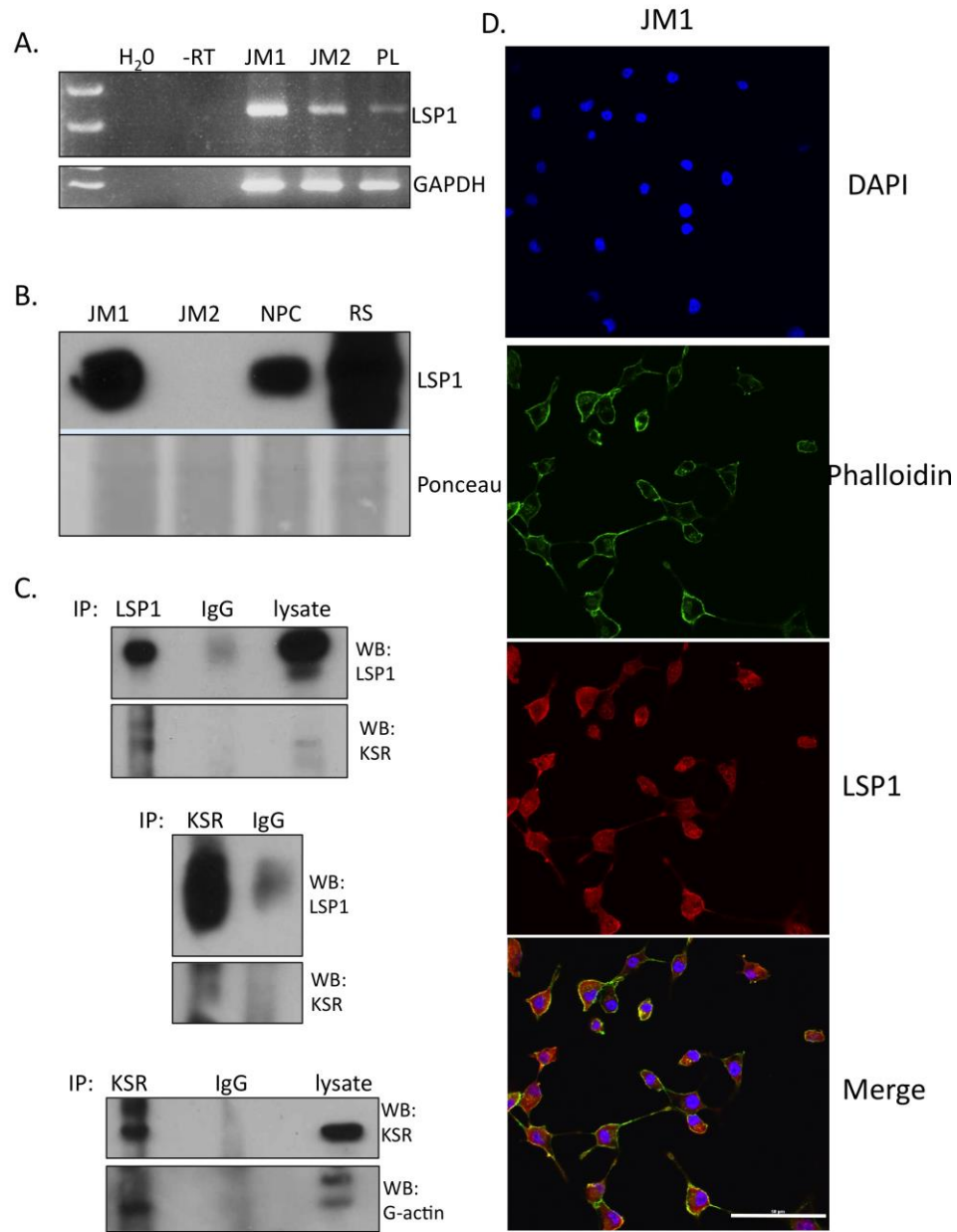


Figure 10. Total and phospho LSP1 expression in rat non-parenchymal cells (NPC) after PHx. Western blot analysis of total LSP1 expression (top panel) and phosphoLSP1 expression (3rd panel) in rat NPC after PHx. Ponceau S stain (loading control).

### **2.3.3 LSP1 expression in hepatoma cell lines and interactions with ERK/MAPK scaffold Kinase Suppressor of Ras (KSR)**

Expression of LSP1 was measured in two rat hepatoma cell lines, JM1 and JM2 (122). JM1 and JM2 cells exhibit different morphological and functional characteristics. Both JM1 and JM2 cells expressed LSP1 mRNA but only JM1 cell line expressed LSP1 protein (Figure 11A and B). Immunofluorescence images demonstrate that LSP1 co-localizes with F-actin in the JM1 cell line as well (Figure 11D). Since the LSP1 immunofluorescence signal in the cytoplasm of the JM1 cells is very strong it is possible that the co-localization with F-actin is an artifact. Therefore, we isolated the cytoskeleton of the JM1 cells and performed immunofluorescence on these extracts, which removes the high LSP1 signal from the cytoplasm. The results demonstrate that LSP1 and F-actin cytoskeleton do co-localize in the JM1 rat hepatoma cells (Figure 12). Next, we utilized co-immunoprecipitation to determine if LSP1 interacts with KSR and G-actin in the JM1 cell line. The results indicate that LSP1 does interact with KSR and KSR interacts with G-actin in these cells (Figure 11C). These findings demonstrate that LSP1 is expressed in a rat hepatoma cell line and targets the ERK/MAPK scaffold KSR to F-actin filaments.



**Figure 11. LSP1 expression in rat hepatoma cell lines and analysis of LSP1, KSR and F-actin interactions. JM1 and JM2 cells were analyzed for expression of LSP1 A. mRNA by RT-PCR and B. protein by western blotting. C. Co-immunoprecipitation analysis on the JM1 cell line for interactions between LSP1, KSR and G-actin. Upper panel: IP of LSP1 and western blot of LSP1 (top) and KSR (bottom). Middle panel: IP of KSR and western blot of LSP1 (top) and KSR (bottom). Bottom panel: IP of KSR and western blot of KSR (top) and F-actin (bottom). D. IF images of JM1 cells for DAPI (top panel), Phalloidin (2nd panel), LSP1 (3rd panel), and merge (bottom panel). Images were taken at 400x magnification. Scale bar = 50 $\mu$ m**

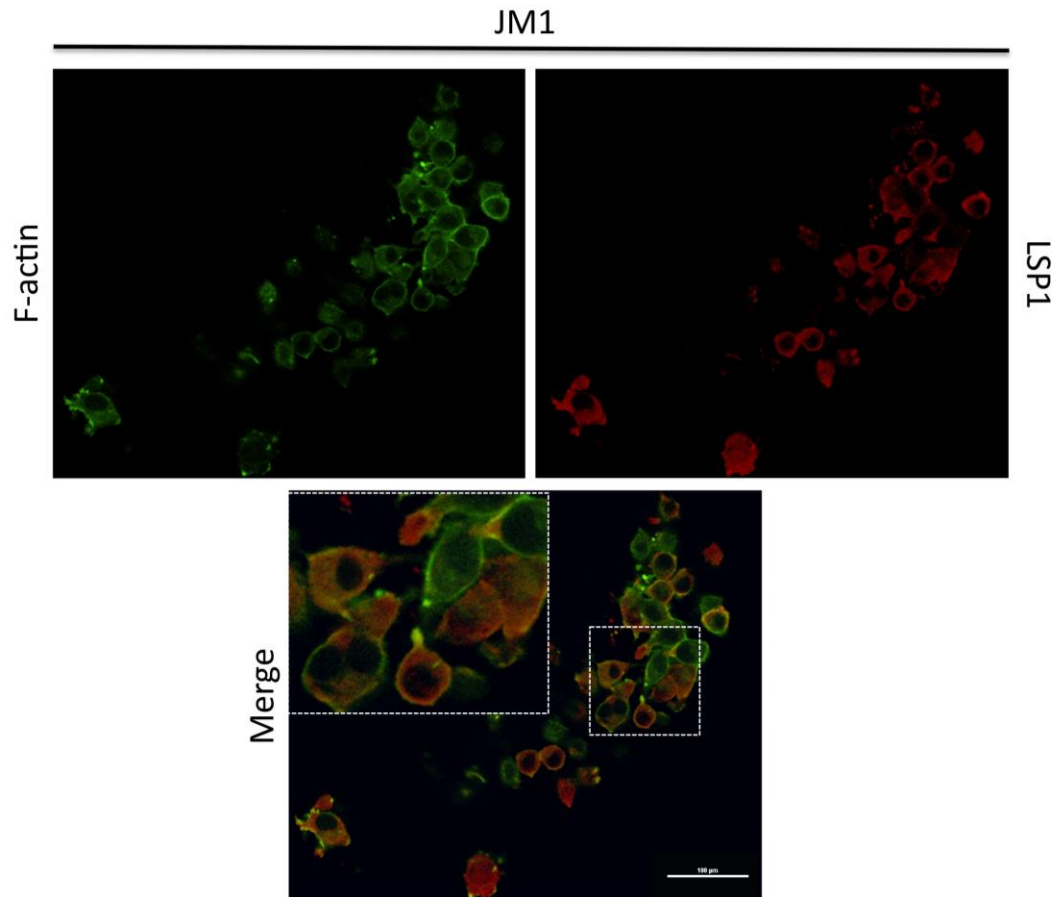


**Figure 12.** LSP1 and f-actin immunofluorescence in cytoskeletal extracts of JM1 rat hepatoma cells. Phalloidin (green, top left), LSP1 (red, top right), and merge (bottom) immunofluorescence images of cytoskeleton that has been extracted from JM1 rat hepatoma cells. Scale bar = 100 $\mu$ m.

## 2.4 DISCUSSION

A previous study from our laboratory demonstrated that in human HCC, LSP1 CNV was found in the highest number of cases (74); however the expression and functional role of LSP1 in both normal liver and HCC is unknown. The finding arrived as a surprise since there is no literature on LSP1 in hepatic biology. In order to place the role of LSP1 in the perspective of normal liver biology, and thus get a framework for understanding its role in hepatic neoplasia, we embarked upon the studies described above, to provide a baseline of LSP1 functions in normal liver and obtain evidence from experimental models as to its functional significance. As a first step in this study, we aimed to determine if LSP1 is expressed in liver, specifically in the hepatocytes, and the role LSP1 plays in hepatocyte growth regulation. LSP1 is intensely expressed in endothelial cells and cells of hematopoietic origin. Thus, studies of LSP1 in whole liver tissue are not likely to be informative since hepatocyte expression of LSP1 is likely to be overwhelmed by the intense expression of LSP1 in hepatic macrophages and endothelial cells. Because of this, we concentrated our studies in hepatocytes in primary culture or in hepatocytes isolated by collagenase perfusion at different stages of regeneration. Our results indicate that LSP1 expression is not observed in normal hepatocytes until day 3 in culture and expression increases over time. Since hepatocytes in culture experience the peak of proliferation between days 2-4 and the highest level of LSP1 expression is observed on day 10, it is reasonable to conclude that LSP1 may be associated with a termination signal for hepatocyte proliferation (36). Analysis of LSP1 expression during liver regeneration demonstrates that the peak of expression occurs on day 7 (Fig. 5E) providing further support for the role of LSP1 as associated with inhibition of hepatocyte growth (7, 12). Measurement of phosphoLSP1 in regenerating hepatocytes also reveals increased expression on day 2 after PHx. Phosphorylation of LSP1 at serine 252

corresponds with increased binding to the F-actin filaments, which was detected in both hepatocytes (day 2) and NPCs (days 1-3).

Our findings revealed changes in LSP1 expression and association with its binding targets (F-actin filaments) during rat liver regeneration. Immunofluorescence analysis shows that LSP1 co-localizes with hepatocyte F-actin on day 2 following PH, which suggests that the ability of LSP1 to bind to the actin filaments may be vital for its role in controlling proliferation. In the CNV study of HCC, all of the amplifications and deletions of LSP1 affected the C-terminal region of the gene, which encodes for the F-actin binding elements of LSP1 (74). We have assumed that amplification of the C-terminal portion of LSP1 may create a situation of a dominant negative protein containing only the C-terminal, which may interfere with the binding of the complete protein. This further supports the role of LSP1 in terminating proliferation and that loss of its ability to bind to F-actin by deletion of c-terminal region could lead to aberrant hepatocyte cell division, leading to or enhancing carcinogenesis.

Since LSP1 CNV was discovered in human HCC and our experimental studies were carried out in the rat, we measured the expression of LSP1 in two distinct rat hepatoma cell lines, JM1 and JM2 (122). JM1 cells expressed LSP1 RNA and protein as demonstrated by RT-PCR, western blot and immunofluorescence. To demonstrate how LSP1 functions in these cells, co-immunoprecipitation and immunofluorescence displayed that LSP1 interacts and co-localizes with F-actin and the ERK/MAPK pathway scaffold KSR, respectively. KSR functions by targeting MEK1 and ERK2 to the actin cytoskeleton. In unstimulated cells, this complex is mainly localized to the cytoplasm. Upon growth factor stimulation, KSR translocates to the plasma membrane thereby targeting ERK2 and its direct activator MEK1 to the plasma membrane (102, 117). KSR functions to both potentiate and attenuate ERK cascade activation thereby regulating

the intensity and duration of ERK pathway signaling from the plasma membrane during growth factor stimulation. The ERK/MAPkinase pathway transmits signals from the plasma membrane to a plethora of cytoplasmic and nuclear targets that affect downstream functions such as proliferation, differentiation and survival. Scaffolding proteins, such as LSP1 and KSR, target the ERK cascade to the appropriate intracellular location, which ensures the correct response of the ERK pathway to various extracellular signals (117). Therefore, in HCC, if LSP1 functions as a growth suppressor and there is a loss of LSP1 expression, this could affect the ERK/MAPK pathway leading to aberrant proliferation or migration.

The literature documents the presence of several isoforms for LSP1 in different cell types as a result of alternative splicing (123). As shown in Fig. 5D, there are two protein isoforms in whole liver homogenates. We also noticed that Fig. 5E demonstrates that hepatocytes express only the higher molecular weight isoform. However, only the lower molecular weight mRNA is expressed in hepatocytes in Fig. 7. The significance of this is not clear. There are multiple isoforms described for LSP1 in the literature (79, 123) and the importance of this should be further investigated.

### **3.0 LEUKOCYTE SPECIFIC PROTEIN-1 REGULATES HEPATOCELLULAR MIGRATION AND PROLIFERATION IN VITRO AND IN VIVO**

Portions of Chapter 3 are adapted from: **Kelly Koral, Shirish Paranjpe, William C. Bowen, Wendy Mars, Jianhua Luo, and George K. Michalopoulos. Leukocyte specific protein-1: a novel regulator of hepatocellular proliferation and migration deleted in human hepatocellular carcinoma. Hepatology. 2015 Feb 6;61(2):537-47.**

#### **3.1 INTRODUCTION**

In chapter 2, we demonstrated that LSP1 is expressed in primary hepatocyte cultures as well as during liver regeneration after partial hepatectomy. Our results also showed a role for LSP1 in the migration and proliferation of hepatoma cell lines in vitro. In chapter 3, we will explore the role of LSP1 in vivo during liver regeneration and provide evidence demonstrating that expression of LSP1, either through hydrodynamic tail vein injection of plasmid DNA or in a transgenic mouse model, will significantly decrease proliferation and ERK activation after partial hepatectomy and, loss of LSP1 expression will cause an increase in ERK phosphorylation as well as hepatocellular proliferation during regeneration. Perfusion of both knockout and transgenic LSP1 mouse livers and culture of hepatocytes will further validate the role of LSP1 in hepatocellular proliferation as well as migration.

## 3.2 EXPERIMENTAL METHODS

### 3.2.1 Transfection of JM1 cells and creation of stable cell lines

JM1 cells were transfected with either GFP-LSP1 shRNA plasmid (Origene, #TG702934) or scrambled shRNA plasmid (Origene) for a control at ~85% confluency in 6 well plates using lipofectamine 2000 (Invitrogen). Briefly, following the manufacturer's protocol, the cells were transfected with 4 $\mu$ g of plasmid DNA in serum free DMEM overnight. Serum free media was replaced with DMEM containing 10% FBS and 72 hours post transfection, the cells were trypsinized and plated in a 10mm dish and treated with 10 $\mu$ g/ml puromycin (Sigma) for the selection of stably transfected cells. Stable clones were screened for the expression of GFP by fluorescence microscopy and only clones expressing GFP were isolated and maintained in the presence of 10 $\mu$ g/ml puromycin.

JM2 cells were transiently transfected with either pExpress-1 vector alone (control) or rat LSP1 cDNA (Dharmacon #MRN1768-202784006) using GenJet In Vitro DNA Transfection Reagent (Ver. II) (SignaGen Laboratories) at 80% confluency in 6 well plates. The cells were transfected with 4 $\mu$ g of plasmid DNA complexed with 8 $\mu$ l of transfection reagent in DMEM supplemented with 10% FBS. Cells were incubated with transfection complexes for 8 hours before the medium was changed and further experimental procedures were performed including BrdU assay and protein isolation at 24 hours post transfection.

### **3.2.2 MTT and Bromodeoxyuridine (BrdU) assays**

For the MTT assay, JM1 stable cells (LSP1 shRNA and scrambled control cell lines) were plated at  $1 \times 10^5$  cells/well in 2- 6 well plates and cultured in DMEM + 10% serum. At approximately 50% confluency, the media in both plates was changed to serum free media. Baseline MTT values were measured at 24 hours after addition of serum free medium. Proliferation was stimulated with 10% FBS in DMEM and absorbance measured after 24 h. MTT absorbance after 24 h was normalized to the baseline measurements.

For BrdU assay, transiently transfected JM2 cells were treated with 2 $\mu$ l of bromodeoxyuridine (BrdU) 8 hours after transfection in DMEM with 10% FBS. At 24 hours post transfection, the cells were fixed in 10% formalin and stained using an antibody against BrdU (Invitrogen) using standard immunohistochemical techniques. Images were taken of the stained cells using Provis Fluoview Microscope and quantified using Image J software.

### **3.2.3 Scratch and Transwell migration assays**

For the scratch assay, cells were plated at  $2 \times 10^5$  cells/well in a 6 well plate and cultured in DMEM + 10% FBS until confluent. Upon confluency, a scratch was made in the monolayer using a 10 $\mu$ l pipette tip and the cells were washed in DMEM to remove unattached cells. An image was taken using an inverted fluorescence microscope at the time of the scratch (time 0) and 24 hours post scratch. Live cell imaging was also performed on the scratch assay cultures. At the time of the scratch, the 6 well plate was placed in the incubation chamber of the live cell-imaging microscope and images were taken of each scratch every 2 hours for 24 hours.

For the transwell assay, cells were seeded at  $1 \times 10^5$  cells per transwell insert in serum free medium. The bottom chamber of the well contained DMEM with 10% serum. Cells were allowed to migrate for 24 hours at 37°C. After 24 hours, the cells that migrated to the bottom of the transwell membrane were fixed in 4% paraformaldehyde and stained with a 0.1% Coomassie blue/ 10% methanol/ 10% acetic acid solution. Cells that did not migrate through the membrane were carefully removed using a cotton tipped applicator. The membranes were imaged using an Olympus Provis inverted microscope and the cells of at least three fields per membrane were counted using Image J software.

#### **3.2.4 Hydrodynamic injection of LSP1 plasmid DNA and 2/3 PHx**

Male FVB mice (4 month old) were subjected to a hydrodynamic tail vein injection of either pExpress-1 control plasmid (n=5) or rat LSP1 cDNA plasmid (n=3) (Open Biosystems Dharmacon). Briefly, 20 µg of endotoxin free plasmid DNA was diluted in 2ml of 0.9% sterile endotoxin free saline solution. The DNA/ saline solution was injected through the tail vein in 7 seconds. Following a three-hour recovery period, the mice were subjected to a 2/3 partial hepatectomy, as previously described (43). The livers were harvested 42 hours post hepatectomy and the tissue was processed for paraffin embedding, frozen OCT embedding and protein isolation. All procedures performed on mice and rats were approved under IACUC protocols and conducted in accordance with the National Institute of Health animal care and use guidelines.

### **3.2.5 LSP1 knockout mouse model**

LSP1 global knockout mice were created by Dr. Jenny Jongstra-Bilen on a 129/SvJ background as previously described (81) and were obtained from Dr. Lixin Liu from the University of Saskatchewan. Since the mouse LSP1 gene encodes 2 different tissue specific isoforms, LSP1 and S37, with the only difference between the two isoforms being a unique amino terminus due to alternative splicing, only the LSP1 specific exon 1 was targeted to prevent embryonic lethality due to the importance of S37 in mouse development. Therefore, the LSP1 isoform is absent in all tissues of these mice leaving the S37 expression intact globally (81). The LSP1 KO mice along with the 129/SvJ WT mice were utilized for PHx studies as well as hepatocyte cultures.

### **3.2.6 Creation of hepatocyte specific LSP1 transgenic mouse model**

Hepatocyte specific LSP1 transgenic mice were created in conjunction with Dr. Kyle Orwig at the Magee Women's Research Institute Transgenic and Molecular Research Core Facility on a C57/BL6 background. Mouse LSP1 cDNA was cloned into the BamHI sites of a plasmid containing an albumin promoter and alpha-fetoprotein enhancer to ensure expression of LSP1 in hepatocytes only since the albumin promoter is only active in the hepatocytes. The transgenic mice were created using the pronuclear injection technique in which the LSP1- albumin promoter plasmid DNA is injected into donor zygotes, which are implanted into pseudopregnant female mice. The offspring were screened for the presence of the transgene using PCR. Mice positive for the transgene were mated to control mice in order to determine if the transgene inserted into the genome multiple times (124). Once a pure line was established the transgenic mice were bred together to create a homozygous transgenic mouse line, which were utilized in

the 2/3 partial hepatectomy studies as well as hepatocyte cultures. Expression of LSP1 protein in the liver was assessed by western blot.

### **3.2.7 Mouse hepatocyte isolation and culturing**

Mouse hepatocytes were isolated from WT C57/Bl6, WT 129/SvJ, LSP1 knockout and transgenic mice using an adaptation of Seglen's calcium two-step collagenase perfusion technique described previously (119, 120). Isolated mouse hepatocytes (300,000 cells/ml) were cultured on collagen-coated six well plates in MHGM supplemented with HGF (40ng/ml) and EGF (20ng/ml) (36, 121, 125). Hepatocyte were treated with BrdU on 0-2, 2-4, 4-6 days and fixed with formalin for immunohistochemistry. Protein samples were collected in RIPA buffer on days 0 (pellet), 2, 4, and 6.

## **3.3 RESULTS**

### **3.3.1 Loss of LSP1 expression using shRNA in vitro leads to increased proliferation and migration**

Since LSP1 protein is expressed in the JM1 cell line, we utilized these cells as a model to measure the functional significance of the loss of LSP1 in HCC. We transfected the JM1 cell line with short hairpin RNA (shRNA) in order to knock down expression of LSP1 and then measured the effect of loss of LSP1 on proliferation and migration. Since the shRNA vector

contained a puromycin resistance gene, we created a stable cell line and first measured the expression of LSP1 (Figure 13). Western blot analysis demonstrates a marked decrease in LSP1 protein expression in the LSP1 shRNA transfected cell in comparison to the scrambled shRNA control cells (Figure 14).

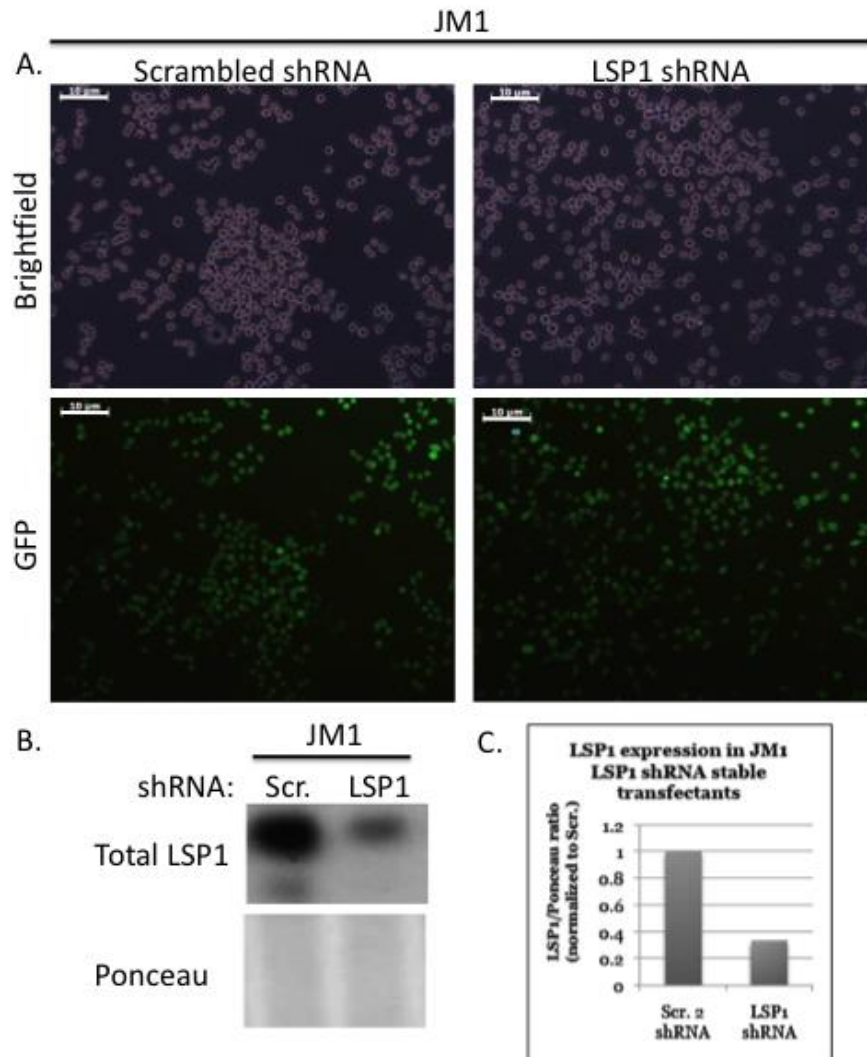


**Figure 13.** Creation of a LSP1 shRNA expression stable JM1 hepatoma cell line. **A.** Representative brightfield (top) and GFP (bottom images of the stable scrambled (left) and LSP1 shRNA (right) expressing JM1 cells. Scale bar = 10µm **B.** Western blot analysis of total LSP1 expression in the scrambled shRNA (scr.) and LSP1 shRNA stable cell lines. Ponceau S was utilized to ensure equal loading. **C.** Quantification of total LSP1 expression in western blots from B. Scale bar = 10µm.

Next, using immunoblotting, we measured the expression of the commonly utilized proliferation marker, cyclin D1. LSP1 shRNA JM1 cells exhibited increased levels of cyclin D1 in comparison to scrambled control indicating an increased proliferation in the LSP1 shRNA cells (Figure 14A). Next, a MTT assay was performed in which two LSP1 shRNA cell lines demonstrated a 3 and 4-fold increase in absorbance in comparison to scrambled controls indicating an increase in mitochondrial activity (Figure 14B). Since LSP1 is known to negatively regulate migration in leukocytes and endothelial cells (75, 92), we measured migration of LSP1 shRNA cells using a “monolayer scratch” assay and a transwell migration/chemotaxis assay. Loss of LSP1 expression led to increased migration into the scratch with an approximately 50% increase in wound closure in the LSP1 shRNA JM1 cells compared to scrambled shRNA cells (Figure 14C and D, Figure 15) as well as a four-fold increase in the number of cells that migrated across the transwell membrane (Figure 16). To determine the mechanism by which LSP1 knockdown resulted in increased proliferation and migration, we analyzed expression of downstream signaling pathways. Since LSP1 is known to interact with KSR and the MEK/ERK pathway signaling proteins, we analyzed expression of phosphorylated ERK2. Loss of LSP1 expression resulted in increased phosphorylated ERK2 indicating increased ERK2 activation and suggesting that the increased proliferation and migration occurs through an ERK activated mechanism (Figure 14E and F).

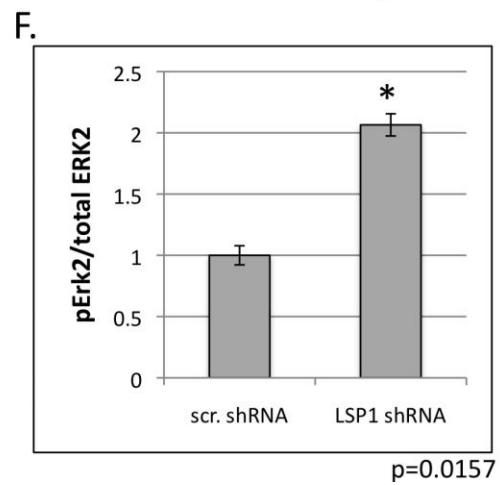
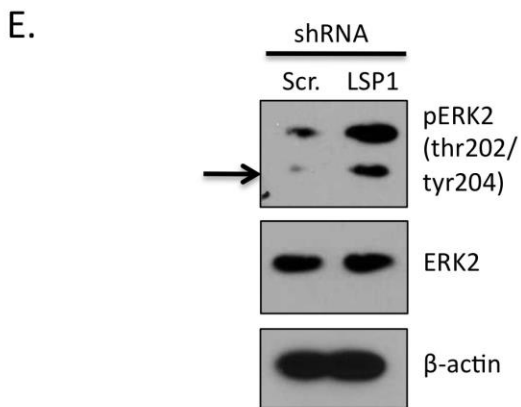
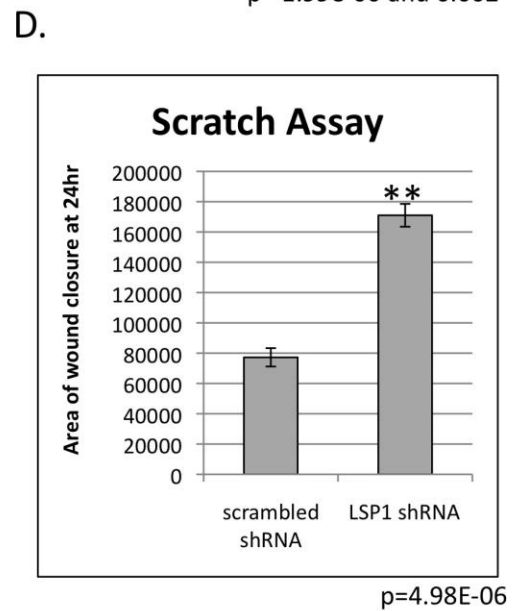
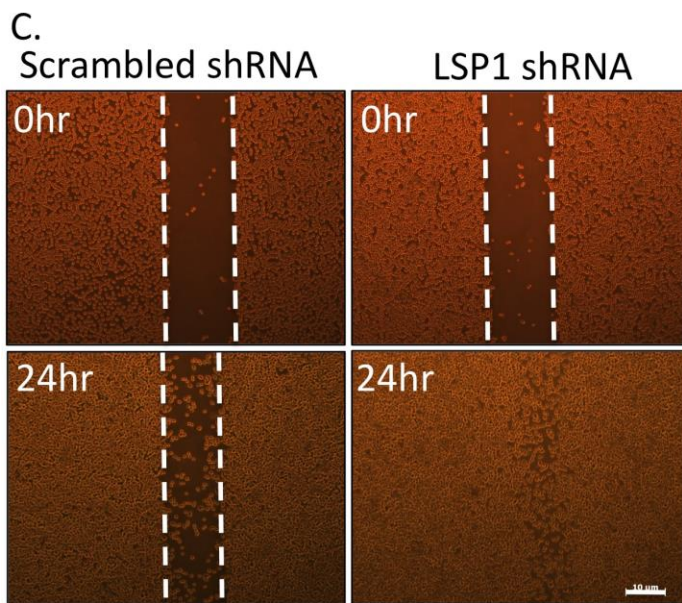
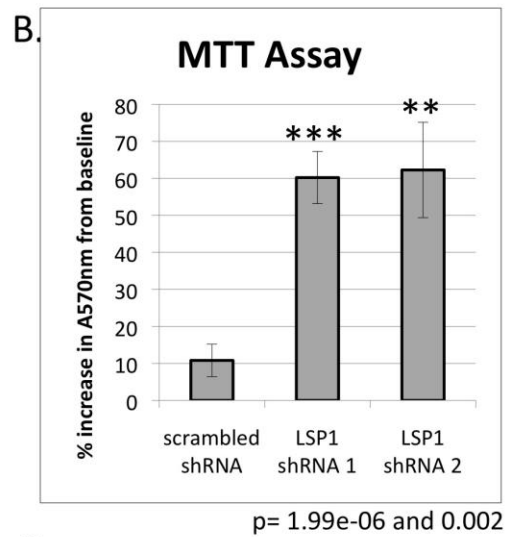
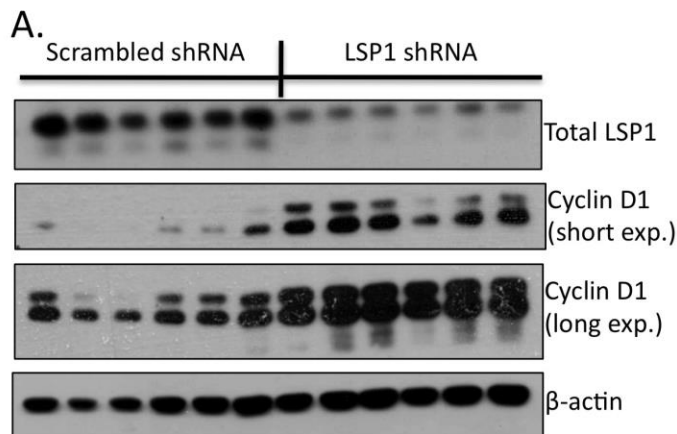


**Figure 14. Functional analysis of loss of LSP1 expression in JM1 hepatoma cell line. JM1 cells were transfected with LSP1 shRNA and a stable cell line was created. A. Western blot analysis of the stable LSP1 shRNA JM1 cell line for total LSP1 (top panel), cyclin D1 (2nd and 3rd panel), and  $\beta$ -actin (bottom panel, loading control). B. MTT assay of scrambled shRNA control cells and two LSP1 shRNA stable clones (LSP1 shRNA 1 and LSP1 shRNA 2). n=18 (experiment repeated at least two independent times), p=1.99e-06 and p=0.002, respectively. C. Representative bright field images of migration “scratch” assay at time 0 (upper panels) and 24 hours post scratch (bottom panel). Scale bar = 10 $\mu$ m. D. Quantification of area of wound closure from scratch assay. n=6, p=4.98e-06. E. Representative western blot of phosphoERK2 (top panel) and total ERK2 (middle panel) in JM1 LSP1 shRNA stable cell lines. F. Quantification of pERK2 and total ERK2. n=7, p=0.0157.**

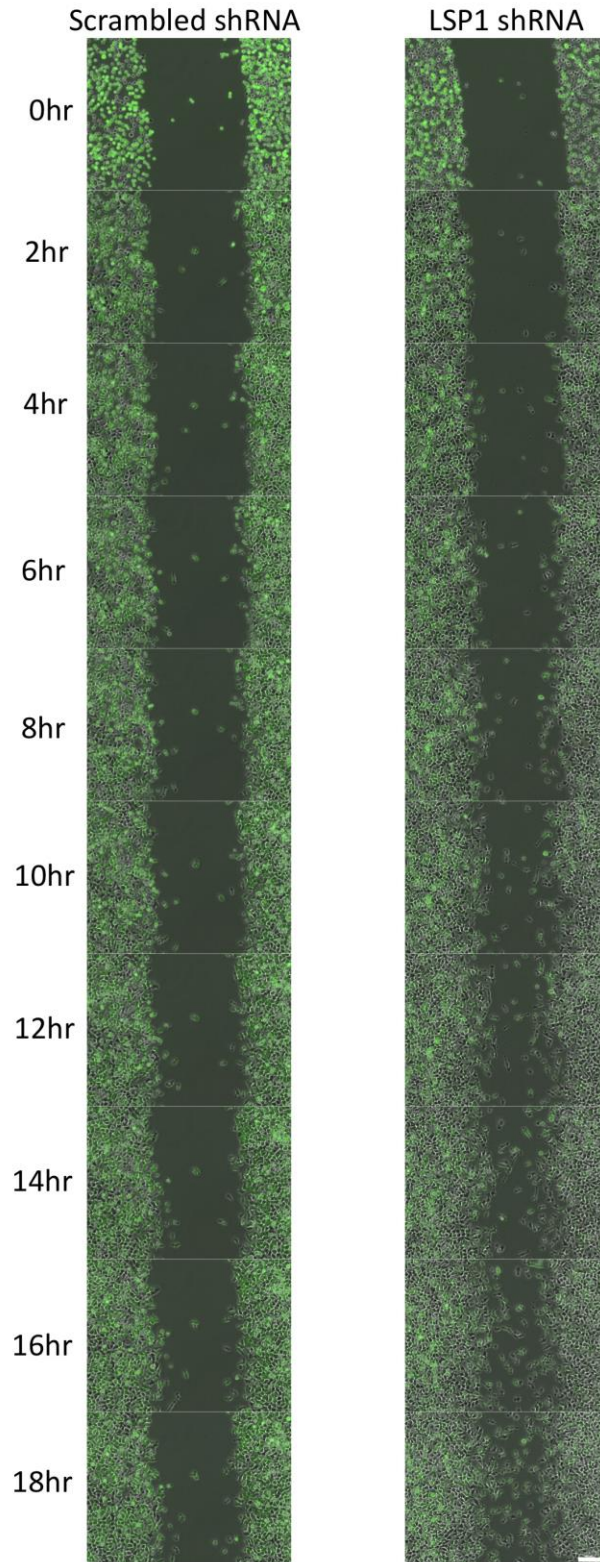
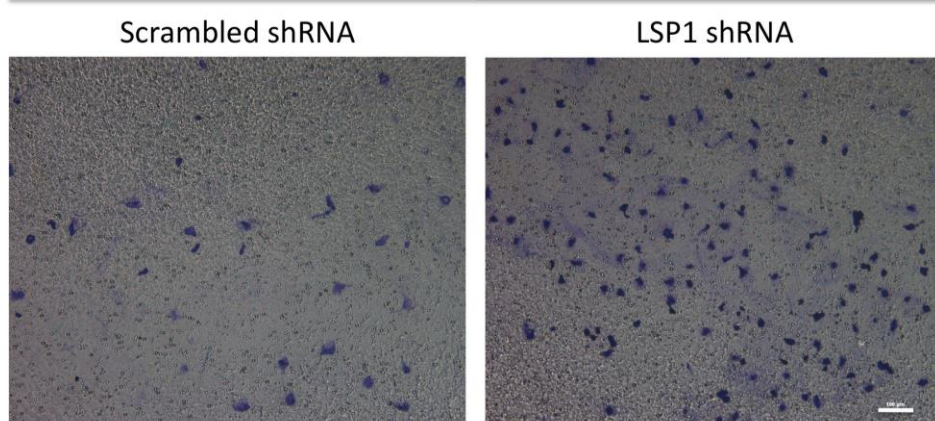


**Figure 15. Live cell imaging of migration scratch assay of JM1 LSP1 shRNA stable cell line. Left panel: scrambled shRNA stable cell line. Right panel: LSP1 shRNA stable cell line. Images were taken every 2 hours for 18 hours. 100x magnification. Scale bar= 100 $\mu$ m.**

A.

JM1



B.

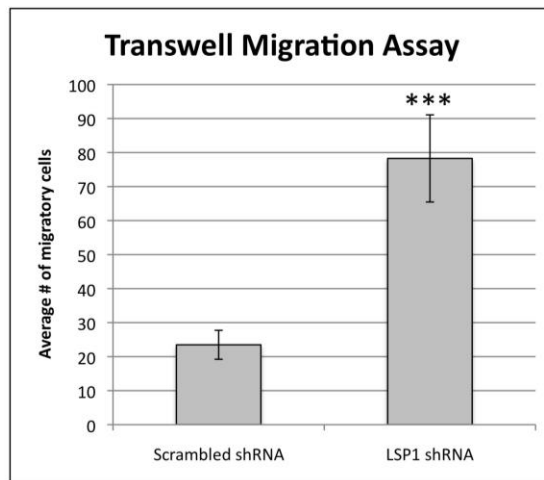


**Figure 16. Transwell Migration Assay of JM1 LSP1 shRNA stable cell line. A. Representative images of 0.1% Coomassie blue/10% methanol/10% acetic acid stained cells that migrated to the bottom of the transwell membrane. Images were taken using Olympus Provis inverted microscope at a 100x magnification. Scale bar = 100µm. Left panel: scrambled shRNA stable cells. Right panel: LSP1 shRNA JM1 stable cell line. B. Quantification of the number of migrating cells. At least 3 random fields per membrane were counted using Image J software**

### **3.3.2 Expression of LSP1 in a LSP1 deficient cell line leads to decreased proliferation**

Loss of LSP1 expression in the JM1 rat hepatoma cell line lead to increased mitochondrial activity and cyclin D1 expression therefore next we wanted to demonstrate if expression of LSP1 in a normally deficient cell line affects proliferation. JM2 rat hepatoma cell line does not express LSP1 protein (Figure 11B). Therefore we utilized these cells to study the role of LSP1 expression on cell proliferation. After transient transfection of JM2 cells with LSP1 cDNA (Figure 17A), we observed a significant decrease in the expression of the proliferation marker, cyclin D1 (Figure 17B and C). Furthermore, LSP1 expression in these normally deficient cells led to an approximate 50% decrease in BrdU labeling indicating a decrease in the rate of proliferation (Figure 17D). These results demonstrate that LSP1 functions as an inhibitor of hepatoma cell proliferation. We did not measure the role of increased LSP1 expression on migration in the JM2 cells however since loss of LSP1 expression leads to increased migration, we would hypothesize that increased LSP1 would greatly reduce migration.

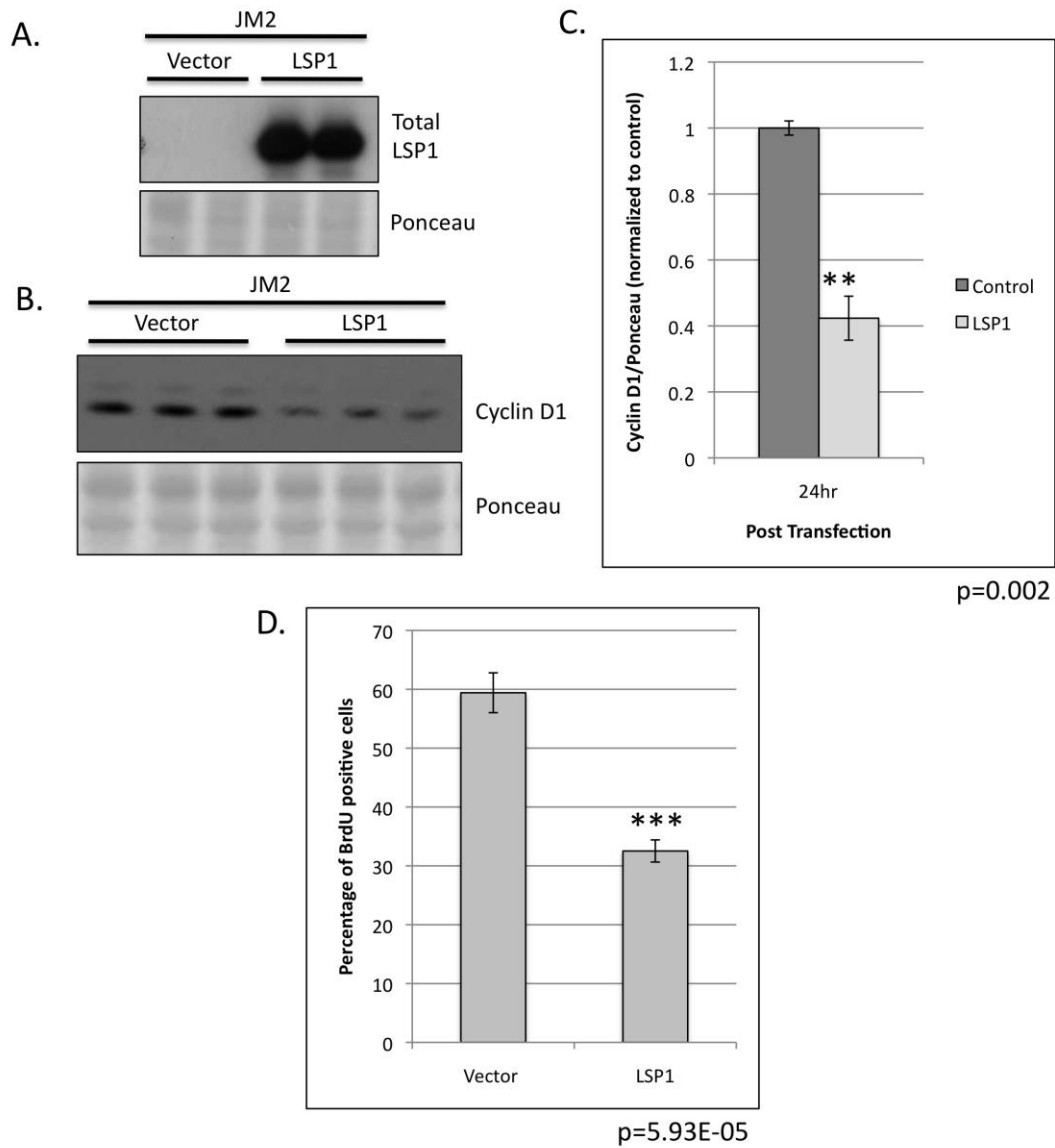


**Figure 17.** JM2 cells were transiently transfected with LSP1 cDNA and pExpress-1 plasmid (control). **A.** Western blot analysis of total LSP1 expression (top panel) at 24 hours post transfection in transiently transfected JM2 cell line. Ponceau S (bottom panel) loading control. **B.** Western blot analysis of cyclin D1 (top panel) expression at 24 hours post transfection. (Ponceau S (bottom panel), loading control). **C.** Quantification of cyclin D1 protein expression from B. n=3, p=0.002. **D.** Quantification of BrdU labeling in D. n=5 per condition, p=5.93E-05.

### **3.3.3 Expression of LSP1 through hydrodynamic tail vein injection leads to decreased proliferation following partial hepatectomy**

To demonstrate a role for LSP1 in the regulation of proliferation *in vivo*, we performed a hydrodynamic tail vein injection of LSP1 cDNA plasmid into male FVB mice and immediately performed a 2/3 partial hepatectomy. To show that the livers, specifically the hepatocytes, were successfully expressing LSP1 following injection, we performed western blot analysis for LSP1 expression and immunofluorescence staining of LSP1 and Hepatocyte Nuclear Factor 4 $\alpha$  (HNF4 $\alpha$ ), a marker of hepatocytes. The LSP1 injected animals expressed LSP1 and the LSP1 expression occurred in the cells also expressing HNF4 $\alpha$ , demonstrating that a majority of the cells expressing LSP1 are hepatocytes (Figure 18A and B). Though there were variations of the percentage of hepatocytes with high expression of LSP1 from one lobule to another, on average, about 30% of hepatocytes were found to have high LSP1 expression following the hydrodynamic injection. The peak of hepatocyte proliferation after PHx in mice is on day 2 (1). Therefore we harvested the livers on day 2 and performed immunohistochemical staining for the proliferation marker Ki67. The livers of the LSP1 injected mice displayed approximately 50% less Ki67 labeled hepatocytes in comparison to the vector control injected mice suggesting that LSP1 plays a role in regulating the proliferation of hepatocytes *in vivo* (Figure 18C and D). Western blot analysis demonstrates that the LSP1 injected mice have decreased cyclin D1 expression as well as decreased pERK expression in two out of the three liver samples (Figure 19). The results show that enhanced expression of LSP1 at the early (proliferative) stages of liver regeneration has inhibitory effects on hepatocyte proliferation.

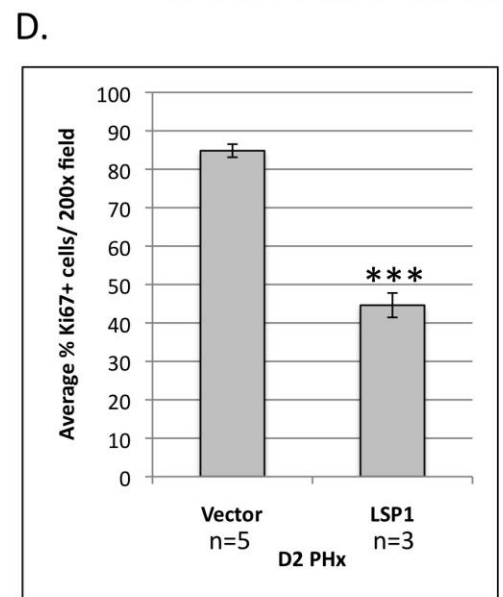
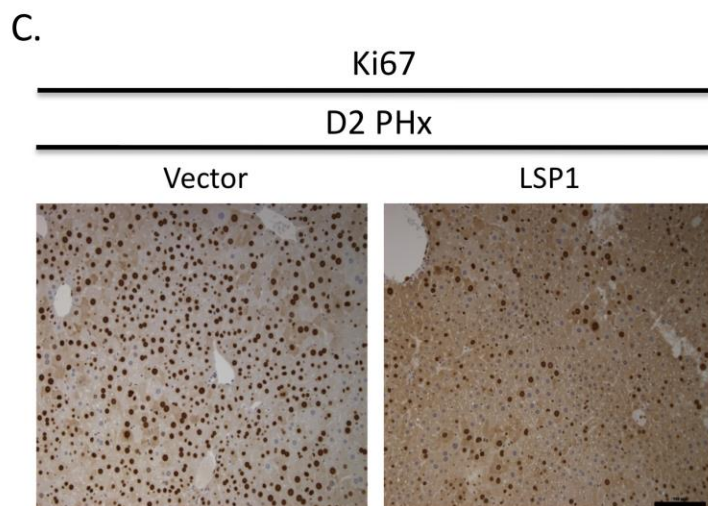
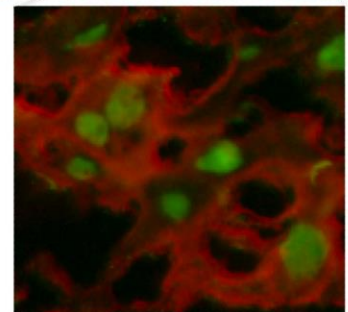
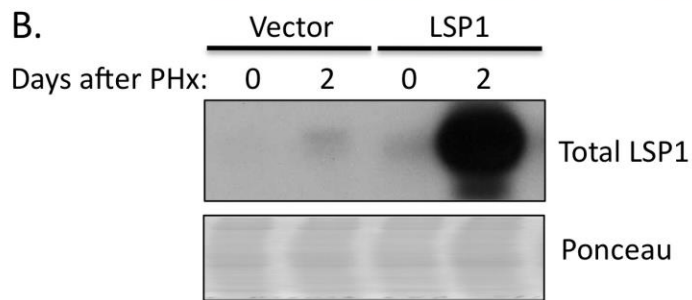
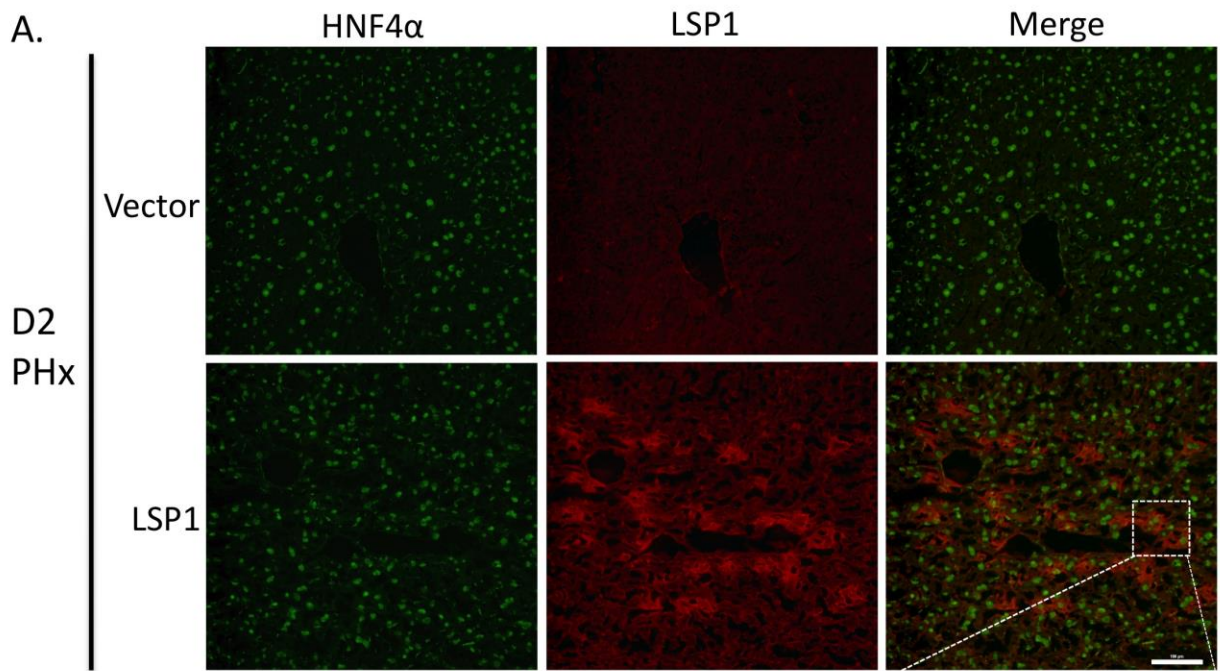


**Figure 18.** In vivo expression of LSP1 in a mouse PHx model. Hydrodynamic tail vein injection was utilized to express LSP1 in vivo during PHx. A. Immunofluorescence images of mouse liver at D2 after PHx (vector control (top panel), and LSP1, (bottom panel)) for HNF4 $\alpha$  (left panel), LSP1 (middle panel), and merge (right panel). Images were taken at 200x magnification. Scale bar =100 $\mu$ m. Inset is shown to demonstrate LSP1 and HNF4 $\alpha$  expression is present in the hepatocytes. B. Western blot analysis of total LSP1 expression (top panel) and Ponceau S (loading control) in total liver lysate from injected mice at Day 0 and 2 after PHx. C. Representative images of Ki67 staining of the injected mouse liver tissue on day 2 after PHx. Right image, vector control and left image, LSP1 injected animal. All images were taken at 200x magnification. Scale bar = 100  $\mu$ m. D. Quantification of the percentage of Ki67 positive hepatocytes in mouse liver tissue on D2 PHx. At least three random fields per slide were quantified using Image J software. Vector control mice n=5, LSP1 mice n=3. p=1.45E-10.

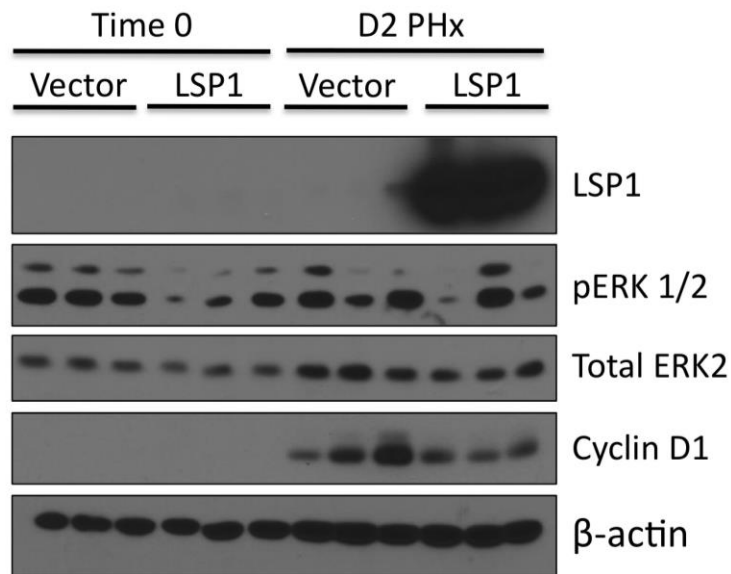


**Figure 19.** Western blot analysis of mouse livers after hydrodynamic tail vein injections. Liver samples from vector control and LSP1 injected mice at the time of PHx (time 0) and on day 2 after PHx were analyzed for expression of LSP1 (top), pERK1/2 (2nd from top), total ERK (3rd from top), Cyclin D1 (4th from top), and  $\beta$ -actin (bottom panel). Each lane represents one mouse. n=3 per condition.

### **3.3.4 LSP1 KO mice display increased ERK activation and proliferation after partial hepatectomy**

Since we have demonstrated that overexpression of LSP1 through hydrodynamic tail vein injection of LSP1 plasmid DNA causes decreased proliferation following PHx, next we wanted to determine what effect the loss of LSP1 expression would have on proliferation after PHx. We hypothesize that the lack of LSP1 expression would result in increased proliferation since LSP1 acts as an inhibitor of cell growth. Therefore, we performed PHx on a global LSP1 knockout (KO) mouse model and using the proliferation marker, Ki67, we measured the percentage of proliferating hepatocytes at various times post-surgery. There was no difference in the number of Ki67 positive hepatocytes at day 2 following PHx between the WT and KO mice, however on day 4, there is a significant increase in the percentage of proliferating hepatocytes in the KO mice (25.7%) as compared to the wild type (15.6%) (Figure 20A and B). By day 7, the amount of dividing hepatocytes in the KO is significantly less than in the WT mice suggesting that in this model, at later time points after PHx, a compensatory mechanism inhibits the increased hepatocellular growth. Although the percentage of Ki67 positive hepatocytes is less on day 7 in the KO, on both day 4 and 7, there is a significant increase in the number of overall hepatocytes in the KO having 144 more hepatocytes on day 4 and 134 more hepatocytes on day 7 than the wild type controls (Figure 20C). Despite the increase in Ki67 positive hepatocytes on day 4 and increased hepatocyte numbers on days 4 and 7, there was no difference in the liver to body weight ratios between the KO and WT mice (Figure 21).

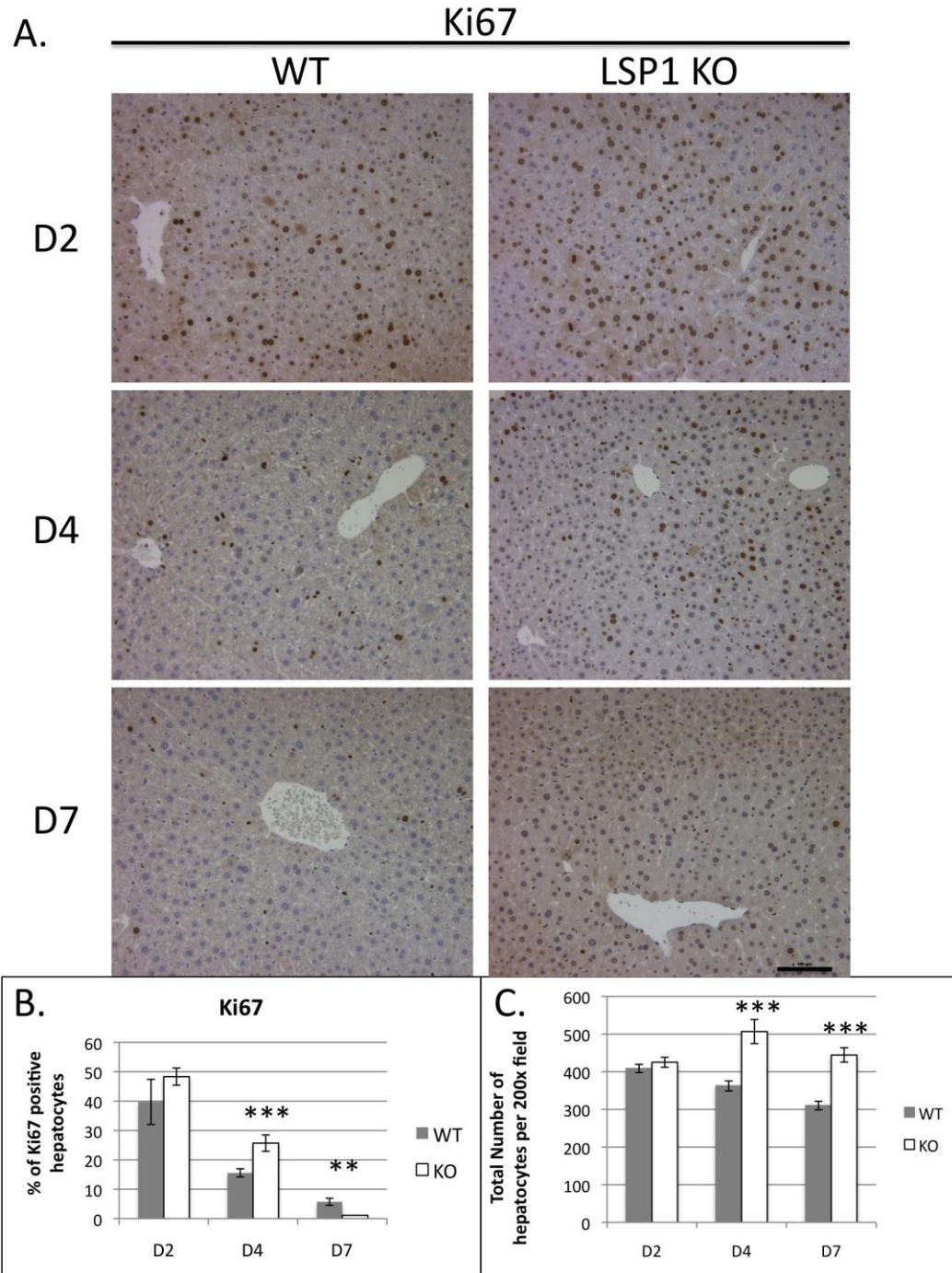


**Figure 20.** LSP1 knockout (KO) mice display increased Ki67 positive hepatocytes on day 4 after PHx and increased hepatocyte numbers on days 4 and 7. **A.** Representative images of Ki67 immunohistochemistry on wild type (WT) (left) and LSP1 KO (right) mouse livers after PHx. 200x magnification. Scale bar = 100 $\mu$ m. **B.** Quantification of the percentage of Ki67 positive hepatocytes in WT and LSP1 KO mouse livers after PHx. **C.** Quantification of the number of hepatocytes per 200x field in WT and LSP1 KO livers after PHx. \*\*  $p < 0.001$ , \*\*\*  $p < 0.0001$ .

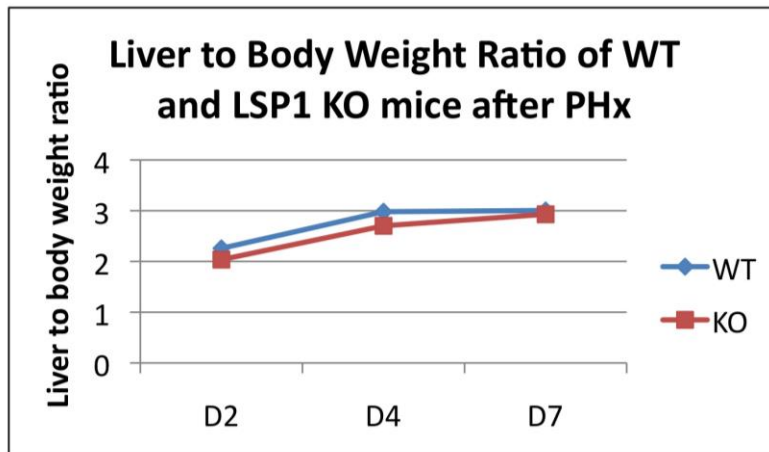


Figure 21. Liver to body weight ratios of WT and LSP1 KO mice after PHx. Ratio of liver weight to body weight was taken on days 2, 4 and 7 after PHx. There is no significant difference in the liver to body weight ratio at any of the time points.

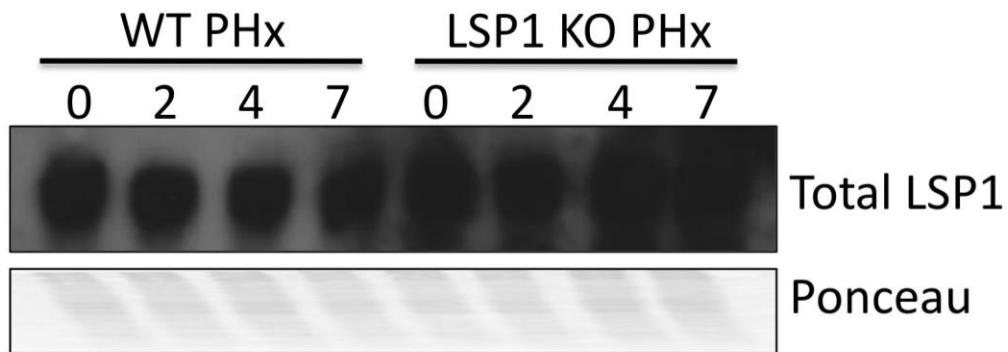
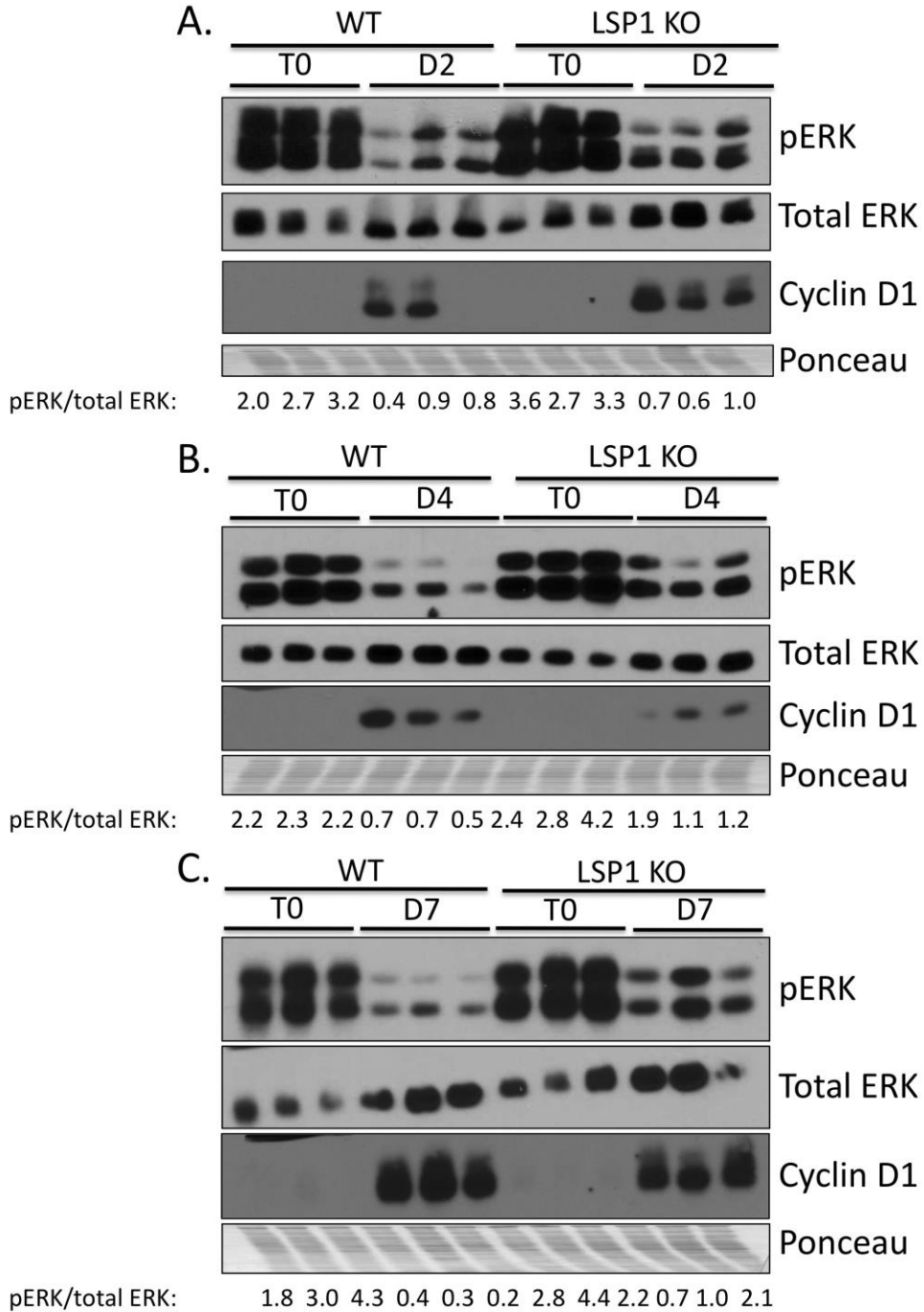


Figure 22. Western blot analysis of LSP1 expression in WT and LSP1 KO mouse livers. Total LSP1 expression was measured at time 0 and days 2, 4 and 7 in both the WT and LSP1 KO mouse livers. Each lane represents a pooled lysate containing protein from 3 separate mouse livers. Ponceau S staining was utilized to ensure equal protein loading.

Next, we measured the expression of total LSP1 in the WT and KO mice and western blot analysis shows that LSP1 expression is increased in the KO mice (Figure 22), which is most likely due to the knockout mice only lacking expression of one isoform of LSP1 leaving expression of the S37 isoform of LSP1 intact. Since the antibody recognizes all LSP1 isoforms, S37 is being expressed at a higher level to compensate for loss of isoform 1. This may also contribute to the modest difference in proliferation that we measured in the KO after PHx. It is possible that one isoform is responsible for effect on proliferation whereas the other isoform S37 plays a role in migration. Another explanation is that the two different isoforms are differentially expressed in hepatocytes and NPCs. We also performed western blot analysis to measure pERK, total ERK and cyclin D1 levels in the KO and WT livers following PHx. The KO mice display increased pERK levels at all of the time points in comparison to controls however, cyclin D1 expression is not effected on day 2 and appears to be decreased on days 4 and 7 (Figure 23). This conflicts with the increased Ki67 staining on day 4 but could be due to the contribution of the other cell types in the lysates since the samples are whole liver lysates and not isolated hepatocytes.



**Figure 23. Western blot analysis of WT and LSP1 KO mouse livers after PHx. A. WT and LSP1 KO livers from time 0 (T0) and day 2 (D2), B. time 0 (T0) and day 4 (D4), and C. time 0 (T0) and day 7 (D7) were analyzed by western blot for pERK (top), total ERK (2nd from top), cyclin D1 (3rd from top) and ponceau S staining (bottom) was utilized to ensure equal protein loading. Each lane represents a whole liver lysate from a separate mouse.**

To determine if the KSR and pERK complex are affected by the loss of LSP1 expression during PHx, we performed an immunoprecipitation with KSR and probed for pERK. Overall, there is more KSR expressed in the KO as compared to the wild type. In the wild type mice, KSR and pERK are in complex on day 2 and day 7 whereas in the KO, KSR and pERK interact at all times points except for day 4, which is when we see increased proliferation in the KO as compared to the WT (Figure 24). One caveat to this study is that these are whole liver lysates so we are unable to determine if the KSR-pERK complex is being formed in the hepatocytes or the other cell types of the liver.

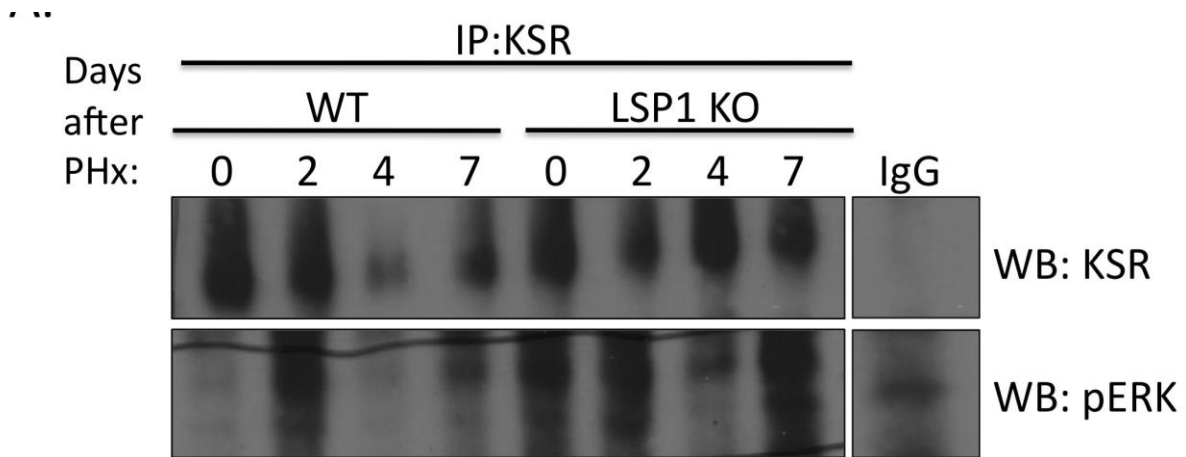


**Figure 24. Immunoprecipitation of KSR in WT and LSP1 KO PHx liver lysates. Top panel: western blot for KSR, bottom panel: western blot for pERK expression in WT and LSP1 KO PHx livers at time 0 and days 2, 4 and 7.**

### **3.3.5 Hepatocytes from LSP1 KO mice exhibit increased proliferation in the absence of growth factors**

Since it is difficult to determine the effect the loss of LSP1 has on hepatocytes when studying the intact liver with the contribution of other cell types, we decided to isolate hepatocytes from the WT and KO mice to study the role of LSP1 on their proliferation in culture. We performed BrdU incorporation assays on hepatocytes cultured in the presence and absence of HGF and EGF. In the presence of growth factors, there was no difference in number of dividing hepatocytes between the WT and KO at all of the time points measured (Figure 25). However, in the absence of growth factors, there was a significant increase in the percentage of KO hepatocytes proliferating in comparison to the WT with approximately 50% of the KO hepatocytes proliferating compared to 10% of the WT on days 2-4 in culture (Figure 26). These results suggest that when growth factors are present, a maximal level of proliferation is achieved that is not affected by loss of LSP1 expression, however, when growth factors are absent and the hepatocytes should not proliferate, a lack of LSP1 expression promotes hepatocellular division.

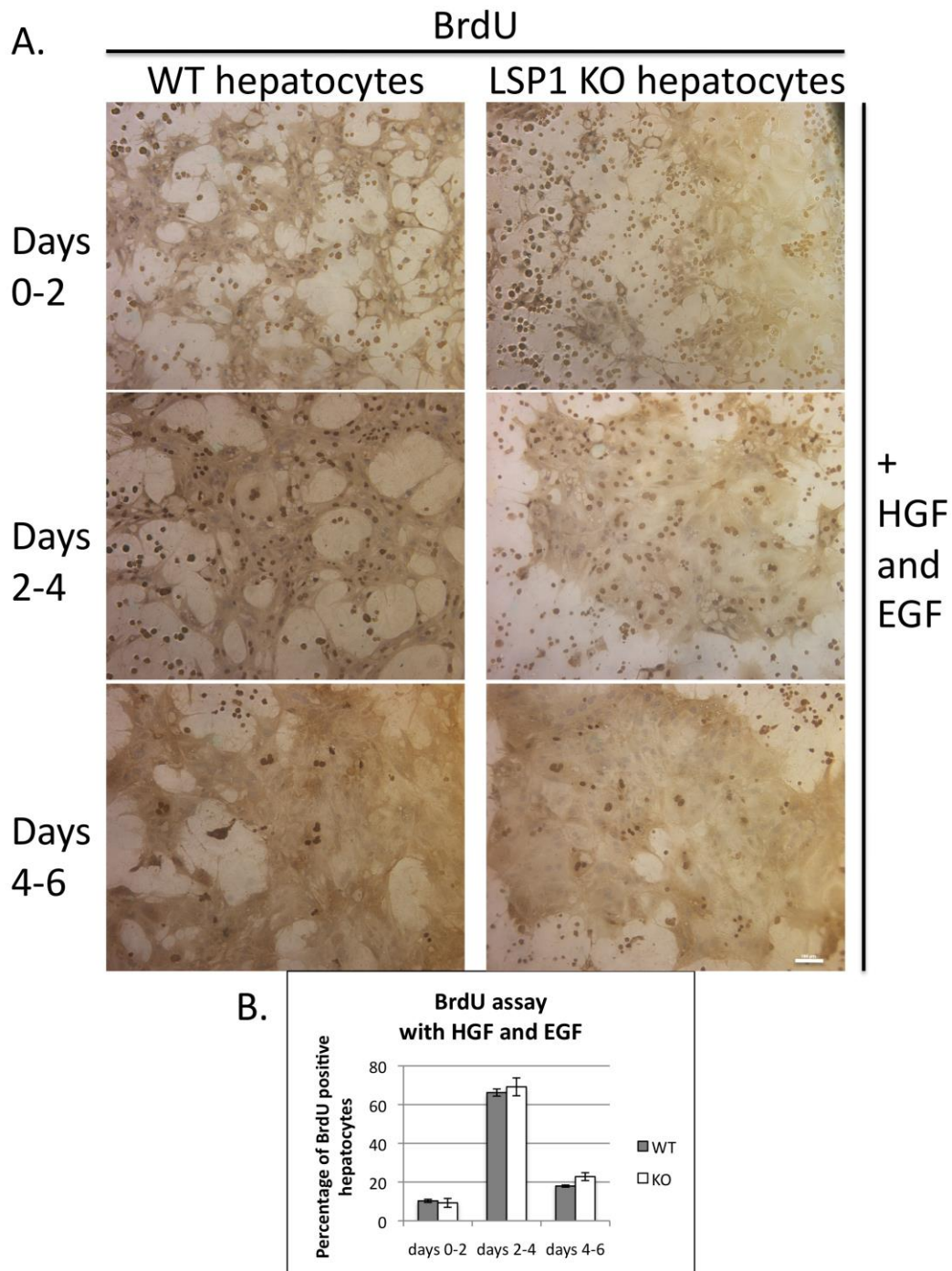


**Figure 25.** BrdU incorporation assay in hepatocytes from WT and LSP1 KO mice cultured in the presence of growth factors. **A.** Representative images of BrdU immunohistochemistry on WT (left) and LSP1 KO (right) hepatocytes cultured in the presence of HGF and EGF. BrdU was added to the culture medium for 2-day pulses. 100x magnification. scale bar = 100 $\mu$ m. **B.** Quantification of BrdU positive hepatocytes cultured in the presence of HGF and EGF at Day 0-2, 2-4, and 4-6.

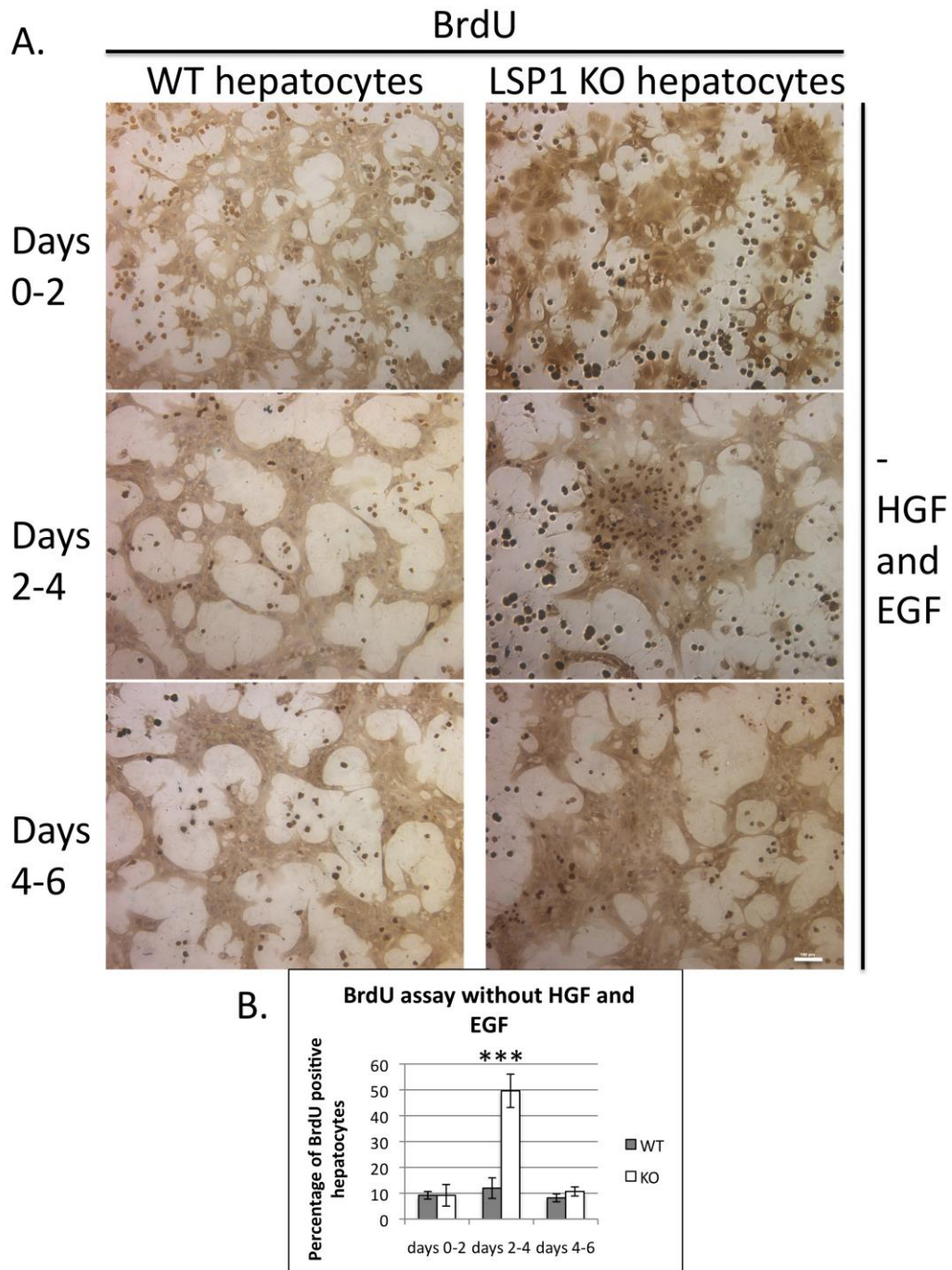


**Figure 26. BrdU incorporation assay in hepatocytes from WT and LSP1 KO mice cultured in the absence of growth factors. A. Representative images of BrdU immunohistochemistry on WT (left) and LSP1 KO (right) hepatocytes cultured in the absence of HGF and EGF. BrdU was added to the culture medium for 2-day pulses. 100x magnification. Scale bar = 100 $\mu$ m. B. Quantification of BrdU positive hepatocytes cultured in the presence of HGF and EGF at Day 0-2, 2-4, and 4-6.**

To determine what downstream signaling pathways are affected by the loss of LSP1 in the hepatocytes, we measured pERK, cyclin D1, and KSR expression in the KO and WT hepatocytes. In the presence of HGF and EGF, KO hepatocytes displayed increase pERK expression at all of the time points as well as increased KSR expression in comparison to WT (Figure 27A). However, cyclin D1 expression remained unchanged between the WT and KO hepatocytes (Figure 27A). These findings correlate with the BrdU incorporation assay in which there was no difference in proliferation between the WT and KO cells (Figure 25). Without HGF and EGF in the medium, KO hepatocytes display increased expression of cyclin D1 and pERK on days 4 and 6 in culture as compared to WT hepatocytes (Figure 27 B), which supports the BrdU proliferation data from figure 26. These results indicate the increased proliferation that occurs due to the loss of LSP1 expression involves an ERK dependent mechanism.

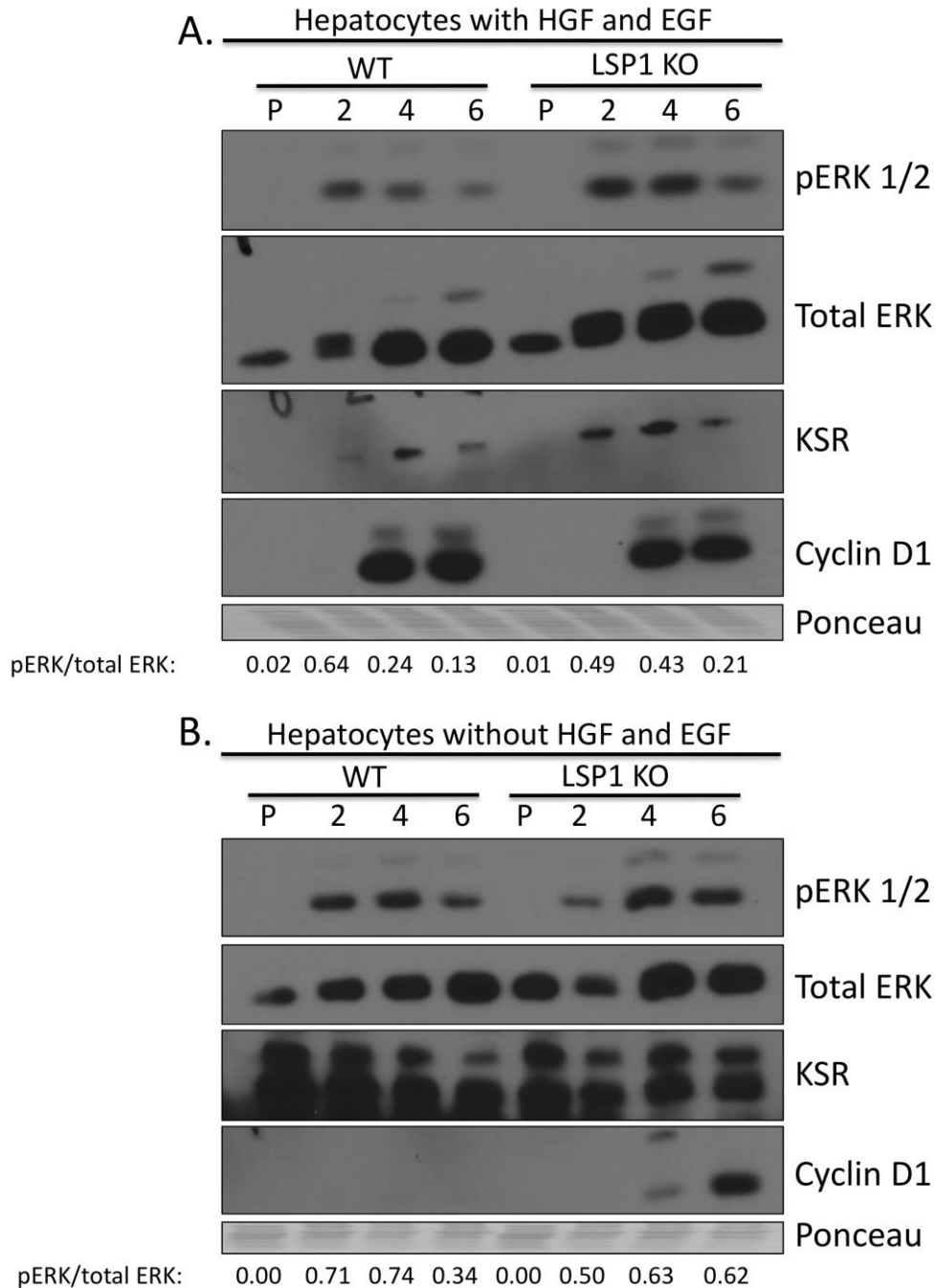


**Figure 27.** Western blot analysis of WT and LSP1 KO hepatocytes cultured in the presence and absence of HGF and EGF. Hepatocytes from WT and KO mice were cultured in the (A) presence and (B) absence of HGF and EGF and the expression of pERK (1st panel), total Erk (2nd panel), KSR (3rd panel) and cyclin D1 (4th panel) were analyzed by western blot. Ponceau S staining was utilized to ensure equal protein loading. P, hepatocyte pellet.

### **3.3.6 LSP1 transgenic mice display decreased proliferation and ERK activation following partial hepatectomy**

We have demonstrated a role for LSP1 in the inhibition of proliferation after PHx through the expression of exogenous LSP1 via hydrodynamic tail vein injection of plasmid DNA. However, one caveat to this experiment is the inability to study the function of LSP1 on proliferation at later time points following surgery since expression of the plasmid DNA only lasts for a short period of time. Another consideration is that although hydrodynamic injection has been shown to target mostly hepatocytes it is possible that other cell types of the liver had taken up the plasmid and contributed to the decreased proliferation of the hepatocytes. Therefore, we decided to create a LSP1 transgenic (TG) mouse model in which LSP1 expression is under the albumin promoter and alpha-fetoprotein enhancer to ensure expression only in hepatocytes. Using this TG model, we performed PHx and measured the number of proliferating hepatocytes using the proliferation marker, Ki67. There is no difference in the percentage of Ki67 positive hepatocytes between the WT and TG livers on day 2 following PHx, however on day 4, we see a significant decrease of 25% fewer hepatocytes proliferating in the TG in comparison to the WT as well as approximately 50 less hepatocytes per 200x field in the TG (Figure 28 A, B and C). By day 7 after PHx, there is no significant difference in the number of dividing hepatocytes between the WT and TG mice. There was no difference in the liver to body weight ratios between the WT and TG mice on days 2 and 4 following surgery, however we did detect a nearly significant decrease in the liver to body weight ratio on day 7 ( $p=0.051$ ) (Figure 29). These results could indicate that in the hydrodynamic tail vein injection experiment the observed decrease in hepatocyte proliferation is not only due to hepatocytes expressing LSP1 but also due to the influence of LSP1 expressing NPCs on hepatocytes.

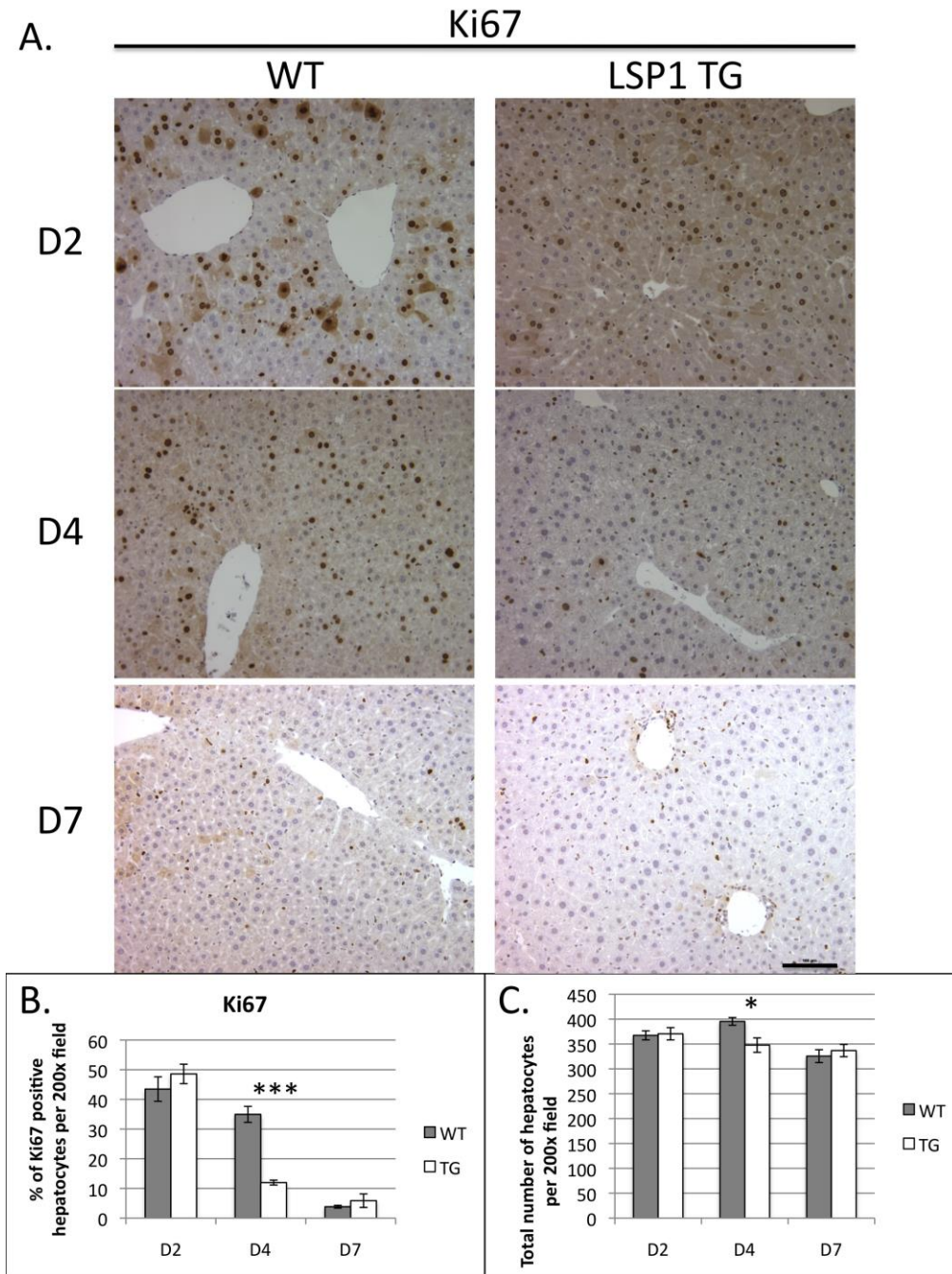


**Figure 28.** LSP1 transgenic (TG) mice display decreased Ki67 positive hepatocytes and decreased hepatocyte numbers on day 4 after PHx. **A.** Representative images of Ki67 immunohistochemistry on wild type (WT) (left) and LSP1 TG (right) mouse livers after PHx. 200x magnification. Scale bar= 100 $\mu$ m **B.** Quantification of the percentage of Ki67 positive hepatocytes in WT and LSP1 TG mouse livers after PHx. **C.** Quantification of the number of hepatocytes per 200x field in WT and LSP1 TG livers after PHx. \*\*  $p < 0.001$ , \*\*\*  $p < 0.0001$ .

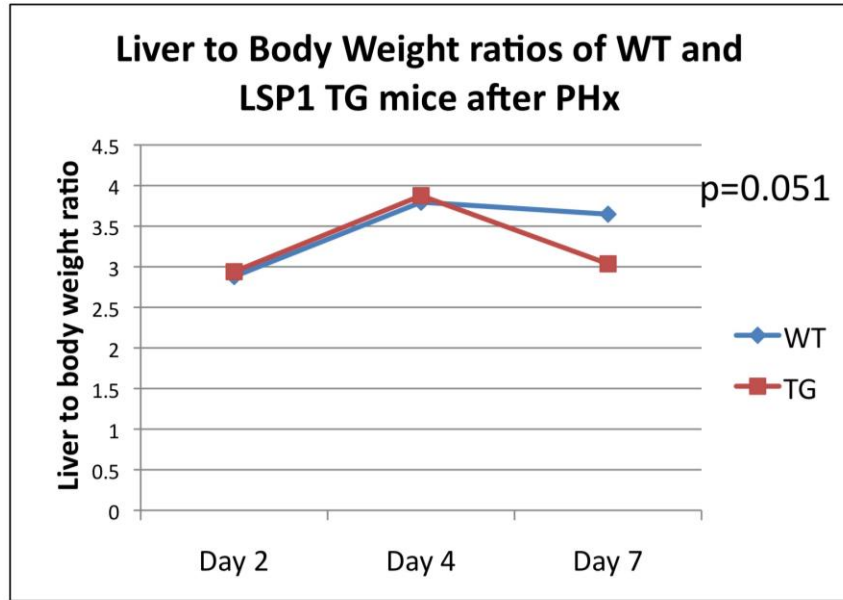


**Figure 29. Liver to body weight ratios of WT and LSP1 TG mice after PHx. Ratio of liver weight to body weight was taken on days 2, 4 and 7 after PHx. There is no significant difference in the liver to body weight ratio at any of the time points. Each time point contains n=3 per condition.**

Next, we measured the expression of total LSP1 in the WT and TG mice by western blot. Total LSP1 expression was increased in the TG at all time points analyzed following PHx as compared to WT indicating that the LSP1 TG was expressing the transgene (Figure 30).

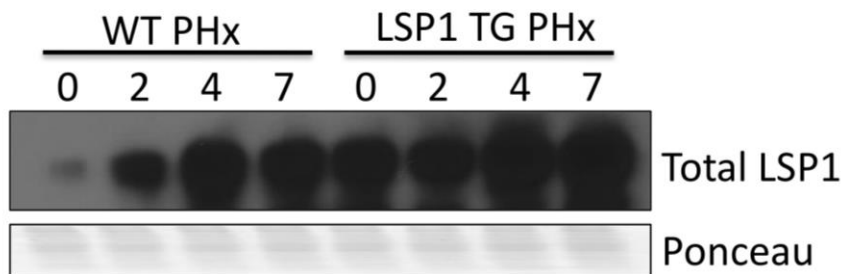


**Figure 30. Western blot analysis of LSP1 expression in WT and LSP1 TG mouse livers. Total LSP1 expression was measured at time 0 and days 2, 4, and 7 in both the WT and LSP1 TG mouse livers. Each lane represents a pooled lysate containing protein from 3 separate mouse livers. Ponceau S staining was utilized to ensure equal protein loading.**

To determine how the increased expression of LSP1 in the TG mouse model affects downstream signaling pathways, we performed western blot analysis to measure the expression of pERK and cyclin D1 after PHx. In the TG livers, we detected decreased pERK expression at all of the time points as compared to WT and the ratio of pERK/ total ERK was decreased in the TG livers on days 2 and 4 in comparison to control. Cyclin D1 expression is decreased in the TG livers on day 2 following PHx but is increased in comparison to WT on day 4 and 7 (Figure 31 A, B and C). Since the samples analyzed are whole liver cell lysates, it is possible that the cyclin D1 expression is increased in the other cell types and not the hepatocytes at these time points. We are unable to distinguish what the level of cyclin D1 expression is in the hepatocytes specifically. However, we could utilize immunofluorescence or immunohistochemistry to visualize which cells are expressing cyclin D1. Decreased pERK expression in the TG livers after PHx suggests that the increased LSP1 expression leads to decreased proliferation on day 4 through an ERK dependent pathway.

Next, we performed immunoprecipitations to determine if the expression of LSP1 affects the KSR and pERK complex in the TG mice following PHx. The TG mice express less KSR than the WT mice at all of the time points. In the TG, the strongest interaction between KSR and pERK occurs at time 0 whereas in the WT livers, KSR is found in complex with pERK on days 2 and 4 after PHx (Figure 32). These results indicate that expression of LSP1 in the TG livers causes an increase in the baseline complex formation but disrupts this KSR, pERK, LSP1 interaction during liver regeneration which may contribute to the decreased proliferation detected after PHx in the transgenic mice.

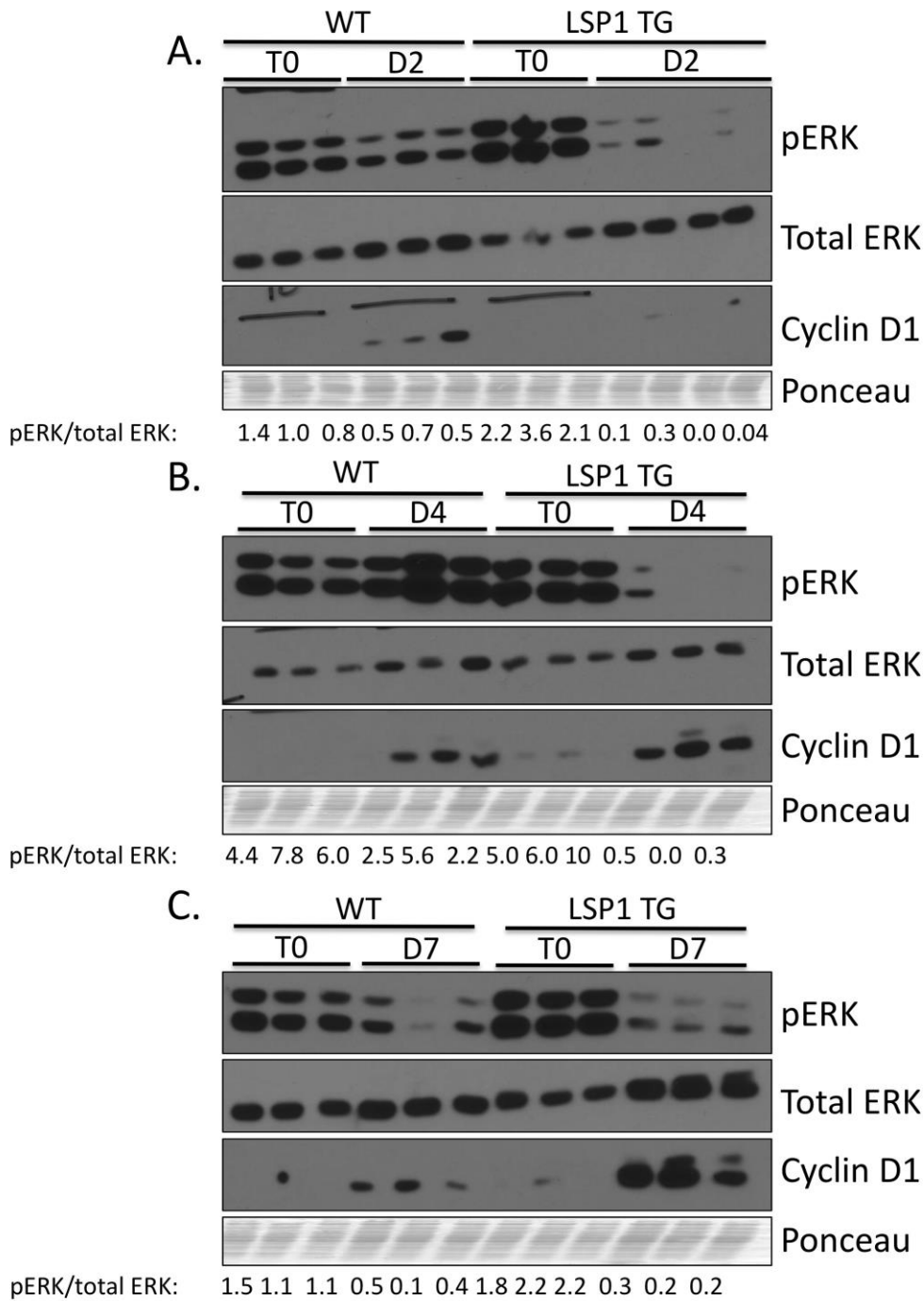


**Figure 31. Western blot analysis of WT and LSP1 TG mouse livers after PHx. A.** WT and LSP1 TG livers from time 0 (T0) and day 2 (D2), **B.** time 0 (T0) and day 4 (D4), and **C.** time 0 (T0) and day 7 (D7) were analyzed by western blot for pERK (top), total ERK (2nd from top), cyclin D1 (3rd from top) and ponceau S staining (bottom) was utilized to ensure equal protein loading. Each lane represents a whole liver lysate from a separate mouse.

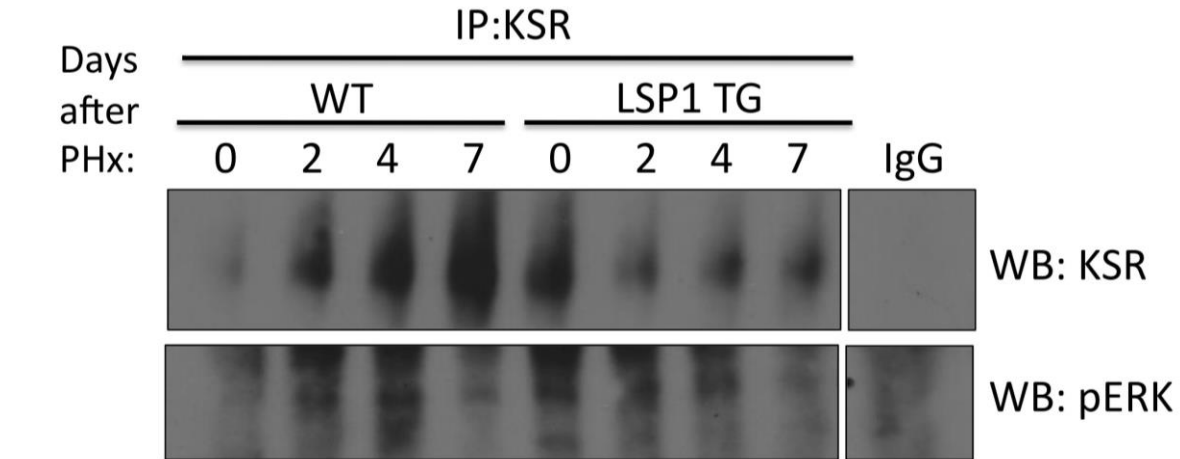


**Figure 32. Immunoprecipitation of KSR in WT and LSP1 TG PHx liver lysates. Top panel: western blot for KSR, bottom panel: western blot for pERK expression in WT and LSP1 TG PHx livers at time 0 and days 2, 4 and 7. Each time point represents a pooled lysate from 3 separate mice.**

### **3.3.7 Hepatocytes from LSP1 transgenic mice display decreased proliferation and pERK expression**

The previous studies on the LSP1 TG mice after PHx were performed on whole liver tissue which impedes our ability to determine which cells are contributing the expression of cyclin D1 and pERK. These studies are also confounded by the presence of the other cell types of the liver. Therefore, we isolated hepatocytes from the WT and TG mice and cultured the cells with and without HGF and EGF to determine how the expression of LSP1 in hepatocytes effects proliferation. Utilizing a BrdU incorporation assay, we were able to show that both in the presence and absence of growth factors, the TG hepatocytes display decreased proliferation in comparison to WT hepatocytes (Figure 33A and B). With HGF and EGF, there is a 4-fold

decrease on days 2-4 and 2.5 fold decrease on days 4-6 in the percentage of BrdU positive TG hepatocytes as compared to WT (Figure 33B). In the absence of growth factors, the significant decrease in proliferation between TG and WT hepatocytes is approximately 2.5 fold (Figure 34 A and B). These findings suggest that LSP1 acts as a negative regulator of hepatocellular proliferation both in the absence and presence of growth factors.

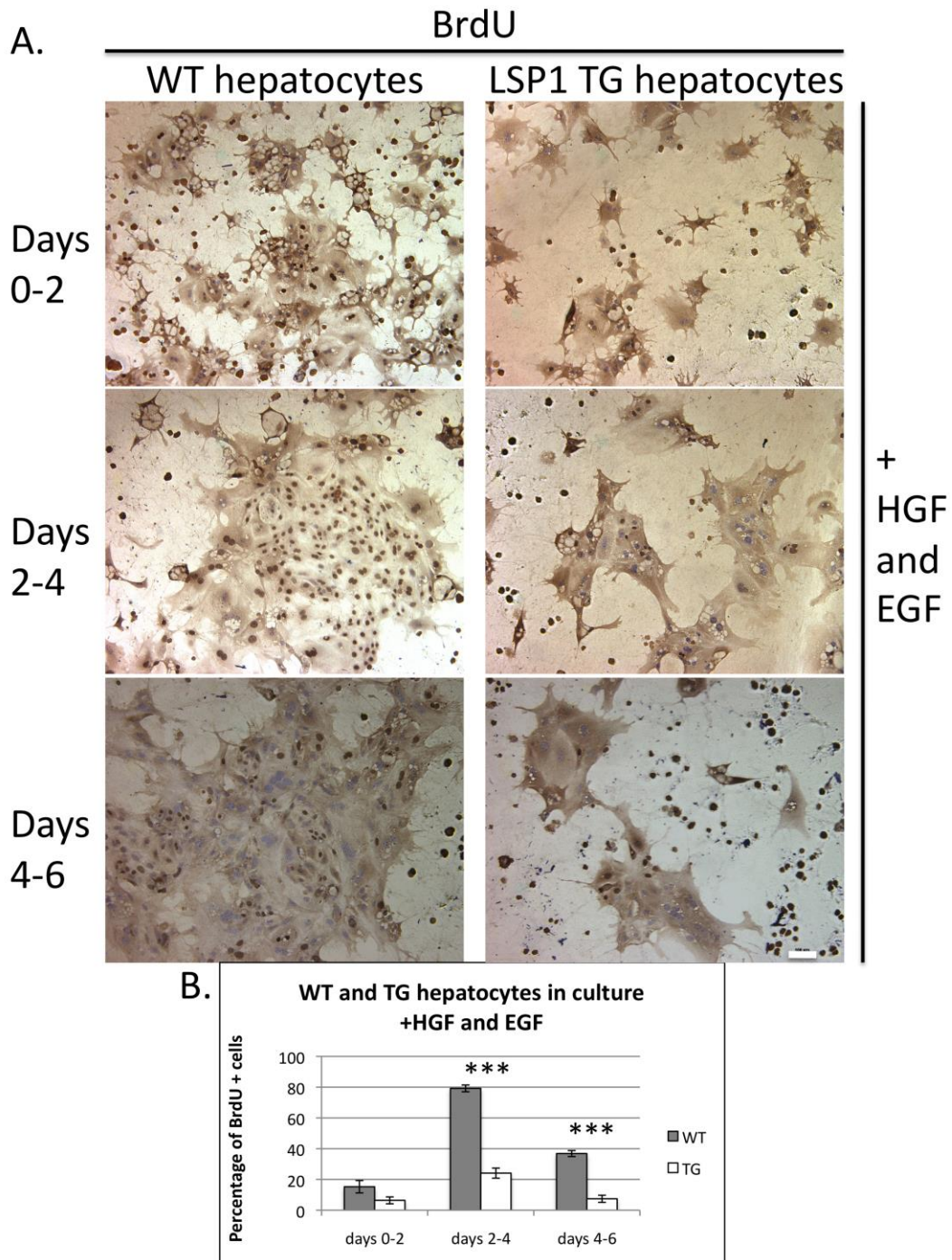


**Figure 33. BrdU incorporation assay in hepatocytes from WT and LSP1 TG mice cultured in the presence of growth factors. A. Representative images of BrdU immunohistochemistry on WT (left) and LSP1 TG (right) hepatocytes cultured in the presence of HGF and EGF. BrdU was added to the culture medium for 2-day pulses. 100x magnification. Scale bar = 100 $\mu$ m. B. Quantification of BrdU positive hepatocytes cultured in the presence of HGF and EGF at Day 0-2, 2-4, and 4-6.**

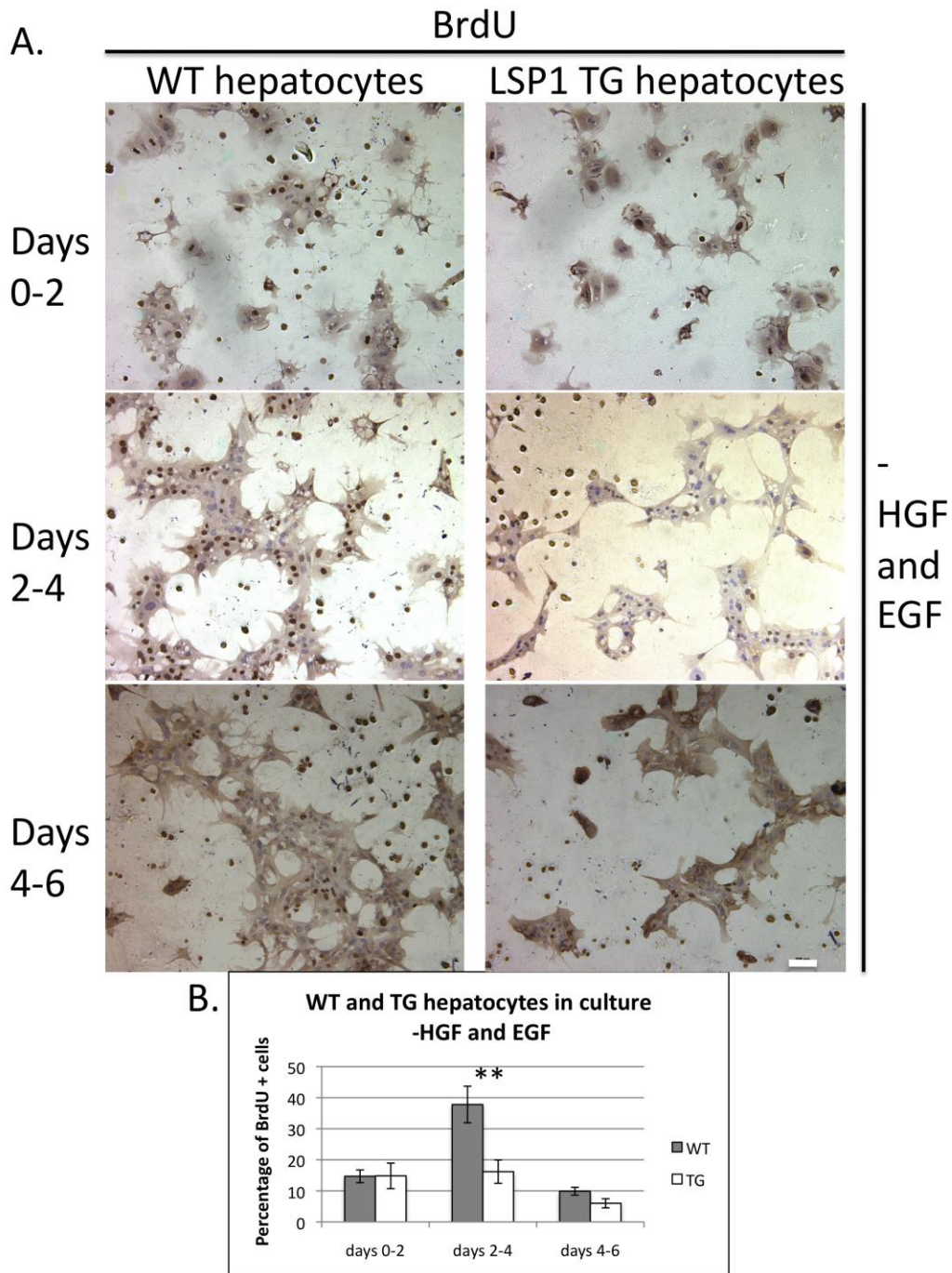


**Figure 34.** BrdU incorporation assay in hepatocytes from WT and LSP1 TG mice cultured in the absence of growth factors. **A.** Representative images of BrdU immunohistochemistry on WT (left) and LSP1 TG (right) hepatocytes cultured in the absence of HGF and EGF. BrdU was added to the culture medium for 2-day pulses. 100x magnification. Scale bar = 100 $\mu$ m. **B.** Quantification of BrdU positive hepatocytes cultured in the presence of HGF and EGF at Day 0-2, 2-4, and 4-6.

Next, we wanted to determine which signaling pathways may be involved in the decreased proliferation detected in the TG hepatocytes. Since our previous results have demonstrated a role for ERK in the modulation of proliferation due to LSP1, we measured pERK expression as well as KSR, which form the complex along with LSP1 to modulate downstream effects, such as proliferation. Western blot analysis shows that pERK expression is decreased in the TG hepatocytes at all of the time points in comparison to WT hepatocytes when cultured with growth factors (Figure 35A). However, the ratio of pERK/total ERK is only decreased in the day TG hepatocytes in comparison to the WT controls (Figure 35A). In the absence of HGF and EGF, pERK levels are decreased as well as the ratio of pERK/total ERK in the hepatocytes from the TG animals on days 4 and 6 in culture. Expression of cyclin D1, a marker of proliferation, is decreased in the TG hepatocytes both in the presence and absence of growth factors (Figure 35 A and B). KSR expression in the TG hepatocytes was greatest at time 0 but dramatically decreased on days 2 and 4 before increasing in both conditions on day 6 in culture. However, in the WT hepatocytes, KSR levels started low in the hepatocyte pellet but steadily increased until day 6 in culture with HGF and EGF (Figure 35A). Without growth factors, KSR expression was high in the WT hepatocyte pellet and on day 4 with levels decreasing on days 2 and 6 (Figure 35B). These results indicate that in the TG hepatocytes, increased LSP1 expression results in decreased KSR expression.

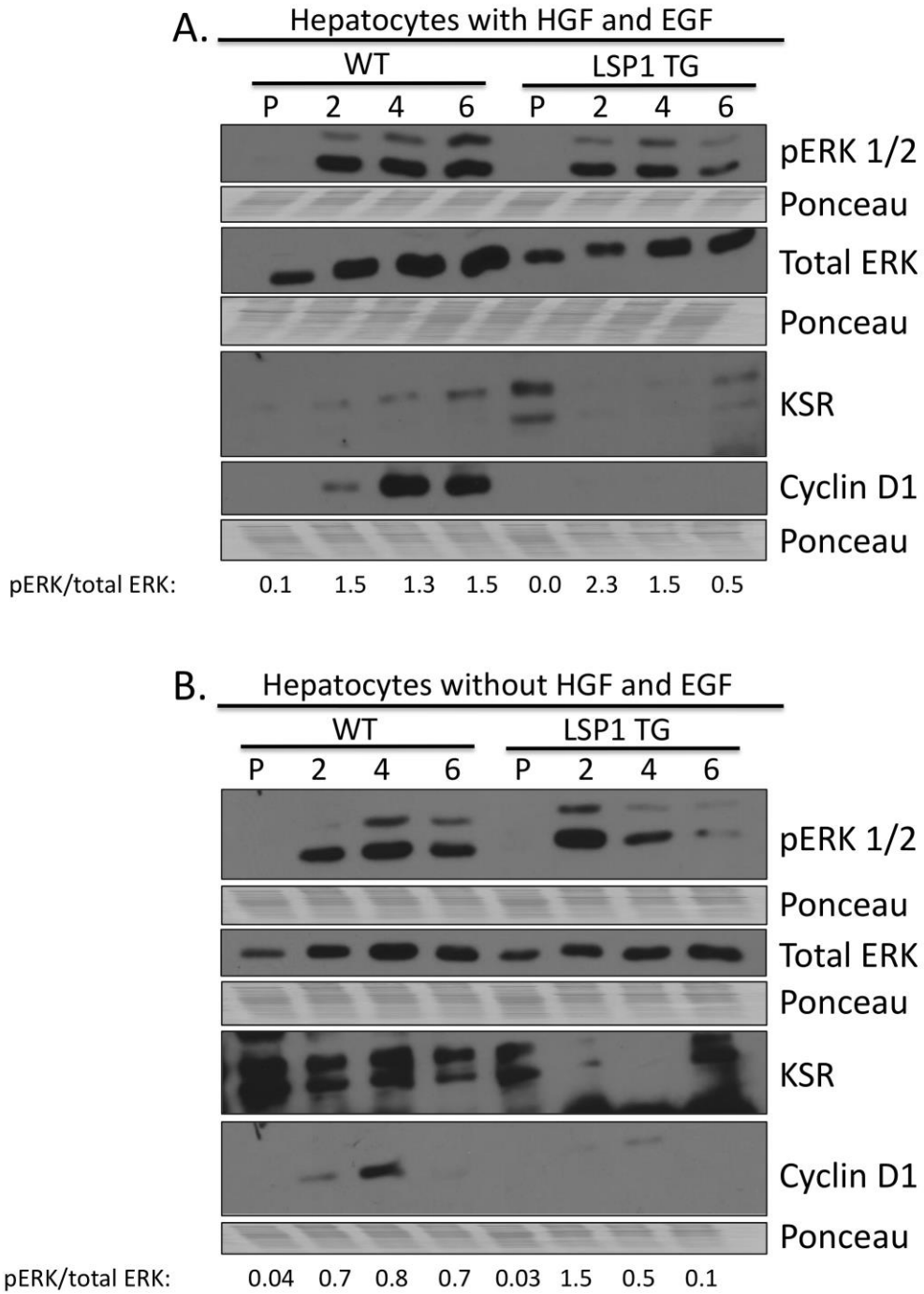


**Figure 35. Western blot analysis of WT and LSP1 TG hepatocytes cultured in the presence and absence of HGF and EGF. Hepatocytes from WT and TG mice were cultured in the (A) presence and (B) absence of HGF and EGF and the expression of pERK (1st panel), total Erk (2nd panel), KSR (3rd panel) and cyclin D1 (4th panel) were analyzed by western blot. Ponceau S staining was utilized to ensure equal protein loading. P, hepatocyte pellet.**

### 3.4 DISCUSSION

Our findings in Figure 14 demonstrate that loss of LSP1 is indeed associated with enhanced migration and enhanced proliferation rate, as evidenced by both increases in cell numbers and a dramatic increase in Cyclin D1 in the rat JM1 HCC cells. We demonstrated that the loss of LSP1 expression in hepatoma cells leads to increased ERK2 activation indicating that the observed increase in proliferation and migration is through an ERK2 dependent pathway. Previous literature has demonstrated that increased LSP1 negatively regulates migration of leukocytes and melanoma cell lines (75, 85, 87) and our data supports this notion in hepatocytes as well. Expression of LSP1 in the LSP1 deficient JM2 cell line and in mouse livers *in vivo* after PHx through hydrodynamic tail vein injection of plasmid DNA led to decreased proliferation as evidenced by decreased cyclin D1 levels and BrdU incorporation as well as decreased Ki67 staining. LSP1 KO mice displayed increased proliferation on day 4 as well as increased pERK expression whereas the LSP1 TG mice displayed decreased hepatocellular proliferation, expression of pERK and liver to body weight ratios. These results corroborate a role for LSP1 in the regulation of hepatocellular proliferation both *in vitro* and *in vivo*.

Cyclin D1 expression has been shown to function not only in proliferation but in the migration of mouse embryonic fibroblasts as well as breast cancer cells (126, 127) therefore it is possible that the increased cyclin D1 expression observed in our experiments may be due to increased migration and not simply proliferation. However, we have clearly demonstrated a role for LSP1 in hepatocellular proliferation *in vivo* with increased Ki67 positive hepatocytes and cell numbers following PHx in the LSP1 KO mouse model as well as the opposite with decreased proliferation in the LSP1 TG mice. In addition to the *in vivo* results, hepatocytes isolated from

LSP1 KO mice display increased BrdU incorporation in the absence of growth factors as well as increased cyclin D1 and phospho ERK expression. Increased expression of LSP1 in the TG hepatocytes results in decreased proliferation and cyclin D1 and pERK levels indicating that LSP1 functions as a regulator of hepatocyte proliferation. As with the cell line studies, all of these effects on proliferation appear to be through an ERK dependent signaling pathway.

Although we observed a significant increase in the percentage of Ki67 positive hepatocytes after PHx in the LSP1 KO livers, the increased proliferation observed was modest and there was no difference in the liver to body weight ratios between the KO and WT animals. In addition to these results, western blot analysis also demonstrated increased expression of LSP1 in the KO. This is due to the KO mice being created by targeting exon 1 of the LSP1 gene leaving expression of the alternative isoform, S37, intact (81). Therefore, the increased levels of LSP1 seen in the KO are most likely caused by compensation of the remaining isoform, S37 and this could contribute to the modest increase in hepatocellular proliferation as well as the lack of a difference in the liver to body weight ratios. Inhibition of the S37 isoform through shRNA could result in a greater increase in hepatocyte proliferation during liver regeneration in the KO mice.

In the experiments with WT and TG hepatocytes, in the absence of growth factors, the percentage of proliferating WT hepatocytes was 40% as compared to 80% in the cultures containing growth factors. Although the percentage of BrdU positive hepatocytes is 2 fold less, in the absence of growth factors, the numbers are higher than we would expect. (Figure 34B) One explanation may be that other components of the medium are able to promote proliferation in the hepatocytes of this mouse strain, C57/Bl6, versus other mouse strains such as, 129/svJ and FVB. Another possible reason for the increased proliferation in the WT hepatocyte cultures

without HGF and EGF may be that contaminating non-parenchymal cells may be present and expressing growth factors promoting hepatocyte proliferation.

#### 4.0 SUMMARY

There have been several recent studies identifying point mutations and large deletions in HCC (72). Driver and “passenger” mutations have been identified and correlated with HCC outcomes. Large size copy number variations (CNV: deletions or amplifications) have also been identified (72). We had concentrated our study (74) in identifying small size CNVs that would otherwise be missed in investigating approaches that would detect CNV of only large size. The latter would be likely to contain many genes in each CNV, thus making it difficult to identify the specific genes whose smaller size CNV would affect neoplastic behavior. LSP1 had the largest number of CNV (51 of 98 cases) (74). In view of this, we believe that elucidation of its function in normal hepatocyte biology is important. We do not believe that genomic alterations in LSP1 alone would be necessarily sufficient to drive a hepatocyte into neoplasia. The high frequency of the LSP1 CNV, however, suggests LSP1 loss of function is important, and that, along with other genomic changes, LSP1 certainly adds to the neoplastic behavior and may be sufficient to convert a low level neoplastic clone into one of a higher malignant potential.

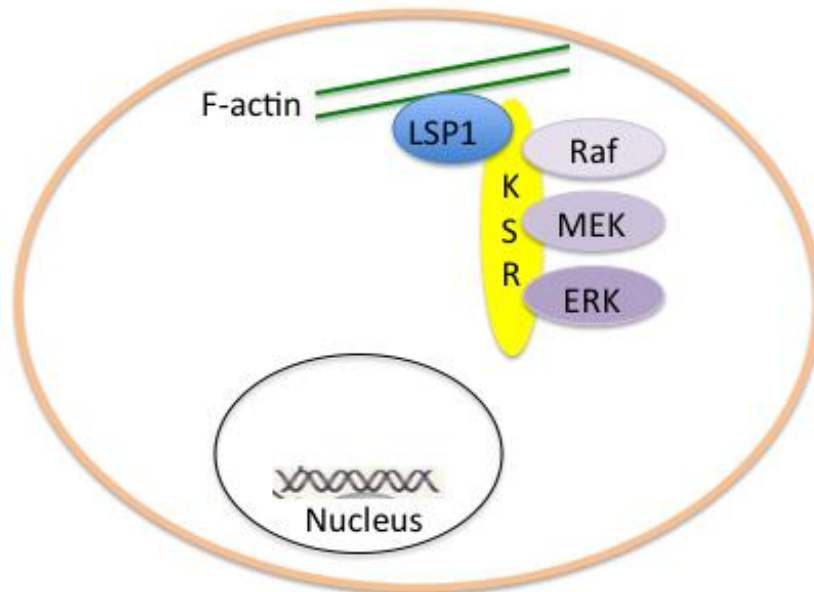


**Figure 36. Schematic of LSP1, KSR, ERK interaction in the cell. LSP1 binds to the F-actin filaments and KSR. KSR acts as a scaffold for the ERK signaling cascade by binding to Raf, MEK and ERK kinase. LSP1 acts to locate the ERK signaling complex to the actin cytoskeleton of the cell. We hypothesize that ERK localization to the cytoskeleton by LSP1 in our system results decreased proliferation and migration however the absence of LSP1 allows ERK to escape binding to the cytoskeleton and can promote migration and proliferation.**

Previous literature has demonstrated that in hematopoietic cells LSP1 interacts with KSR and the Raf, MEK and ERK signaling proteins. LSP1 functions to target the MAPK pathway to the actin cytoskeleton of these cells through its F-actin binding domain in the C-terminal region of the protein (102). LSP1 is also known to function as a negative regulator of migration in neutrophils (86). Our data demonstrates that loss of LSP1 expression leads to increased proliferation and migration in hepatoma cell lines as well as during liver regeneration. One possible explanation for the role of LSP1 in these cellular functions is that LSP1 acts to

negatively regulate ERK activity. We have shown that loss of LSP1 expression leads to increased ERK phosphorylation whereas overexpression of LSP1 causes the opposite phenomenon. One hypothesis is that LSP1 in conjunction with KSR acts as a scaffold for the ERK signaling cascade and functions to sequester ERK at the cytoskeleton, preventing ERK from translocating to the nucleus and activating transcription of targets involved in proliferation and migration of the cell. (Figure 36) To test this hypothesis, we could perform immunofluorescence in our LSP1 shRNA stable cell line to detect where pERK is localized in comparison to scrambled controls or we could fractionate the cell to isolate the cytoskeletal fraction as well as the nucleus to determine if loss of LSP1 leads to increased pERK in the nucleus.

In summary, LSP1 is expressed at the time of cessation of growth in hepatocytes in culture and increases gradually toward the end of liver regeneration. LSP1 functions as a regulator of hepatocyte proliferation and migration most likely by interacting and negatively regulating the function of the ERK/MAPK scaffold KSR. Our studies with LSP1 knockout and transgenic mouse models have demonstrated a role for LSP1 in liver regeneration. Future studies are aimed at elucidating if loss and overexpression of LSP1 will affect liver carcinogenesis in vivo as well as the role LSP1 may play in HCC sensitivity to sorafenib. Understanding the function of LSP1 in liver regeneration and cancer may lead to the development of novel targeted therapies for HCC.

## 5.0 FUTURE DIRECTIONS

Future studies aim to address the role of LSP1 in hepatocarcinogenesis since our studies stem from the finding that in HCC LSP1 has the most CNV cases. We have clearly demonstrated that LSP1 functions to negatively regulate the proliferation of hepatocytes both in culture and during liver regeneration therefore, we hypothesize that loss of LSP1 expression in hepatocytes could lead to a neoplastic phenotype with increased proliferation and metastasis whereas increased LSP1 expression would have a protective effect against hepatocarcinogenesis. We plan to inject both the LSP1 knockout and transgenic mice with diethylnitrosamine (DEN), a complete carcinogen in that at low doses it induces carcinogenesis initiation and higher doses leads to promotion and progression, in order to induce carcinogenesis in the liver (128, 129). We would expect that the LSP1 knockout mice would have larger tumors since LSP1 inhibits proliferation in hepatocytes whereas in the transgenic animals, we would observe smaller tumors. One caveat to this experiment is that LSP1 may affect the level of cytochrome P450 enzyme expressed by the hepatocytes, which would affect the metabolism of DEN (129). Therefore, we must measure the level and activity of the Cyp enzymes in order to ensure equal activity and expression of these proteins in both sets of animals.

Another possibility is that loss of LSP1 expression is an event that occurs during liver fibrosis and cirrhosis and before the liver tumor forms. Therefore, it would be important to study the role of LSP1 in liver fibrosis by using the carbon tetrachloride model to induce liver fibrosis

in the LSP1 KO and TG animals. If LSP1 plays a role in the development and progression of fibrosis, we hypothesize that loss of LSP1 would lead to increased fibrosis whereas the LSP1 TG mice would display a decrease in fibrosis since LSP1 functions as a negative regulator of proliferation and migration, which are hallmarks of stellate cell activation to the myofibroblast phenotype. (130)

Genome wide associate studies in breast cancer samples have demonstrated that single nucleotide polymorphisms (SNPs) in LSP1 are associated with increased susceptibility to breast cancer. (131) This suggests that LSP1 may play an important role in the carcinogenesis of not only liver but other tissues as well. It may be useful to screen other cancers to determine if CNV or SNP of LSP1 is detectable in these other tumor types and to determine if LSP1 functions as a negative regulator of proliferation and migration in these cancers. It is important to understand the role of LSP1 in carcinogenesis in order to develop novel therapeutics that can target this important signaling molecule not only in HCC but other cancers as well.

In addition to studying the role of LSP1 on the development and progression of HCC, we plan to investigate using LSP1 expression status in liver tumors as a diagnostic tool for a personalized medicine approach to treating HCC. Since our data has demonstrated that loss of LSP1 expression leads to increased activity of the ERK kinase signaling pathway, it is conceivable that these LSP1 negative tumors would be more sensitive to inhibitors that target the MAPK/ERK signaling pathway, such as sorafenib (132). Sorafenib is currently the only FDA approved multikinase inhibitor for treatment of advanced HCC (46). In a phase III clinical trial, the median overall survival of patients on sorafenib increased by 3 months in comparison to placebo (68). However, patients were not screened to determine which would have a positive outcome with sorafenib. We believe patient's tumors should be screened for LSP1 or pERK

expression and the efficacy of sorafenib on tumors both with and without LSP1 expression should be assessed. We hypothesize that the tumors lacking LSP1 expression would respond better to sorafenib since tumors expressing LSP1 would most likely not have increased ERK activation and therefore not respond as well to sorafenib treatment. Preliminary results demonstrate that the LSP1 shRNA expressing JM1 hepatoma cells, which express higher levels of ERK phosphorylation, are more sensitive to sorafenib than the scrambled control cells (Figure 37).

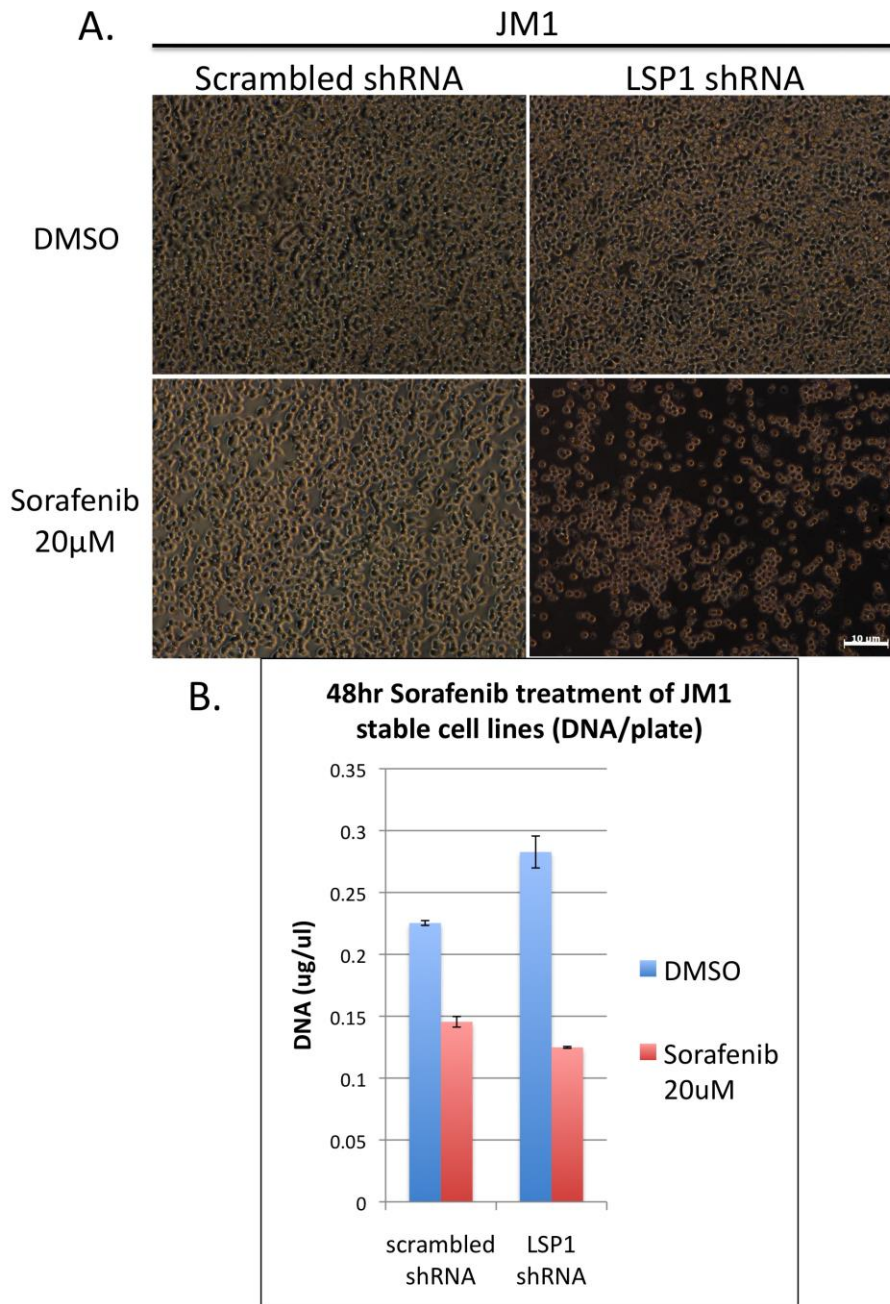


**Figure 37. Treatment of LSP1 shRNA JM1 stable cells with sorafenib causes increased cell death in comparison to scrambled control cells. A. Representative phase contrast images of scrambled shRNA control and LSP1 shRNA JM1 cells treated with DMSO (control) (Top) or 20μM sorafenib for 48 hours. Scale bar = 10μm. B. Quantification of the amount of DNA (μg/μl) per plate for scrambled control and LSP1 shRNA JM1 cells treated with DMSO and sorafenib (20μM) for 48 hours.**

LSP1 is a known regulator of migration and our data demonstrates that LSP1 functions to negatively regulate migration in hepatoma cell lines. However, we have not studied the role LSP1 plays on migration in vivo which is technically challenging in a PHx model of liver regeneration. One method to circumvent this challenge is to utilize a different model of liver regeneration, the carbon tetrachloride model (CCl<sub>4</sub>), which causes the death of the hepatocytes around the central vein because only these hepatocytes express the enzyme that activates CCl<sub>4</sub> to its toxic form, CYP2E1. The remaining hepatocytes proliferate to restore the necrotic region and liver architecture is intact after about 10 days (133). Hoehme, et al. demonstrated through mathematical modeling as well three dimensional reconstruction that during regeneration after CCl<sub>4</sub> administration, daughter hepatocytes migrate into the necrotic region and align along the sinusoids and that this phenomenon is necessary to restore normal liver microarchitecture (133). Therefore, using this model, we can determine if loss of LSP1 expression can lead to increased hepatocyte migration into the necrotic region created in the pericentral region of the liver by CCl<sub>4</sub> administration.

Another area of LSP1 research that needs to be explored further is the function of the different isoforms of LSP1 in our model system. It is conceivable that one of the isoforms functions to regulate proliferation while the other plays a role in migration since cells that are dividing are not migrating and vice versa. To test this hypothesis, we could overexpress each isoform of LSP1 in our JM2 hepatoma cell line and measure the effect on proliferation and migration of these cells. Since isoform 1 of LSP1 is the isoform deleted in the LSP1 KO animals and overexpressed in the LSP1 TG animals and we have demonstrated an effect on proliferation

during regeneration, we would expect that isoform 2 (S37) functions as the negative regulator of migration.

## BIBLIOGRAPHY

1. Michalopoulos GK (2007) Liver regeneration. *J Cell Physiol* 213(2):286-300.
2. Kang LI, Mars WM, & Michalopoulos GK (2012) Signals and cells involved in regulating liver regeneration. *Cells* 1(4):1261-1292.
3. Malarkey DE, Johnson K, Ryan L, Boorman G, & Maronpot RR (2005) New insights into functional aspects of liver morphology. *Toxicol Pathol* 33(1):27-34.
4. Limaye PB, *et al.* (2008) Mechanisms of hepatocyte growth factor-mediated and epidermal growth factor-mediated signaling in transdifferentiation of rat hepatocytes to biliary epithelium. *Hepatology* 47(5):1702-1713.
5. Michalopoulos GK, Barua L, & Bowen WC (2005) Transdifferentiation of rat hepatocytes into biliary cells after bile duct ligation and toxic biliary injury. *Hepatology* 41(3):535-544.
6. Friedman SL (2008) Hepatic stellate cells: protean, multifunctional, and enigmatic cells of the liver. *Physiol Rev* 88(1):125-172.
7. Michalopoulos GK & DeFrances MC (1997) Liver regeneration. *Science* 276(5309):60-66.
8. Parker GA & Picut CA (2012) Immune functioning in non lymphoid organs: the liver. *Toxicol Pathol* 40(2):237-247.

9. Gebhardt R & Matz-Soja M (2014) Liver zonation: Novel aspects of its regulation and its impact on homeostasis. *World J Gastroenterol* 20(26):8491-8504.
10. Christoffels VM, *et al.* (1999) A mechanistic model for the development and maintenance of portocentral gradients in gene expression in the liver. *Hepatology* 29(4):1180-1192.
11. Higgins GM, Anderson R.M. (1934) Experimental pathology of the liver. I. Restoration of the liver of the white rat following partial surgical removal. . *Arch. Pathol.* 12:186-202.
12. Michalopoulos GK (2010) Liver regeneration after partial hepatectomy: critical analysis of mechanistic dilemmas. *Am J Pathol* 176(1):2-13.
13. Taub R (2004) Liver regeneration: from myth to mechanism. *Nat Rev Mol Cell Biol* 5(10):836-847.
14. Fausto N, Campbell JS, & Riehle KJ (2006) Liver regeneration. *Hepatology* 43(2 Suppl 1):S45-53.
15. Rabes HM (1977) Kinetics of hepatocellular proliferation as a function of the microvascular structure and functional state of the liver. *Ciba Found Symp* (55):31-53.
16. Gebhardt R, Baldysiak-Figiel A, Krugel V, Ueberham E, & Gaunitz F (2007) Hepatocellular expression of glutamine synthetase: an indicator of morphogen actions as master regulators of zonation in adult liver. *Prog Histochem Cytochem* 41(4):201-266.
17. Sakamoto T, *et al.* (1999) Mitosis and apoptosis in the liver of interleukin-6-deficient mice after partial hepatectomy. *Hepatology* 29(2):403-411.
18. Bupathi M, Kaseb A, Meric-Bernstam F, & Naing A (2015) Hepatocellular carcinoma: Where there is unmet need. *Mol Oncol* 9(8):1501-1509.

19. Mars WM, *et al.* (1995) Immediate early detection of urokinase receptor after partial hepatectomy and its implications for initiation of liver regeneration. *Hepatology* 21(6):1695-1701.
20. Mohammed FF & Khokha R (2005) Thinking outside the cell: proteases regulate hepatocyte division. *Trends Cell Biol* 15(10):555-563.
21. Masumoto A & Yamamoto N (1991) Sequestration of a hepatocyte growth factor in extracellular matrix in normal adult rat liver. *Biochem Biophys Res Commun* 174(1):90-95.
22. Stolz DB, Mars WM, Petersen BE, Kim TH, & Michalopoulos GK (1999) Growth factor signal transduction immediately after two-thirds partial hepatectomy in the rat. *Cancer Res* 59(16):3954-3960.
23. Yamada Y & Fausto N (1998) Deficient liver regeneration after carbon tetrachloride injury in mice lacking type 1 but not type 2 tumor necrosis factor receptor. *Am J Pathol* 152(6):1577-1589.
24. Huang W, *et al.* (2006) Nuclear receptor-dependent bile acid signaling is required for normal liver regeneration. *Science* 312(5771):233-236.
25. Cressman DE, *et al.* (1996) Liver failure and defective hepatocyte regeneration in interleukin-6-deficient mice. *Science* 274(5291):1379-1383.
26. Lesurtel M, *et al.* (2006) Platelet-derived serotonin mediates liver regeneration. *Science* 312(5770):104-107.
27. Monga SP, Pediaditakis P, Mule K, Stolz DB, & Michalopoulos GK (2001) Changes in WNT/beta-catenin pathway during regulated growth in rat liver regeneration. *Hepatology* 33(5):1098-1109.

28. Kohler C, *et al.* (2004) Expression of Notch-1 and its ligand Jagged-1 in rat liver during liver regeneration. *Hepatology* 39(4):1056-1065.
29. Houck KA & Michalopoulos GK (1989) Altered responses of regenerating hepatocytes to norepinephrine and transforming growth factor type beta. *J Cell Physiol* 141(3):503-509.
30. Braun L, *et al.* (1988) Transforming growth factor beta mRNA increases during liver regeneration: a possible paracrine mechanism of growth regulation. *Proc Natl Acad Sci U S A* 85(5):1539-1543.
31. Ichikawa T, *et al.* (2001) Transforming growth factor beta and activin tonically inhibit DNA synthesis in the rat liver. *Hepatology* 34(5):918-925.
32. Yee KS, Wilkinson S, James J, Ryan KM, & Vousden KH (2009) PUMA- and Bax-induced autophagy contributes to apoptosis. *Cell Death Differ* 16(8):1135-1145.
33. Gkretsi V, *et al.* (2008) Liver-specific ablation of integrin-linked kinase in mice results in abnormal histology, enhanced cell proliferation, and hepatomegaly. *Hepatology* 48(6):1932-1941.
34. Dong J, *et al.* (2007) Elucidation of a universal size-control mechanism in *Drosophila* and mammals. *Cell* 130(6):1120-1133.
35. Apte U, *et al.* (2009) Enhanced liver regeneration following changes induced by hepatocyte-specific genetic ablation of integrin-linked kinase. *Hepatology* 50(3):844-851.
36. Block GD, *et al.* (1996) Population expansion, clonal growth, and specific differentiation patterns in primary cultures of hepatocytes induced by HGF/SF, EGF and TGF alpha in a chemically defined (HGM) medium. *J Cell Biol* 132(6):1133-1149.
37. Song HH & Filmus J (2002) The role of glypicans in mammalian development. *Biochim Biophys Acta* 1573(3):241-246.

38. Luo JH, *et al.* (2006) Transcriptomic and genomic analysis of human hepatocellular carcinomas and hepatoblastomas. *Hepatology* 44(4):1012-1024.
39. Filmus J & Capurro M (2004) Glypican-3 and alphafetoprotein as diagnostic tests for hepatocellular carcinoma. *Mol Diagn* 8(4):207-212.
40. Pilia G, *et al.* (1996) Mutations in GPC3, a glypican gene, cause the Simpson-Golabi-Behmel overgrowth syndrome. *Nat Genet* 12(3):241-247.
41. Cano-Gauci DF, *et al.* (1999) Glypican-3-deficient mice exhibit developmental overgrowth and some of the abnormalities typical of Simpson-Golabi-Behmel syndrome. *J Cell Biol* 146(1):255-264.
42. Liu B, *et al.* (2009) Investigation of the role of glypican 3 in liver regeneration and hepatocyte proliferation. *Am J Pathol* 175(2):717-724.
43. Liu B, *et al.* (2010) Suppression of liver regeneration and hepatocyte proliferation in hepatocyte-targeted glypican 3 transgenic mice. *Hepatology* 52(3):1060-1067.
44. Farazi PA & DePinho RA (2006) Hepatocellular carcinoma pathogenesis: from genes to environment. *Nat Rev Cancer* 6(9):674-687.
45. Society AC (2016) What are the key statistics about liver cancer?
46. Bruix J, Reig M, & Sherman M (2016) Evidence-based Diagnosis, Staging, and Treatment of Patients With Hepatocellular Carcinoma. *Gastroenterology*.
47. Sanyal AJ, Yoon SK, & Lencioni R (2010) The etiology of hepatocellular carcinoma and consequences for treatment. *Oncologist* 15 Suppl 4:14-22.
48. Lotersztajn S, Julien B, Teixeira-Clerc F, Grenard P, & Mallat A (2005) Hepatic fibrosis: molecular mechanisms and drug targets. *Annu Rev Pharmacol Toxicol* 45:605-628.

49. El-Serag HB & Rudolph KL (2007) Hepatocellular carcinoma: epidemiology and molecular carcinogenesis. *Gastroenterology* 132(7):2557-2576.
50. Rehermann B & Nascimbeni M (2005) Immunology of hepatitis B virus and hepatitis C virus infection. *Nat Rev Immunol* 5(3):215-229.
51. McClain CJ, Hill DB, Song Z, Deaciuc I, & Barve S (2002) Monocyte activation in alcoholic liver disease. *Alcohol* 27(1):53-61.
52. Hoek JB & Pastorino JG (2002) Ethanol, oxidative stress, and cytokine-induced liver cell injury. *Alcohol* 27(1):63-68.
53. Ozturk M (1991) p53 mutation in hepatocellular carcinoma after aflatoxin exposure. *Lancet* 338(8779):1356-1359.
54. Riley J, Mandel HG, Sinha S, Judah DJ, & Neal GE (1997) In vitro activation of the human Harvey-ras proto-oncogene by aflatoxin B1. *Carcinogenesis* 18(5):905-910.
55. Minouchi K, Kaneko S, & Kobayashi K (2002) Mutation of p53 gene in regenerative nodules in cirrhotic liver. *J Hepatol* 37(2):231-239.
56. Chin R, *et al.* (2007) Modulation of MAPK pathways and cell cycle by replicating hepatitis B virus: factors contributing to hepatocarcinogenesis. *J Hepatol* 47(3):325-337.
57. Zhao LJ, *et al.* (2005) Hepatitis C virus E2 protein promotes human hepatoma cell proliferation through the MAPK/ERK signaling pathway via cellular receptors. *Exp Cell Res* 305(1):23-32.
58. Urabe Y, *et al.* (1996) Telomere length in human liver diseases. *Liver* 16(5):293-297.
59. Nagao K, Tomimatsu M, Endo H, Hisatomi H, & Hikiji K (1999) Telomerase reverse transcriptase mRNA expression and telomerase activity in hepatocellular carcinoma. *J Gastroenterol* 34(1):83-87.

60. Shimojima M, *et al.* (2004) Detection of telomerase activity, telomerase RNA component, and telomerase reverse transcriptase in human hepatocellular carcinoma. *Hepatol Res* 29(1):31-38.
61. Farazi PA, *et al.* (2003) Differential impact of telomere dysfunction on initiation and progression of hepatocellular carcinoma. *Cancer Res* 63(16):5021-5027.
62. Gollin SM (2005) Mechanisms leading to chromosomal instability. *Semin Cancer Biol* 15(1):33-42.
63. Llovet JM, Burroughs A, & Bruix J (2003) Hepatocellular carcinoma. *Lancet* 362(9399):1907-1917.
64. Llovet JM & Bruix J (2008) Molecular targeted therapies in hepatocellular carcinoma. *Hepatology* 48(4):1312-1327.
65. Okada S (1999) Local ablation therapy for hepatocellular carcinoma. *Semin Liver Dis* 19(3):323-328.
66. Llovet JM, *et al.* (2002) Arterial embolisation or chemoembolisation versus symptomatic treatment in patients with unresectable hepatocellular carcinoma: a randomised controlled trial. *Lancet* 359(9319):1734-1739.
67. Lo CM, *et al.* (2002) Randomized controlled trial of transarterial lipiodol chemoembolization for unresectable hepatocellular carcinoma. *Hepatology* 35(5):1164-1171.
68. Llovet JM, *et al.* (2008) Sorafenib in advanced hepatocellular carcinoma. *N Engl J Med* 359(4):378-390.

69. Cheng AL, *et al.* (2012) Efficacy and safety of sorafenib in patients with advanced hepatocellular carcinoma according to baseline status: subset analyses of the phase III Sorafenib Asia-Pacific trial. *Eur J Cancer* 48(10):1452-1465.
70. Lee JS & Thorgeirsson SS (2005) Genetic profiling of human hepatocellular carcinoma. *Semin Liver Dis* 25(2):125-132.
71. Lee JS, *et al.* (2004) Classification and prediction of survival in hepatocellular carcinoma by gene expression profiling. *Hepatology* 40(3):667-676.
72. Guichard C, *et al.* (2012) Integrated analysis of somatic mutations and focal copy-number changes identifies key genes and pathways in hepatocellular carcinoma. *Nat Genet* 44(6):694-698.
73. Schulze K, *et al.* (2015) Exome sequencing of hepatocellular carcinomas identifies new mutational signatures and potential therapeutic targets. *Nat Genet* 47(5):505-511.
74. Nalesnik MA, *et al.* (2012) Gene deletions and amplifications in human hepatocellular carcinomas: correlation with hepatocyte growth regulation. *Am J Pathol* 180(4):1495-1508.
75. Jongstra-Bilen J & Jongstra J (2006) Leukocyte-specific protein 1 (LSP1): a regulator of leukocyte emigration in inflammation. *Immunol Res* 35(1-2):65-74.
76. Jongstra-Bilen J, Janmey PA, Hartwig JH, Galea S, & Jongstra J (1992) The lymphocyte-specific protein LSP1 binds to F-actin and to the cytoskeleton through its COOH-terminal basic domain. *J Cell Biol* 118(6):1443-1453.
77. Wong MJ, Malapitan IA, Sikorski BA, & Jongstra J (2003) A cell-free binding assay maps the LSP1 cytoskeletal binding site to the COOH-terminal 30 amino acids. *Biochim Biophys Acta* 1642(1-2):17-24.

78. Huang CK, Zhan L, Ai Y, & Jongstra J (1997) LSP1 is the major substrate for mitogen-activated protein kinase-activated protein kinase 2 in human neutrophils. *J Biol Chem* 272(1):17-19.
79. Misener VL, *et al.* (1994) Expression of mouse LSP1/S37 isoforms. S37 is expressed in embryonic mesenchymal cells. *J Cell Sci* 107 ( Pt 12):3591-3600.
80. Klein DP, Jongstra-Bilen J, Ogryzlo K, Chong R, & Jongstra J (1989) Lymphocyte-specific Ca<sup>2+</sup>-binding protein LSP1 is associated with the cytoplasmic face of the plasma membrane. *Mol Cell Biol* 9(7):3043-3048.
81. Jongstra-Bilen J, *et al.* (2000) LSP1 modulates leukocyte populations in resting and inflamed peritoneum. *Blood* 96(5):1827-1835.
82. Howard TH, Hartwig J, & Cunningham C (1998) Lymphocyte-specific protein 1 expression in eukaryotic cells reproduces the morphologic and motile abnormality of NAD 47/89 neutrophils. *Blood* 91(12):4786-4795.
83. Coates TD, Torkildson JC, Torres M, Church JA, & Howard TH (1991) An inherited defect of neutrophil motility and microfilamentous cytoskeleton associated with abnormalities in 47-Kd and 89-Kd proteins. *Blood* 78(5):1338-1346.
84. Southwick FS, Dabiri GA, & Stossel TP (1988) Neutrophil actin dysfunction is a genetic disorder associated with partial impairment of neutrophil actin assembly in three family members. *J Clin Invest* 82(5):1525-1531.
85. Li Y, Zhang Q, Aaron R, Hilliard L, & Howard TH (2000) LSP1 modulates the locomotion of monocyte-differentiated U937 cells. *Blood* 96(3):1100-1105.

86. Hannigan M, Zhan L, Ai Y, & Huang CK (2001) Leukocyte-specific gene 1 protein (LSP1) is involved in chemokine KC-activated cytoskeletal reorganization in murine neutrophils in vitro. *J Leukoc Biol* 69(3):497-504.
87. Wang C, *et al.* (2002) Modulation of Mac-1 (CD11b/CD18)-mediated adhesion by the leukocyte-specific protein 1 is key to its role in neutrophil polarization and chemotaxis. *J Immunol* 169(1):415-423.
88. Coxon A, *et al.* (1996) A novel role for the beta 2 integrin CD11b/CD18 in neutrophil apoptosis: a homeostatic mechanism in inflammation. *Immunity* 5(6):653-666.
89. Jongstra-Bilen J, Wielowieyski A, Misener V, & Jongstra J (1999) LSP1 regulates anti-IgM induced apoptosis in WEHI-231 cells and normal immature B-cells. *Mol Immunol* 36(6):349-359.
90. Cao MY, *et al.* (2001) Inhibition of anti-IgM-induced translocation of protein kinase C beta I inhibits ERK2 activation and increases apoptosis. *J Biol Chem* 276(27):24506-24510.
91. Petri B, *et al.* (2011) Endothelial LSP1 is involved in endothelial dome formation, minimizing vascular permeability changes during neutrophil transmigration in vivo. *Blood* 117(3):942-952.
92. Liu L, *et al.* (2005) LSP1 is an endothelial gatekeeper of leukocyte transendothelial migration. *J Exp Med* 201(3):409-418.
93. Hossain M, Qadri SM, Su Y, & Liu L (2013) ICAM-1-mediated leukocyte adhesion is critical for the activation of endothelial LSP1. *Am J Physiol Cell Physiol* 304(9):C895-904.

94. Martin P (1997) Wound healing--aiming for perfect skin regeneration. *Science* 276(5309):75-81.
95. Wang J, *et al.* (2007) Accelerated wound healing in leukocyte-specific, protein 1-deficient mouse is associated with increased infiltration of leukocytes and fibrocytes. *J Leukoc Biol* 82(6):1554-1563.
96. Wang J, *et al.* (2008) Increased severity of bleomycin-induced skin fibrosis in mice with leukocyte-specific protein 1 deficiency. *J Invest Dermatol* 128(12):2767-2776.
97. Zu YL, *et al.* (1996) Activation of MAP kinase-activated protein kinase 2 in human neutrophils after phorbol ester or fMLP peptide stimulation. *Blood* 87(12):5287-5296.
98. Ohira T, *et al.* (2004) A stable aspirin-triggered lipoxin A4 analog blocks phosphorylation of leukocyte-specific protein 1 in human neutrophils. *J Immunol* 173(3):2091-2098.
99. Zu YL, *et al.* (1998) p38 mitogen-activated protein kinase activation is required for human neutrophil function triggered by TNF-alpha or FMLP stimulation. *J Immunol* 160(4):1982-1989.
100. Hannigan MO, *et al.* (2001) Abnormal migration phenotype of mitogen-activated protein kinase-activated protein kinase 2<sup>-/-</sup> neutrophils in Zigmond chambers containing formyl-methionyl-leucyl-phenylalanine gradients. *J Immunol* 167(7):3953-3961.
101. Tan SM, *et al.* (2000) Effect of integrin beta 2 subunit truncations on LFA-1 (CD11a/CD18) and Mac-1 (CD11b/CD18) assembly, surface expression, and function. *J Immunol* 165(5):2574-2581.

102. Harrison RE, Sikorski BA, & Jongstra J (2004) Leukocyte-specific protein 1 targets the ERK/MAP kinase scaffold protein KSR and MEK1 and ERK2 to the actin cytoskeleton. *J Cell Sci* 117(Pt 10):2151-2157.
103. Brunet A, *et al.* (1999) Nuclear translocation of p42/p44 mitogen-activated protein kinase is required for growth factor-induced gene expression and cell cycle entry. *EMBO J* 18(3):664-674.
104. Pearson G, *et al.* (2001) Mitogen-activated protein (MAP) kinase pathways: regulation and physiological functions. *Endocr Rev* 22(2):153-183.
105. Roy F, Laberge G, Douziech M, Ferland-McCollough D, & Therrien M (2002) KSR is a scaffold required for activation of the ERK/MAPK module. *Genes Dev* 16(4):427-438.
106. Denouel-Galy A, *et al.* (1998) Murine Ksr interacts with MEK and inhibits Ras-induced transformation. *Curr Biol* 8(1):46-55.
107. Stewart S, *et al.* (1999) Kinase suppressor of Ras forms a multiprotein signaling complex and modulates MEK localization. *Mol Cell Biol* 19(8):5523-5534.
108. Yu W, Fantl WJ, Harrowe G, & Williams LT (1998) Regulation of the MAP kinase pathway by mammalian Ksr through direct interaction with MEK and ERK. *Curr Biol* 8(1):56-64.
109. Michaud NR, *et al.* (1997) KSR stimulates Raf-1 activity in a kinase-independent manner. *Proc Natl Acad Sci U S A* 94(24):12792-12796.
110. Muller J, Ory S, Copeland T, Piwnica-Worms H, & Morrison DK (2001) C-TAK1 regulates Ras signaling by phosphorylating the MAPK scaffold, KSR1. *Mol Cell* 8(5):983-993.

111. Xing H, Kornfeld K, & Muslin AJ (1997) The protein kinase KSR interacts with 14-3-3 protein and Raf. *Curr Biol* 7(5):294-300.
112. Therrien M, Michaud NR, Rubin GM, & Morrison DK (1996) KSR modulates signal propagation within the MAPK cascade. *Genes Dev* 10(21):2684-2695.
113. Cacace AM, *et al.* (1999) Identification of constitutive and ras-inducible phosphorylation sites of KSR: implications for 14-3-3 binding, mitogen-activated protein kinase binding, and KSR overexpression. *Mol Cell Biol* 19(1):229-240.
114. Gringhuis SI, den Dunnen J, Litjens M, van der Vlist M, & Geijtenbeek TB (2009) Carbohydrate-specific signaling through the DC-SIGN signalosome tailors immunity to Mycobacterium tuberculosis, HIV-1 and Helicobacter pylori. *Nat Immunol* 10(10):1081-1088.
115. Talarmin H, *et al.* (1999) The mitogen-activated protein kinase kinase/extracellular signal-regulated kinase cascade activation is a key signalling pathway involved in the regulation of G(1) phase progression in proliferating hepatocytes. *Mol Cell Biol* 19(9):6003-6011.
116. Wortzel I & Seger R (2011) The ERK Cascade: Distinct Functions within Various Subcellular Organelles. *Genes Cancer* 2(3):195-209.
117. McKay MM, Ritt DA, & Morrison DK (2009) Signaling dynamics of the KSR1 scaffold complex. *Proc Natl Acad Sci U S A* 106(27):11022-11027.
118. Koral K, *et al.* (2015) Leukocyte-specific protein 1: a novel regulator of hepatocellular proliferation and migration deleted in human hepatocellular carcinoma. *Hepatology* 61(2):537-547.
119. Seglen PO (1976) Preparation of isolated rat liver cells. *Methods Cell Biol* 13:29-83.

120. Michalopoulos GK, *et al.* (1999) Morphogenetic events in mixed cultures of rat hepatocytes and nonparenchymal cells maintained in biological matrices in the presence of hepatocyte growth factor and epidermal growth factor. *Hepatology* 29(1):90-100.
121. Liu BW, *et al.* (2009) Investigation of the Role of Glypican 3 in Liver Regeneration and Hepatocyte Proliferation. *American Journal of Pathology* 175(2):717-724.
122. Novicki DL, Jirtle RL, & Michalopoulos G (1983) Establishment of two rat hepatoma cell strains produced by a carcinogen initiation, phenobarbital promotion protocol. *In Vitro* 19(3 Pt 1):191-202.
123. Thompson AA, *et al.* (1996) Alternatively spliced exons encode the tissue-specific 5' termini of leukocyte pp52 and stromal cell S37 mRNA isoforms. *Genomics* 32(3):352-357.
124. Ittner LM & Gotz J (2007) Pronuclear injection for the production of transgenic mice. *Nat Protoc* 2(5):1206-1215.
125. Bowen WC, *et al.* (2014) Development of a chemically defined medium and discovery of new mitogenic growth factors for mouse hepatocytes: mitogenic effects of FGF1/2 and PDGF. *PLoS One* 9(4):e95487.
126. Li Z, *et al.* (2006) Cyclin D1 regulates cellular migration through the inhibition of thrombospondin 1 and ROCK signaling. *Mol Cell Biol* 26(11):4240-4256.
127. Dai M, *et al.* (2013) Cyclin D1 cooperates with p21 to regulate TGFbeta-mediated breast cancer cell migration and tumor local invasion. *Breast Cancer Res* 15(3):R49.
128. Park DH, *et al.* (2009) Diethylnitrosamine (DEN) induces irreversible hepatocellular carcinogenesis through overexpression of G1/S-phase regulatory proteins in rat. *Toxicol Lett* 191(2-3):321-326.

129. Verna L, Whysner J, & Williams GM (1996) N-nitrosodiethylamine mechanistic data and risk assessment: bioactivation, DNA-adduct formation, mutagenicity, and tumor initiation. *Pharmacol Ther* 71(1-2):57-81.
130. Moreira RK (2007) Hepatic stellate cells and liver fibrosis. *Arch Pathol Lab Med* 131(11):1728-1734.
131. Turnbull C, *et al.* (2010) Genome-wide association study identifies five new breast cancer susceptibility loci. *Nat Genet* 42(6):504-507.
132. Wilhelm S, *et al.* (2006) Discovery and development of sorafenib: a multikinase inhibitor for treating cancer. *Nat Rev Drug Discov* 5(10):835-844.
133. Hoehme S, *et al.* (2010) Prediction and validation of cell alignment along microvessels as order principle to restore tissue architecture in liver regeneration. *Proc Natl Acad Sci U S A* 107(23):10371-10376.